Freie Universität Berlin

Analysis of mutant huntingtin aggregation and toxicity in *Drosophila* models of Huntington's disease

Inaugural-Dissertation to obtain the academic degree
Doctor rerum naturalium (Dr. rer. nat.)

submitted to the Department of Biology, Chemistry and Pharmacy of Freie Universität Berlin

by

Franziska Schindler
from Erfurt

October 2016

The work was conducted from November 2011 until October 2016 under supervision of Prof. Dr. Erich E. Wanker at the Max Delbrück Center for Molecular Medicine in the Helmholtz-Association.

I hereby confirm that I have written the thesis independently using solely the aids mentioned and without illicit assistance from third parties.

1. Reviewer: Prof. Dr. Erich E. Wanker

2. Reviewer: Prof. Stephan Sigrist

Thesis defense on 17.02.2017

Acknowledgment

First of all, I would like to thank Prof. Erich Wanker, who allowed me to work very independently on my PhD project. He gave me the opportunity to share and discuss my work with researches in different countries. Besides the valuable talks with him, I would like to thank him for the generous supply of tools and equipment for my research. Despite his many responsibilities, he always found time to discuss the work and to give useful input.

I would like to thank Prof. Stephan Sigrist for the interest and the supervision of my thesis and to provide a working place in his fly lab for the first 1.5 years of my PhD. Also, I want to thank the group members of Prof. Sigrist, especially Christine, Tanja, Harald and Anuradha, for their support in the fly lab. Thanks also goes to Prof. Bertram Gebrer and Dr. Sören Diegelmann, who supported me in establishing the olfactory learning method in our lab.

Thanks to my colleagues and labmates, particular Anne, Young-In, Alexander, Konrad, Philipp, Nadine, Eileen and Kirstin for the help, advice, patience and enjoyment during the last five years.

I would like to thank Anne, Eileen, Alex, and Michael for their helpfulness and support to create this thesis. And especially my husband Alexander who has encouraged me to create this thesis with LaTeX.

Most importantly, I would like to my husband Alexander and the rest of my family who supported me during the last five years, thanks for everything.

Contents

1 Introduction

1.1 Neurodegenerative diseases

Neurodegenerative diseases are an umbrella term of hereditary and sporadic disorders which are characterized by degeneration and selective progressive death of particular neuron subtypes in the human brain [1]. A common symptom of neurodegenerative diseases is cognitive decline and partially impairments in movement [2]. A hallmark of neurodegenerative diseases are protein deposits that are present in the brain in Alzheimer's disease (AD), Parkinson's disease (PD), amyotrophic lateral sclerosis (ALS), frontotemporal dementia (FTD) and polyglutamine diseases including Huntington's disease (HD) [3]. The involved disease-related proteins such as amyloid-β and tau in AD [4], α-synuclein and parkin in PD [5, 6], transactive response DNA-binding protein 43 (TDP-43) in ALS and FTD [7, 8] and the huntingtin protein in HD [9] accumulate and form aggregates, which can be localized in the cytoplasmic, the nuclear or the extracellular space [10].
Major efforts have been made to identify the molecular causes of these diseases. Several intracellular processes, including oxidative metabolism, ubiquitin-proteasome system and axonal transport seem to be altered in neurodegenerative diseases [11]. Mitochondrial and synaptic dysfunction, altered vesicle transport, increased oxidative stress and disruption of the proteasome system are implicated in neurodegenerative diseases [11]. However, the exact molecular mechanisms involved in the origin and pathogenesis of neurodegenerative diseases are still poorly understood.

1.2 Polyglutamine diseases

Nine inherited neurological disorders are linked to an expansion of a trinucleotide repeat (CAG), including Huntington's disease (Table 1.1). The CAG triplet repeat encodes for the amino acid glutamine, which results in a polyglutamine (polyQ) tract in the transcribed protein and causes the production of a mutated form of the protein. The elongated polyQ tract provokes the disease either through a loss-of-function or a gain-of-function or a combination of both [12]. The first described polyQ disease is the X-linked spinal bulbar muscular atrophy (SBMA) that is caused by a mutation in the androgen receptor (AR) gene. It leads to a progressive weakness resulting

from a loss of motor neurons [13]. Nine other diseases caused by polyQ-expanded proteins including Machado-Joseph disease (MJD / SCA3), dentatorubro-pallidoluysian atrophy (DRPLA) and six forms of spinocerebellar ataxia (SCA1, 2, 6, 7 and 17) were identified so far [14, 15].

Table 1.1: Polyglutamine- associated diseases and their affected proteins.
Modified from [15, 16].

Disease	Protein	Normal CAG(n)	Expanded CAG(n)	Most affected brain areas
SCA1	Ataxin-1	6 – 39	41 – 83	Cerebellum
SCA2	Ataxin-2	14 – 32	34 – 77	Cerebellum
SCA6	CACNA1A	4 – 18	21 – 30	Cerebellum
SCA7	Ataxin-7	7 – 18	38 – 200	Cerebellum, Eye retina
SCA17	TBP	25 – 43	45 – 63	Cerebellum
MJD / SCA3	Ataxin-3	12 – 40	63 – 86	Spinal cord
HD	Huntingtin	6 – 35	36 – 180	Striatum
DRPLA	Atrophin-1	3 – 38	49 – 88	Cerebellum
SBMA	Androgen receptor	6 – 36	38 – 62	Spinal cord and brainstem

The prevalence of polyQ diseases averages one – ten cases per 100,000 people [17]. The most common polyQ diseases are HD and SCA3 [18], though the occurrence differs between nations. Many cases of SCA2 were reported from Cuba [19], SCA3 was frequently observed in Portugal [20] and DRPLA predominantly occurs in Japan [21].
In already two of the polyQ diseases, SCA8 and HD, repeat-associated non-ATG (RAN) translation have been reported [22, 23]. RAN translation was first discovered in SCA8 by Zu and colleagues [24]. The group mutated the ATG initiation codon of the SCA8 gene and showed the expression of homopolymeric polyglutamine, polyalanine and polyserine proteins in transfected cells. Additional, the SCA8 polyalanine proteins were detected in mouse models and human tissue. A recent study demonstrated the accumulation of homopolymeric expansion proteins such as polyAla, polySer, polyLeu and polyCys in HD human brains, indicating that RAN translation could also contribute to other polyQ diseases [23].

1.3 Chorea Huntington

Huntington's disease (also Huntington's chorea) was first described in 1872 by George Huntington [25]. HD is an autosomal dominant inherited, progressive neurodegenerative disorder with a prevalence of about five – seven cases per 100,000 in Europe [26]. The disease is characterized by adult-onset motor abnormalities, cognitive defects and psychiatric disturbances [26].

1.3.1 Symptoms

Cognitive and psychiatric problems can be evident up to 15 years before the motor symptoms manifest [27]. These include personality changes such as depression, anxiety, impulsiveness and aggression [26, 27]. With disease progression, cognitive impairments develop into dementia. In 5 – 10 % of the cases, the depression results in suicide [26]. Motor symptoms include involuntary movements, also known as "chorea", and akinesia and rigidity at a later stage of the disease [26, 28]. The decline of the motor function decreases the speech output and even affects the ability to chew and swallow, which can lead to the commonly observed weight loss [29]. Many HD patients succumbs heart diseases due to aspiration pneumonia caused by swallowing problems. The typical duration from onset of symptoms to death is 10 to 20 years [30].

1.3.2 Neuropathology

The most notable neuropathological feature of HD is the selective neuronal loss of the striatum (caudate nucleus and putamen) and the cerebral cortex (Fig. 1.1) [31]. The most severely affected region in HD is the striatum that is comprised of approximately 95 % medium spiny neurons (MSNs) and 5 % interneurons [32]. The MSNs are characterized by a long axon, medium-size cell bodies and spiny dendrites. In contrast, interneurons are characterized by short axons, large cell bodies and dendrites [33, 34]. Striatal MSNs, which are the main and earliest cell type, affected in HD show differences in vulnerability among specific subpopulations of MSNs. The enkephalin-expressing MSNs projecting to the external segment of the globus pallidus die earlier than the P-expressing MSNs projecting to the internal segment of the globus pallidus. In comparison the interneurons are mildly affected at a late stage of the disease. Loss of cortical neurons, in special large pyramidal projection neurons in cortical layers III, V and VI that project to the striatum, is only evident in late stage HD [33, 34].
The neuropathology of HD is classified in five grades (0 – 4) depending on the severity of neuronal loss within the brain [35]. For example, grade 0 brains show a neuronal loss of 30 to 40 % of the caudate nucleus, whereby the brains of grade 1 exhibit 50 % atrophy of the caudate and grade 4 displays 95 % loss of the caudate and widespread loss of the putamen [35]. In addition to the atrophy of specific brain regions, abnormalities in peripheral tissues have been reported.

Here, altered glucose homeostasis and sub-cellular abnormalities in fibroblasts, lymphocytes and erythrocytes were observed [36].

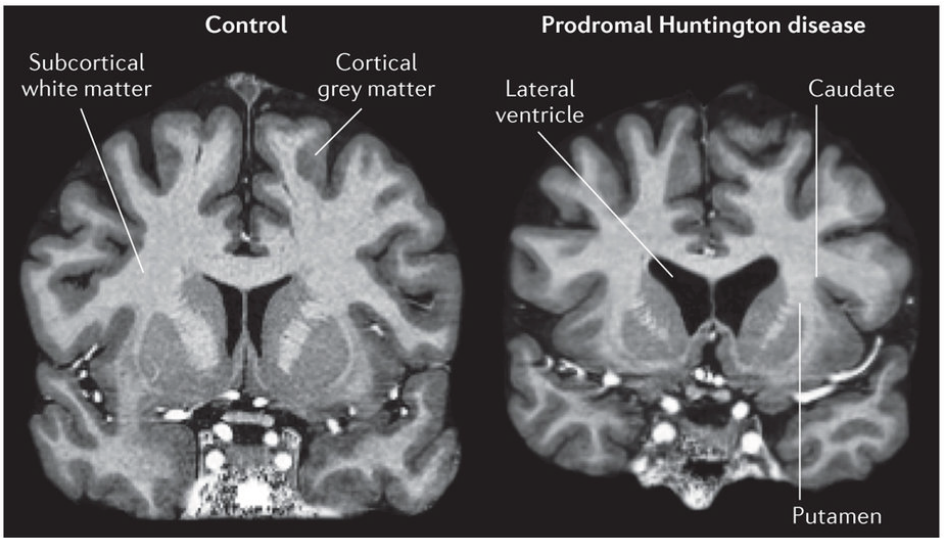

Figure 1.1: Macroscopic analysis of a Huntington's disease brain (right) compared to a normal brain (left).
The brain shows atrophy of the caudate and putamen and an increase of the fluid-filled lateral ventricle in the HD brain. Moreover, changes in cortical grey matter and white matter are observable. Adapted from [37].

1.3.3 Genetics

In 1993 the Huntington's disease Collaborative Research Group (HDCRG) identified the responsible gene for HD, the *IT15* gene also known as *huntingtin* (*HTT*) [38]. The *huntingtin* gene is located on the short arm of chromosome 4 and encodes for the protein huntingtin (HTT). The *HTT* gene is characterized by a CAG trinucleotide repeat located in the first of 67 exons and encodes sequential glutamines [38]. In healthy individuals the *HTT* gene contains up to 35 CAG repeats, whereas individuals with 36 – 39 CAG repeats are at risk to develop the disease. Full penetrance is observed for a repeat length of > 40. Extremely large repeats of > 60 CAGs are associated with a disease onset during childhood or adolescence (juvenile HD) [38, 39]. There is an inverse correlation between the CAG repeat length and the onset of disease. Patients with a large number of glutamines develop symptoms at an earlier age [39, 40]. Moreover, genetic anticipation, environmental as well as genetic factors influence the variance in the age of onset [41, 42].

1.3.4 The huntingtin protein

The human wild-type huntingtin (wHTT) consists of 3144 amino acids that encode a ~350 kDa protein (Fig. 1.2). It is characterized by a polyQ tract at the N-terminus of the protein of up to 35 glutamines (in healthy individuals), two polyproline regions (polyP) and several HEAT (Huntingtin elongation factor 3, the PR65/A subunit of protein phosphatase2A and the lipid kinase Tor) repeats downstream of the polyP regions [42]. The polyQ tract is a key regulator of huntingtin binding to its cellular partners [43, 44]. X-ray crystallography has been shown that the polyQ tract in HTT can adopt multiple flexible conformations, including α-helixes, random coils and an extended loop [45]. These data also indicate that the structure of the polyQ tract may be influenced by the polyP region. The specific conformations depends on its binding partners, sub-cellular location and differentiation of a given cell type and tissue [45, 46]. It has been shown that the polyQ region stabilize protein-protein-interactions [47]. A number of 37 putative HEAT repeats were found in HTT, which are clustered in three main groups. This structural motif was found to be involved in protein-protein interactions [48]. Moreover, HTT harbors a nuclear localization signal (NLS) and a functionally very active carboxy nuclear export signal (NES) sequence, indicating that the protein can shuttle in and out of the nucleus [49].

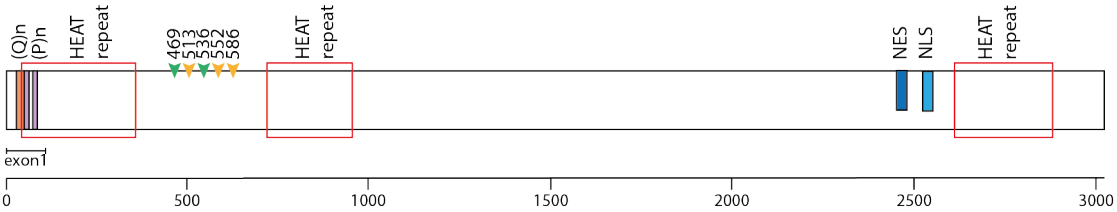

Figure 1.2: Schematic diagram of the HTT amino acid sequence.
Full-length HTT consist of 3144 amino acids in length. It contains a polyglutamine tract, two proline-rich regions and three clusters of HEAT repeats. The yellow and green arrows indicate potential cleavage sites by caspases and calpains. The polyQ tract is labeled in orange and the polyP regions in purple.

The HTT protein contains consensus cleavage sites and can be cleaved by several intracellular proteases, resulting in the formation of a large number of N-terminal fragments. Many studies have demonstrated that proteolytically cleaved HTT fragments are sufficient to cause an HD-like phenotype in model organisms [50] - [52]. HTT can be cleaved by caspase-3 at amino acid 513 and 552, caspase-2 at amino acid 552, caspase-6 at amino acid 586 and calpain at amino acids 469 and 536 [50, 53]. Inhibition of caspase-3 and caspase-6 cleavage reduces pathogenicity, whereby further analysis showed no contribution of HTT proteolysis by caspase-6 [54]. Even smaller N-terminal fragments, such as the cleavage products A and B (cp-A and -B) produced by an aspartyl protease and unidentified proteases were detectable [55]. The potential importance of smaller N-terminal HTT fragments is substantiated by their presence in HD postmortem brain

[9]. Many studies currently use the HTT exon-1 fragment as a model of HD [56] - [58]. Recently, it was shown that the pathogenic HTT exon-1 fragment is produced by aberrant splicing in HD patient tissue [59]. In this way, the exon-1 fragment represents a very important disease relevant fragment.
Various post-translational modifications of the HTT protein have been described [42]. This includes sumoylation, ubiquitination, phosphorylation and palmitoylation. Ubiquitination has been linked to reduced toxicity most probably by increased clearance of HTT by the proteasome, whereas sumoylation of HTT exacerbates toxicity in a *Drosophila* model of HD [60]. The HTT protein has several known phosphorylation sites including phosphorylation at serines-13, -16, -421 and -434 and threonine-3 [46]. The importance of phosphorylation has been shown by Yang and colleagues, who developed a BACHD mice model that expressed full-length mutant HTT with a mutation of serine-13 and -16 to either aspartate or alanine [61]. The disease pathogenesis was reversed in these mice. Phosphorylation at serine-13 and -16 has been shown to target the clearance of wildtype-huntingtin by the proteasome and lysosome [61, 62].
HTT is ubiquitously expressed with the highest levels found in neurons in the CNS [63]. In cells, HTT is associated with various subcellular compartments, including the endoplasmic reticulum, the Golgi complex, mitochondria and the nucleus [64]. It is also found at various vesicular structures within neurites and synapses [46]. Furthermore, HTT is involved in anti-apoptotic processes, transcriptional regulation, microtubule transport, synaptic transmission and endocytosis [43]. Finally, it was demonstrated that HTT is essential for embryonic development, as knock-out mice die before gastrulation [65].

1.4 Aggregation and toxicity of mutant HTT

One pathological characteristic of HD is the appearance of nuclear or cytoplasmic inclusion bodies. Often, these nuclear inclusion bodies contain small N-terminal huntingtin fragments that were first discovered in transgenic mice and later examined in postmortem brains of HD patients [9, 66].
Currently, two major aggregation mechanisms for mutant HTT are discussed. Perutz proposed that HTT with an elongated polyQ undergo a conformational change from a random coil structure to a stable hairpin structure when the number of glutamines exceeds 41 [67]. This stable structure is called polar zipper that consists of two antiparallel β-sheet strands of polyQ repeats linked together by hydrogen bonds between their man-chain and side-chain amides. The polyQ containing hairpins could associate with each other and causes formation of fibrillar aggregates. Evidence for this hypothesis came from Scherzinger *et al.* who showed that short huntingtin fragments with elongated polyQ tract self-assemble *in vitro* into fibrillar or ribbon-like aggregates [68]. To initiate the aggregation, a critical concentration of mutant HTT has to be exceeded. The

aggregation follows a nucleation-dependent pathway (Fig. 1.3 A), meaning the formation of a nucleus is essential before the polymerization into ordered fibrils occur [69].
The other pathway was found for the polyQ containing N-terminal 17 amino acids sequence of HTT exon-1 (Fig. 1.3 B). Thakur *et al.* proposed that with increasing polyQ length this structure unfolds and self-assembles to globular-intermediate structures with the first 17 amino acids in its core and the polyQ sequences exposed to the surface [70]. The polyP region does not incorporate into the core [71]. Subsequently, the globular intermediate collapses and rearranges into protofibrillar structures with high β-sheet content that grow by the addition of monomer.

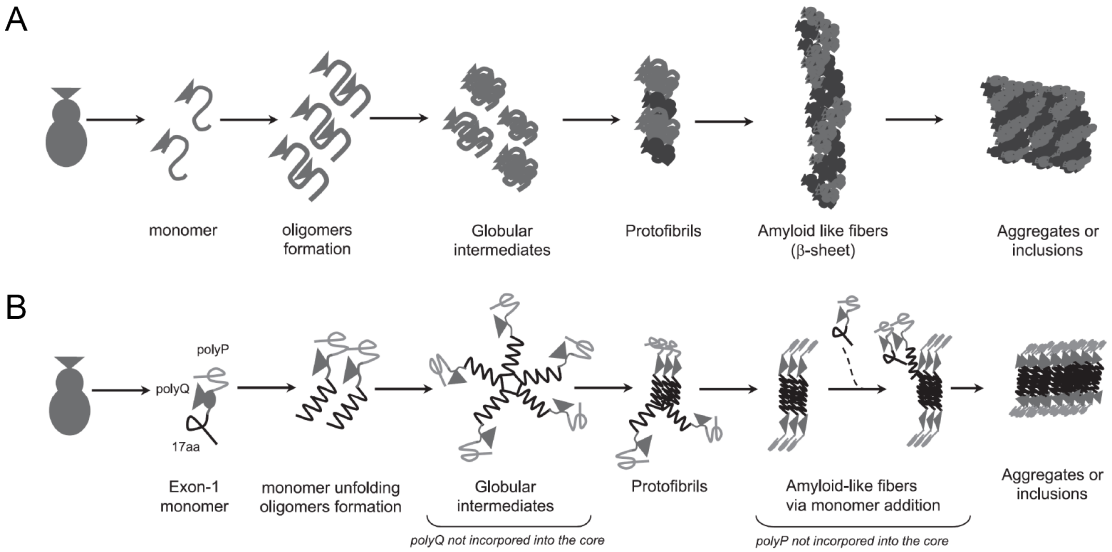

Figure 1.3: The process of aggregate formation.
(A) Nucleation-dependent polymerization mechanism. The mutant protein undergoes a conformational change from a random coil to a hairpin structure. After exceeding a critical concentration, the nucleus is formed during the lag phase. Subsequently, oligomers arise, that grow by adding further monomers. Mutant huntingtin forms amyloid-like structures rich in β-sheet strands forming molecular zipper. **(B)** 17-amino-acid flanking sequence mediated aggregation pathway. The first 17 amino acids unfold in the presence of elongated polyQ tracts. Non-fibrillar oligomers are formed, with the N-terminal fragment in the core and the polyQ tracts exposed on the surface. With increasing polyQ tract, the structure decompacts and oligomers or protofibrils rearrange into amyloid-like structure, which rapidly propagate by monomer addition and producing aggregates. Adapted from [70].

The *in vitro* polymerization of polyQ-containing HTT exon-1 fragments can be accelerated by addition of preformed fibrils / aggregates, which can act as seeds for the polymerization and accelerate the transition into an insoluble state [68]. Even the accumulation of wild-type HTT exon-1 fragments in aggregates of mutant HTT was observed [72]. Besides HTT itself, it has been shown that proteins with Q-rich domains such as transcription factors like TBP (TATA-binding protein) and CBP (CREB-binding protein) are able to co-aggregate with HTT [73]. Also other proteins without a Q- or N-rich domain can be sequestered into HTT aggregates. For example, components of the ubiquitin-proteasome pathway and molecular chaperones co-aggregate with HTT [64].

Several studies revealed that N-terminal fragments of HTT are essential for the spontaneous formation of insoluble aggregates [9, 57]. Often, neuronal inclusions could only be detected with antibodies that bind to the N-terminus of HTT [9, 57, 74]. Cell-free and cell-based studies demonstrated that N-terminal fragments of HTT with expanded polyQ tracts effectively form aggregates, whereas neuroblastoma cells transfected with full-length huntingtin show a diffuse localization of the protein [55, 75]. Moreover, the inhibition of the production of N-terminal HTT fragments produced by proteolytic cleavage leads to a reduction in toxicity and aggregate formation [50]. The spontaneous aggregation of N-terminal HTT fragments is highly dependent on their length and the size of the polyQ repeat [76, 77]. Cell culture experiments exhibited an increasing toxicity with decreasing protein length and increasing polyQ size [77, 78]. These data suggest that the truncation of full-length HTT is a crucial step in the disease process and a prerequisite for the aggregation of the protein in patients and disease models.

The question whether the native protein, the misfolded protein, aggregation intermediates or mature aggregates are the toxic species in HD is still unanswered. An increasing body of evidence indicates that mutant HTT aggregates are toxic structures [9]. Several studies showed that large cytoplasmic inclusions as well as nuclear inclusions cause toxicity [9, 75, 78]. Also, the localization of the inclusions seems to play a role, since nuclear but not cytoplasmic inclusions lead to dramatic cell death in a cell culture and mouse model [79, 80]. In contrast, a recent study claimed that cytoplasmic aggregates cause the pathology [81]. The toxic behavior of aggregates has also been demonstrated in a number of cell types that take up and internalize HTT aggregates supplied by the medium [79, 82]. Moreover, a recent study by Jeon and colleagues exhibited the transmission of HTT aggregates from patient's fibroblasts as well as induced pluripotent stem cells to healthy tissue of neonatal mice [83]. After implantation into the cerebral ventricles, transmitted HTT aggregates increased motor and cognitive symptoms and loss of striatal medium spiny neurons. The transmission of mutant HTT aggregates from cell to cell was also exhibited by the integration of human stem cell-derived neurons into mouse organotypic brain slices and by investigating the localization of tagged HTT aggregates in a fly model of HD [84, 85].

In contrast, it has been demonstrated that the presence of HTT aggregates / inclusions does not

correlate with neuronal cell death in mouse model systems [86, 87]. Arrasate and colleagues demonstrated that the formation of inclusion bodies reduces the level of free diffusible mutant HTT in the cytoplasm resulting in decreased neuronal death [88]. Other studies showed that the formation of inclusion bodies is protective. The suppression of inclusion body formation in cells even increased death [89]. Also aggresomes, which are microtubule-dependent cytoplasmic inclusion bodies, have been shown to be cytoprotective in a cellular model of X-linked spinobulbar muscular atrophy and a yeast model of HD [90, 91]. Muchowski and others suggested that active transport processes along microtubules are required for inclusion body formation that might contribute to a decrease in toxicity in mammalian cells [92].

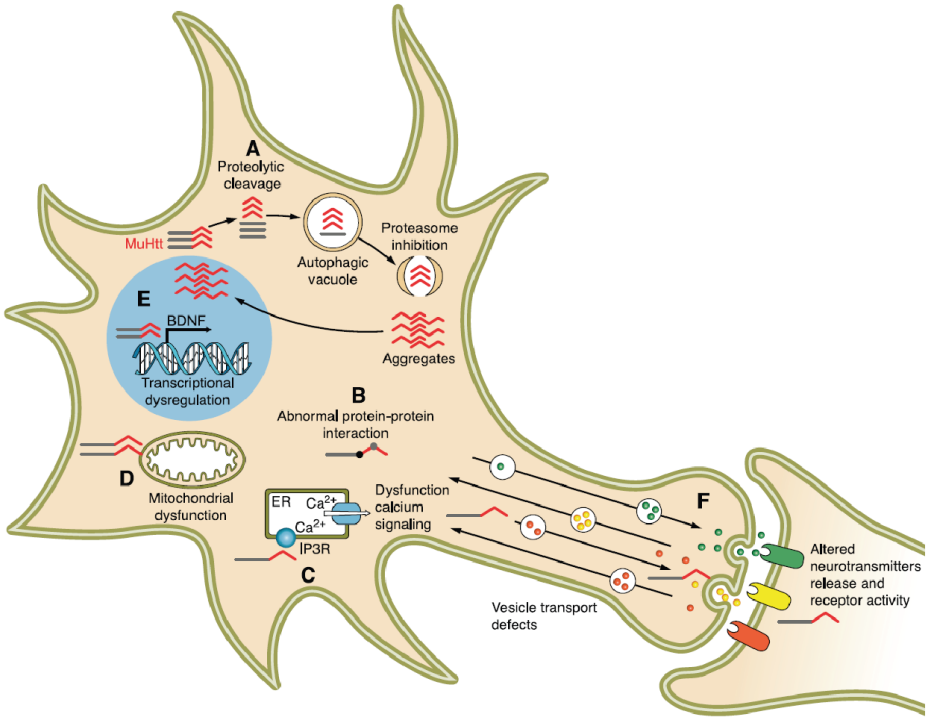

Figure 1.4: Potential pathogenic mechanisms in Huntington's disease.
(A) Full-length HTT is cleaved by several proteases. The generated fragments are ubiquitinated and targeted to the proteasome. **(B)** N-terminal HTT fragments accumulate and cause impairments in calcium signaling and homeostasis **(C)** and mitochondrial dysfunction **(D)**. Mutant HTT translocates to the nucleus and impairs gene transcription **(E)**. Also vesicular transport and recycling are altered by mHTT **(F)**. Adapted from [46].

Many cellular processes are dysregulated in HD (Fig. 1.4). The ubiquitin-proteasome system (UPS), which degrades ubiquitin-labeled proteins and plays a critical role in the clearance of misfolded proteins, found to be impaired [93]. It was shown that components of the proteasome such as subunits of the 26S proteasome and the molecular chaperones Hsp40 and Hsp70 co-

localize with HTT inclusions [94]. Reduced neuronal UPS activity may be responsible for the preferential accumulation of misfolded proteins in neurons [95]. N-terminal fragments of mutant HTT have been shown to translocate to the nucleus and cause transcriptional dysregulation [96]. One major pathway is the sequestration of transcription factors into HTT aggregates and the modulation of their transcriptional activity. The aberrant form of HTT results also in global cellular impairments such as mitochondrial dysfunction, defective energy imbalance, synaptic dysfunction and axonal transport impairment [37].

1.5 Modulation of mutant HTT aggregation by other proteins

In cells, misfolded proteins are refolded into the correct conformation by molecular chaperones or targeted for degradation by the proteasomal or lysosomal pathway [97]. Molecular chaperones provide the first line of defense against misfolded, aggregation-prone proteins [98]. Analysis of molecular chaperone levels in mice and flies exhibit a biphasic response in neurodegenerative diseases [99]. At first, the expression of chaperones shows an increase in the early stage of the disease caused by aggregate-induced cellular stress [100]. In the late stage, the levels decrease due to the sequestration into HTT aggregates [99]. Several chaperones have been identified that suppress protein aggregation in different HD and other polyQ disease models [101] - [106]. The Overexpression of both HSPA1A (Hsp70) and DnaJB1 (Hsp40), but not HSPA1A alone, prevents the formation of insoluble HTT inclusions in cells [101]. Another member of the DNAJ-chaperone family, DnaJB6, potently delays the aggregation of a 6.5 kb polyQ peptide by overexpression as well [102]. In yeast, Hsp70 and Hsp40 co-expression inhibits the formation of large and detergent-insoluble aggregates [103]. Another study demonstrated a suppression of polyQ mediated toxicity by co-expression of the human chaperones Hsp70 and Hsp40 chaperone (dHdj1) in a Drosophila model of Machado-Joseph disease (MJD) [104, 105]. Also, the chaperonin TRiC (TCP1-ring complex) inhibits HTT aggregation *in vitro* and *in vivo* [106]. The chaperonin binds to fibril tips and encapsulates small oligomers, which lead to an inhibition of large fibrillary structures *in vitro* [106]. Further modifiers of mutant HTT aggregation and toxicity such as CRMP1 were described to reduce toxicity and aggregation in transgenic HD flies by overexpression [107]. Another therapeutic strategy targeting the transcriptional dysregulation is the inhibition of histone deacetylases (HDAC). The HDAC inhibitor 4b ameliorates transcriptional abnormalities and the disease phenotype in HD mice [108]. In other studies, positive modulators of HTT aggregation were identified such as MOAG-4 that induces a conformational change in aggregation-prone proteins and promotes the aggregate formation process [109].
The clearance of mutant HTT is primarily mediated by the ubiquitin-proteasomal system and autophagy, whereby the UPS is more efficient to remove soluble N-terminal HTT fragments [110]. The degradation of aggregates is mainly promoted by macroautophagy [111] - [113]. Ravikumar

and colleagues found that overexpression of the early endosomal protein Rab5 attenuates toxicity in cell and fly models of HD by macroautophagy [114].

1.6 Therapeutic approaches against polyQ mediated toxicity

At the present time, no treatments can alter the course of Huntington's disease. Currently used pharmaceutics ameliorate the primary symptomatology, as for instance psychiatric drugs to control behavioral symptoms, motor sedatives and cognitive enhancers, to improve the quality of life [115]. Several potential therapeutic agents have been tested and have shown improvement of motor and cognitive dysfunction. Drugs against mitochondrial dysfunction or excitotoxicity such as tetrabenazine were analyzed. Tetrabenazine is a dopamine pathway inhibitor and reduces chorea in HD patients with side effects [116]. Other studies examined drugs that target caspase activities and the proteolysis of HTT by using caspase inhibitors [117]. Transcriptional dysregulation is an early event in the pathology of HD and is considered as a target for therapeutic intervention. Therefore, several HDAC inhibitors such as soidium butyrate and phenylbutyrate were already examined and showed a neuroprotective effect in a transgenic mouse model of HD [118, 119]. Another approach is to target aggregates or the aggregation process of HTT using anti-aggregation compounds such as Epigallocathechin gallate (EGCG) or drugs that increase the level of molecular chaperones [120]. Compounds may also induce degrading pathways, such as Sulforaphane that increases proteasome and autophagy activity in transgenic mice or small-molecule enhancers that enhance autophagy [121, 122].
A recently announced clinical trial "Huntingtin Lowering Trial" aims at reducing HTT levels in patient brains using an antisense oligonucleotide (ASO) [123]. The administration of the ASO drug IONIS-HTTRx that has entered phase I in 2015, specifically binds HTT RNAs and inhibits the production of the protein. The reduction of mutant HTT levels should slow the disease progression as has been shown in animal studies before [124, 125].

1.7 Animal model for studying the molecular mechanism in HD

After the identification of the *HTT* gene, a variety of genetic animal models that express a mutant HTT protein with an expanded polyQ tract were generated [126, 127]. The significance for these transgenic models is indisputable, since fundamental studies in humans are limited. Studies with animal models are relatively fast, allow expression of the transgene in specific tissues and provide the opportunity to interfere with disease progression using therapeutic molecules.
Rodents are the most commonly used animals for modelling HD [127]. The most frequently used rodents models are the R6/2, N171-82Q, BACHD and YAC128 mice that express various

HTT fragments or full-length HTT, respectively [56], [128] - [130]. These mouse models show a progressive HD phenotype with motor and cognitive impairments. Furthermore, large animal models such as transgenic HD rhesus monkeys, transgenic pigs and sheep that revealed a mild HD phenotype have been developed [131]. The large transgenic models show typical clinical features of HD and provide a powerful tool for preclinical experiments and long-term safety studies [132, 133]. In addition to rodent or large animal models, invertebrate models like *Caenorhabditis elegans* and *Drosophila melanogaster* HD models were also established and are often used for mechanistic investigations [72, 85], [134] - [137]. These model systems allow a fast analysis of potential disease underlying mechanisms and can also be applied for testing of therapeutic strategies [138] - [140].

The fruit fly *Drosophila melanogaster* offers many advantages like easy cultivation and handling, a development cycle as short as two weeks, simple genetics and well-established transgenesis technologies and experimental tools [141]. Flies are a multicellular organism and are more suitable to mimic human diseases compared to yeast or cell culture. The currently used Drosophila models of HD displayed in Table 1.2 were generated by P-element mutagenesis, which leads to random insertion of the transgene into the fly genome [142].

Table 1.2: Representative *Drosophila melanogaster* models of HD.
The stated phenotypes were observed in the highlighted (underlined) flies. Modified from [131, 143].

Model	Transgene product	Promotor	Phenotype	Ref.
HTTQ2, HTTQ75, HTTQ120	1-142 a.a. HTT	GMR	Degeneration of photoreceptor neurons	[144]
HTT.Q20.ex1p, HTT.Q93.ex1p	1-90 a.a. HTT	GMR, Elav	Loss of rhabdomers and reduced survival	[58]
HTT.128Q.1-336	1-336 a.a. HTT	GMR, Elav	Progressive deficit in climbing, reduced survival and neurodegenerative phenotype in eye	[145]
HTT.Q0, HTT.Q128	1-548 a.a. HTT	GMR, Elav	Abnormal motor behavior, reduced survival and photoreceptor degeneration	[146]
HTT.16Q.FL, HTT.128Q.FL	Full-length HTT	GMR, Elav	Progressive eye degeneration and climbing deficits and electrophysiological abnormalities	[147]

The HTT.128Q.FL flies show neuronal degeneration, impaired motor function and reduced lifespan with no detectable huntingtin aggregates [147]. In contrast, the truncated HTT.Q128 flies, which produce a 548 amino acid long HTT fragment, display a behavioral disease phenotype and cytoplasmic HTT aggregates in neuronal and non-neuronal tissue [146]. The expression of the HTTQ75 and HTTQ120 proteins in flies induces retinal degeneration and causes the formation of nuclear inclusions [144]. Likewise, flies carrying the labeled N-terminal fragment with the first 588 amino acids (RFP.Htt.138Q) exhibit the formation of HTT aggregates, which spread rapidly

from one region to another in the brain [85]. Experimental evidence that small N-terminal HTT fragments are critical for the formation of aggregates in flies was also shown by Pearce *et al.*. Finally, it was demonstrated that the expression of the exon1 fragment with 91 glutamine repeats in flies leads to the formation of aggregates that can converts the wild-type protein with 25 glutamines into an aggregated state [72].
Since the pathology of HD including the formation of nuclear inclusions, behavioral defects and progressive degeneration of neurons can be emulated in fruit fly, they are very valuable models for the identification of potential therapeutic compounds [139, 148]. Thus, drugs that are initially identified in cell-based assays as modulators of mutant HTT aggregation can next be validated in transgenic flies, which is fast and cost effective prior to their analysis in transgenic mouse models [149].

1.8 *Drosophila melanogaster*, a versatile model organism for studying disease mechanism

The common fruit fly, *Drosophila melanogaster*, has been used since the last century to study biological processes, including inheritance, embryonic development, learning, behavior and aging [150]. Despite the outward difference, fundamental biological mechanisms are conserved across evolution between the fruit fly and humans [140]. Approximately 77 % of the human genes associated with diseases are found in the fly genome [151]. The fly harbors ~14,000 genes on four chromosomes and exhibits a higher density of genes per chromosome compared to humans, which harbors 22,000 genes that are allocated on 23 chromosomes [150].

1.8.1 The life cycle of *Drosophila melanogaster*

The life cycle of fruit flies comprises of four stages, the egg, the larva, the pupa and the adult fly (Fig. 1.5) [150]. After fertilization, the embryos develop in the eggs for one day before the larva hatches. The larvae consume a lot of food when they growth through the first, second and third larva stage [150]. The *Drosophila* larva is characterized by the presence of giant polytene chromosomes in the salivary glands [152]. Giant polytene chromosomes are over-sized chromosomes, which develop from normal chromosomes that begin repeated rounds of DNA replication without cell division (endoreplication). The centromeric regions of the chromosomes do not endoreplicate with the result that the centromeres of all chromosomes bundle together in the chromocenter [152]. The polytene chromosomes allow high levels of gene expression and a fast larval growing. The third instar larva stage is followed by the pupal stage, which is characterized by dramatic reorganization during the metamorphosis into the adult fly. The developmental period of flies takes about twelve days at 25 °C. After the adult flies emerge from the pupae, it

takes eight – twelve hours until female flies become receptive to courtship. The average lifespan of wild-type fruit flies is ~50 days [153].

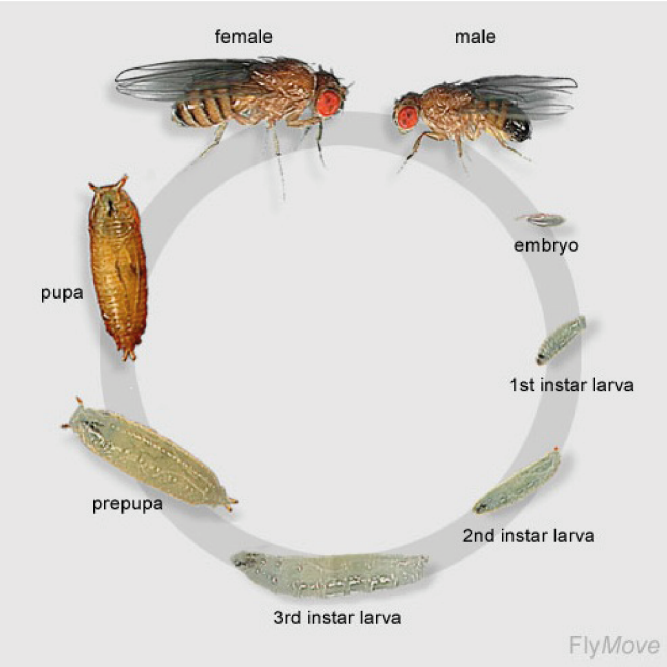

Figure 1.5: The *Drosophila* life cycle.
The development stages of a fertile egg to an adult fly over a ten day period at 25 °C. Following the hatching (eclosion), the larvae goes through three instars before reaching the pupation stage at which the metamorphosis to the adult fly takes place. Figure taken from [154].

1.8.2 *Drosophila* anatomy

The adult body of a Drosophila fly is divided into three main body parts, the head, the thorax and the abdomen [155]. The abdomen consists of five or six segments in male flies and seven or eight segments in female flies. The thorax is built up of three segments (prothorax, mesothorax and metathorax), the wings and the legs. The fly head consists of the brain and the compound eye, which is composed of approximately 800 ommatidia with eight photoreceptor cells each [156]. The major regions of the Drosophila brain are the optical lobes and central brain including the antennal lobes and the mushroom bodies (Fig. 1.6). The antennal lobes are the primary olfactory centers and consist of projection neurons and local interneurons. The projection neurons receive signals form the olfactory receptor neurons and pass the olfactory information to the lateral horn and the mushroom body neuron dendrites in the calyx. The mushroom bodies are prominent neu-

ropil structures in the fly brain that are arranged as pairs. The mushroom bodies can be divided in α, α', β, β' and γ lobes and are composed of Kenyon cells [157].

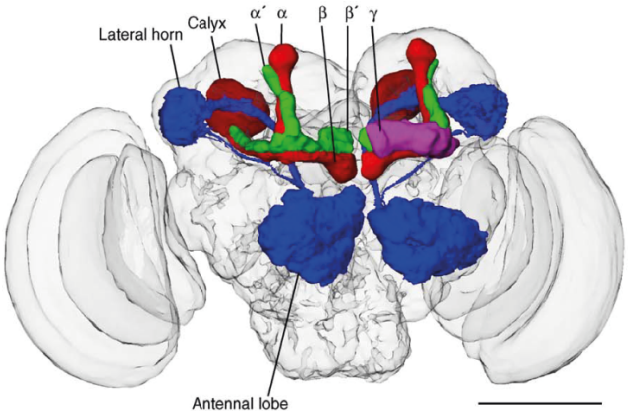

Figure 1.6: Detailed model of the fly brain and anatomy of the mushroom bodies.
Sown is a dorsal view of a fly head with the main parts of the olfactory pathway in the brain. The mushroom body comprises α, α', β, β' and γ lobes. Adapted from [158].

1.8.3 Transgenesis of *Drosophila melanogaster*

Transgenesis in *Drosophila melanogaster* has undergone some revolution in recent years. The first established tool and classical technique for mutagenesis in fruit flies was the P-element transposition system [159]. The system has been used to knock-out genes as well as to insert genes in the *Drosophila* genome [160]. P-elements are transposable elements found in the fly genome and encode the functional P transposase protein with flanking inverted terminal repeats to enable the cut-and-paste mechanism in the genome [161, 162]. After some modifications the transposase protein has been transferred to an additional vector, called helper-plasmid. A multiple cloning site and a visible marker gene were introduced between the inverted terminal repeats instead of the transposase. The multiple cloning site facilitates the insertion of the gene of interest [163]. The marker gene, which is used to identify the transformants, is commonly the *white* mini-gene [164]. A sex-linked mutation in the *white* gene causes a white-eye phenotype (w^{1118} strain). An insertion of the modified P-element leads to a colored eye phenotype induced by the mini-*white* gene in the *white* mutant background [164]. A drawback of this system is the random insertion of transgenes in the genome, because position effects can influence gene expression and impede a direct comparison of transgenic flies.
A suitable alternative method to P-element mutagenesis is the site-specific ΦC31 integration system [165, 166]. The ΦC31 integrase is a sequence-specific recombinase and is encoded in the

genome of the bacteriophage ΦC31. The ΦC31 integrase mediates a recombination between a bacterial attachment site (attB) in the expression vector and a phage attachment site (attP) in the fly genome as shown in Figure 1.7. In comparison to the P-element mutagenesis, a site-specific integration is mediated [167]. In recent years, a number of well-characterized and highly efficient landing sites throughout the four chromosomes of *Drosophila* have been developed [168, 169]. Additionally, the ΦC31 integrase was integrated in the fly genome to overcome the need of coinjecting the integrase [169]. Similar as the P-element mutagenesis, a plasmid containing the transgene, the mini-*white* gene and the attB site is injected into eggs of a *Drosophila* strain with a *white* mutation. The integration of the plasmid in the fly genome leads to colored eye phenotype, which can be easily monitored [165].

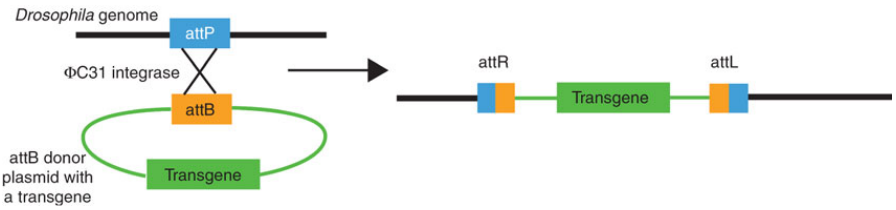

Figure 1.7: Principle of the ΦC31 integration system.
The ΦC31 integrase mediates the site-specific integration of the donor plasmid containing the attB site, the transgene and a mini-white gene into the attP site in the fly genome. Adapted from [170].

One challenge of the work with *Drosophila melanogaster* is that flies cannot be archived and mutant or transgenic flies have to be propagated continuously [171]. Moreover, genetic manipulations without a marker gene like deletions are difficult to track from generation to generation. Also mutations, which are lethal or sterile in a homozygote state, are successively abolished during strain maintenance of heterozygote flies. A solution is the usage of balancer chromosomes that stabilize chromosomes and carry at least one phenotypic marker gene [171, 172]. Balancer chromosomes contain multiple inverted sections to prevent homologous recombination between two chromosomes, called crossing over. These chromosomes contain a lethal recessive allele, which leads to lethality in a homozygote state. Therefore, the combination of a chromosome carrying a mutation or a transgene with a balancer chromosome leads to a stable fly line with no need for selection of transgenic flies in each generation. This arrangement is called the ”balanced system” [172]. It provides a predictable and verifiable tool for genetic crossings and therefore avoids the sequencing step required for mouse experiments.

1.8.4 Expression of transgenes in *Drosophila melanogaster*

The GAL4 / UAS expression system is a powerful tool for the constitutive expression of transgenes in transgenic flies [173] - [175]. The GAL4 protein, originally found in *Saccharomyces*

cerevisiae, regulates the transcription of genes by a defined binding site. This specific binding site, called Upstream Activating Sequences (UAS), is fused upstream to the target gene of interest (Fig. 1.8 A). The GAL4 gene is placed close to a promotor or enhancer that directs the expression in a cell- or tissue-specific manner. As a consequence, the tissue-specifically expressed GAL4 protein binds to the UAS sequence of the target gene and activates transcription of this gene in the same cells or tissues [176]. The man feature of this bipartite expression system is that the GAL4 gene and the UAS-target gene are separated in two different fly lines until expression is desired. The fly strain harboring the GAL4 protein expresses the transcription activator, but not the target gene. Flies containing the UAS-target gene, miss the transcription activator, hence the target gene is silent. Exclusively through the cross-breeding of these two fly strains both elements are combined in the progeny, which leads to the expression of the target gene. This bipartite system allows the strain maintenance of viable UAS lines for which tissue-specific expression is lethal. Furthermore, target genes can be analyzed in a wide range of tissues through the application of different GAL4 lines [176]. A drawback of this spatially controlled expression system is the lack of temporal control over the expression of the target gene.

Recently, several alternatives expression systems were generated, including the temporal and regional gene expression targeting (TARGET) system and the hormone-inducible chimeric GAL4 activator system, also termed the Gene-Switch system [178, 179].
The TARGET system is based on a temperature-sensitive GAL80 protein (Fig. 1.8 B). In yeast, the GAL80 protein represses the GAL4 protein in the absence of galactose. A temperature-sensitive mutant of GAL80 ($GAL80^{ts}$), found in yeast, regulates the repression of GAL4 in a temperature-dependent manner. At 19 °C the $GAL80^{ts}$ protein is in an active state and represses the activity of the GAL4 protein. At 29 °C or higher temperatures the $GAL80^{ts}$ is in an inactive state and the expression of the target gene through binding of the GAL4 protein to the UAS takes place. $GAL80^{ts}$ lines can be combined with existing GAL4 driver lines. The resulting system offers the combination of spatial and temporal control of the target gene expression through the conventional GAL4 / UAS system [177, 180].
In contrast, the Gene-Switch system is based on a modified GAL4 protein (Fig. 1.8 C). The DNA-binding domain of the GAL4 protein is fused to the p65 activation domain and a mutant progesterone receptor ligand binding domain, enabling a ligand-stimulated activation of the GAL4 protein complex [179]. The hormone ru-486 (ligand) is able to bind to the ligand binding domain of the progesterone receptor. In the absence of ru-486, the Gene-Switch protein complex is inactive. In the presence of the hormone, however, the GAL4 complex changes into an active conformation that can bind to the UAS sequence and stimulate the expression [173, 177]. The activation of the ru-486 mediated expression is carried out by feeding the hormone to flies. The expression can be turned off by transferring the flies on hormone-free food.

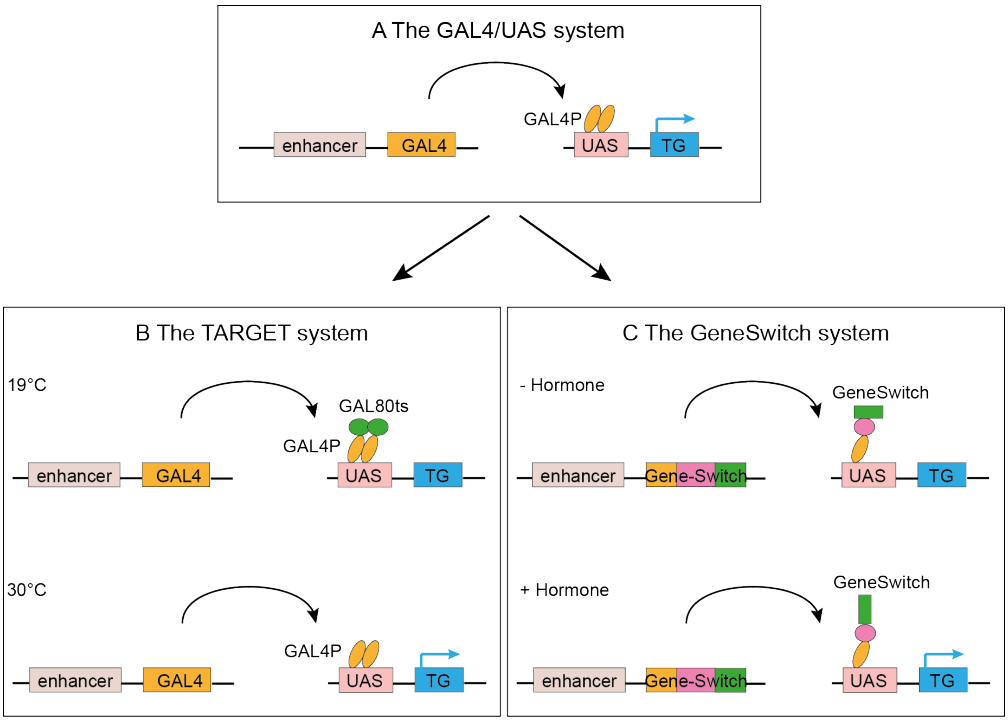

Figure 1.8: The GAL4 / UAS, TARGET and Gene-Switch system.
(A) The GAL4 / UAS expression system. The yeast transcription activator GAL4, driven by a specific enhancer or promoter, binds to the UAS sequence and activates the transcription of the target gene (TG) cloned downstream of the UAS. **(B)** The TARGET expression system. The GAL4 / UAS system is regulated by a temperature sensitive mutant of GAL80. At 19 °C the transcription is repressed. After a temperature shift to 30 °C the $GAL80^{ts}$ protein is inactive and the target gene is expressed. **(C)** The GeneSwitch expression system. In the absence of the hormone the system is in the "off" state. Addition of the hormone leads to a change to an active conformation that binds the UAS and activates expression of the target gene. Modified from [177].

1.9 Aim of this work

One aim of my study was the establishment of new *Drosophila* models for HD that should be produced by ΦC31-mediated integration in the fly genome to ensure direct comparability of different HD fly models. Flies containing HTT fragments with various amino acids in length, combined with non-pathogenic or pathogenic polyQ lengths should be generated. The newly generated flies should to be characterized using a combination of biochemical and behavioral approaches. Another aim was the development of an adult-onset *Drosophila* model of HD. To understand the underlying mechanisms of disease progression, HTT with a wild-type or a mutant polyQ tract should be inducible expressed in the nervous system of the adult fly. Subsequently, short-term and long-term induced flies shall be systematically analyzed. Additionally, the modulation of mutant HTT toxicity should to be analyzed in proof-of-principle experiments by co-expression

of a chaperone. This should provide the basis for the analysis of the effect of small compounds on the aggregation of mutant HTT and its toxicity in flies.

2 Results

2.1 Establishment of new *Drosophila* transgenic models of HD

Existing and commonly used *Drosophila* models of HD were produced by p-element-mediated integration, which leads to a random integration of the transgenes in the genome of *Drosophila melanogaster* [58, 147]. Position effects might influence the expression of different HTT fragments [181], suggesting that the generated fly lines cannot be compared directly. To overcome these limitations and to avoid chromosomal position effects, new transgenic models of HD were generated using the ΦC31-mediated insertion of different HTT transgenes at the same genomic insertion site.

Previous studies indicate that N-terminal HTT fragments play an important role in HD pathogenesis [50] - [52]. Several proteases have been identified which cleave the full-length HTT protein, resulting in the production of N-terminal HTT fragments of different [50, 53]. For instance, the caspase-3 produces a HTT fragment with 513 amino acids in length. In addition, the N-terminal HTT exon-1 fragment has been shown to be produced by aberrant splicing [59]. To investigate and compare the pathogenic effects of different HTT fragments, I generated transgenic fly lines, which harbor N-terminal HTT fragments of different sizes. The transgenic flies contain either HTT exon-1 fragment (HTTex1), HTT fragment with the first 513 amino acids (HTT513) or full-length HTT (HTTfl). The different HTT fragments were combined with different CAG repeats, including wild-type and mutant-associated repeats (Table 2.1). The corresponding proteins, which are produced by the transgenic flies, contain consequential different polyQ-lengths. To monitor the polyQ length-dependent effects of HTTex1 fragments, flies containing a non-pathogenic length of 17 CAG repeats (HTTex1Q17) and flies with expanded length of 49 (HTTex1Q49) and 97 CAG repeats (HTTex1Q97) were generated. Additionally, flies containing the HTT fragment without CAG repeats (HTTex1Q0) were created. Furthermore, flies were generated that harbor HTT513 fragments with a non-pathogenic length of 17 CAG repeats (HTT513Q17) and a pathogenic length of 68 (HTT513Q68) and 145 CAG repeats (HTT513Q145). In terms of full-length HTT, flies were produced which contain a wild-type length of 23 CAG repeats (HTTflQ23) and mutant lengths of 73 (HTTflQ73) and 145 CAG repeats (HTTflQ145).

2.1.1 Generation of expression plasmids containing different huntingtin fragments

In order to generate the above described transgenic flies, the required HTT cDNAs were constructed if they were not yet available in the plasmid library of the Wanker lab. The cDNA encoding the HTTexQ0 protein was amplified by polymerase chain reaction (PCR) from the fragment HTT336Q0, which was available in the library. The template (HTT336Q0) consists of codons that were optimized for expression in yeast. However, this modified DNA sequence does not affect the amino acid sequence so that it is still comparable to the other HTTex1 proteins. The inclusion of attB sites at the 5' and 3' ends, which are essential for gateway cloning, were added by amplification using the attB-HTT-ex1-fwd and attB-HTT-ex1-Stop1-rev primers. The HTTex1Q97 cDNA was produced by PCR using a template (HTTex1Q97-stop) without a stop codon. The primers attB-HTT-ex1-fwd and attB-HTT-ex1-Stop2-rev were used to introduce the stop codon. The attB-flanked PCR products were purified from an agarose gel and were shuttled into the gateway-compatible pDONR221 vector. The remaining HTT cDNAs did already exist as entry clones in the plasmid library. To assess whether the generated plasmids are correct, entry clones were examined by restriction digestion with the BsrGI restriction enzyme (data not shown).

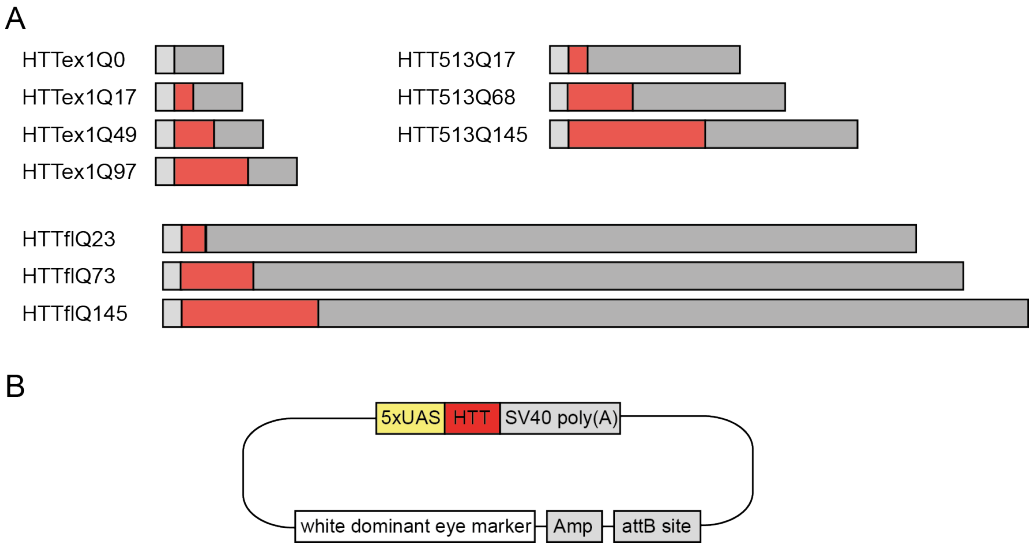

Figure 2.1: Generation of expression vectors (pUAST) containing different HTT cDNAs.
(A) Schematic representation of the different HTT fragments that are encoded by the generated expression plasmids. The light gray box represents the N-terminus, the red box the polyQ tract and the middle gray box represents the C-terminus of HTT. **(B)** A schematic representation of the pUAST-HTT-attB vector for ΦC31 mediates integration in the fly genome [169].

The different HTT cDNAs were transferred from the generated entry clones into the gateway-based destination vector pUAST-attB-rfA [169] (Fig. 2.1 A and B). This *Drosophila* specific destination vector contains an attB site downstream of the UAS-transgene for site-specific integration in the genome of the fly by ΦC31 integration [165, 166]. The vector also contains the eye-specific white$^+$ marker gene, which allows the selection of fly transformants [165]. The correct sequences of the HTT cDNA fragments and the size of the CAG repeats encoding glutamine tracts (Fig. 2.1) were confirmed by DNA sequencing. The obtained sequences are shown in Figure 7.1 - 7.5.

The generated destination vectors containing different HTT transgenes were sent to the company Rainbow Transgenic Flies for injection in *Drosophila melanogaster* embryos. The *Drosophila* strain y[1] M{vas-int.Dm}ZH-2A, M{3xP3-RFP.attP'}ZH-68E that includes a phage attachment site (attP) on the third chromosome (2A3, 68E) in the fly genome, which is complementary to the bacteriophage attachment site (attB) of the Gateway-based destination vectors was used. All destination vectors were integrated on the pre-selected site within the genome using the co-injected ΦC31 integrase. The offspring was selected for white$^+$ expression and was sent to our laboratory. The transgenic flies were crossed with the balancer strain $\frac{CyO}{Sp}$;$\frac{TM6,Tb,Hu}{MKRS,Sb}$ to generate stable HTT fly-lines (Table 2.1).
For a clear representation, flies were named after the transgenes they carry. For example, flies carrying the cDNA encoding the HTTflQ23 protein are called HTTflQ23 flies. The gene-drivers used will be introduced at the beginning of the corresponding chapter.

Table 2.1: Established transgenic fly models of Huntington's disease.

HTTex1Q0	HTT513Q17	HTTflQ23
HTTex1Q17	HTT513Q68	HTTflQ73
HTTex1Q49	HTT513Q145	HTTflQ145
HTTex1Q97		

2.2 Characterization of transgenic *Drosophila* models expressing the full-length HTT protein

2.2.1 Expression of full-length huntingtin in transgenic flies

In order to confirm the correct genetic identity of the newly generated *Drosophila* HD models, transgenic flies were genotyped using genomic DNA. The full-length transgenes were examined by amplification of the exon-1 fragment with the pUAST-fwd and HTT-ex1-rev-end primer, to display the appropriate size of the CAG repeats. The analysis in the agarose gel obtained expected PCR products with ~450 bp for HTTflQ23, ~600 bp for HTTflQ73 and ~800 bp for HTTflQ145 (Fig. 2.2 A).

To investigate whether HTT proteins are expressed in the full-length HD models, fly head lysates from flies that were obtained from cross-breeding with Elav-GAL4 flies were examined by SDS-Page and Western blotting. Elav-GAL4 driven pan-neuronal expression of the transgenes leads to HTT protein synthesis in neurons at all developmental stages [182]. The C-terminal HTT-specific antibody MAB2166, which binds to amino acid 181 – 810, was used to detect the full-length HTT proteins. The full-length HTT proteins display protein bands that have a molecular weight above 250 kDa (Fig. 2.2 B), suggesting that the full-length HTT proteins are expressed in transgenic flies. Since no high molecular weight marker was used, the real molecular weight could not be confirmed.

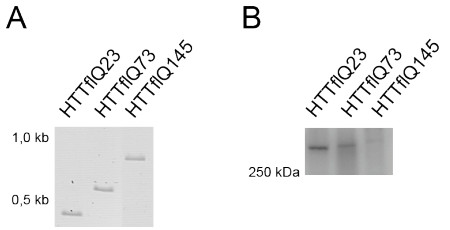

Figure 2.2: Analysis of the CAG repeat sequence size in transgenes and of the protein expression in HD transgenic flies.
(A) PCR analysis of flies containing the full-length transgenes using the ex1 primer pair. The expected PCR products of 433 bp (HTTflQ23), 583 bp (HTTflQ73) and 799 bp (HTTflQ145) were obtained. **(B)** Western blot analysis of the full-length HTT proteins produced in HD transgenic flies using the C-terminal HTT-specific MAB2166 antibody.

2.2.2 Behavioral analysis of the full-length models

In order to investigate whether the expression of HTT proteins with pathogenic polyQ lengths influences locomotion and circadian rhythm, male flies expressing the full-length proteins HTTflQ23, HTTflQ73 and HTTflQ145 were analyzed using the *Drosophila* Activity Monitor (DAM) System [183]. The DAM harbors 32 glass tubes with an individual male fly in each tube. The locomotor activities of flies were measured over 30 days every five minutes by counting the beam breaks of three infrared light beams that are distributed over the glass tube. Flies containing the UAS-transgenes were crossed with Elav-GAL4 flies to receive Elav;HTT flies that express the transgenes pan-neuronal.

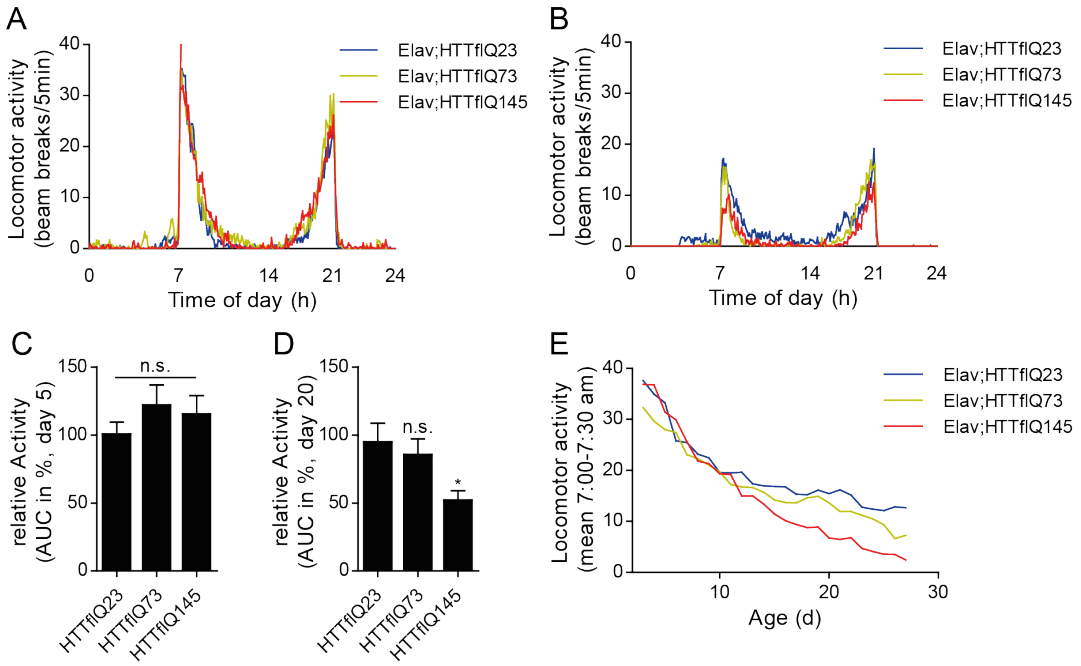

Figure 2.3: Effects of pan-neuronal expression of HTTflQ23, HTTflQ73 or HTTflQ145 on circadian locomotor behavior in *Drosophila melanogaster*.
(A) Average locomotor activity of five days old male flies (HTTflQ23 n = 18; HTTflQ73 n = 16; HTTflQ145 n = 18) under 12:12 light-dark cycle (light switching-on 7 am, light switching-off 7 pm). The full-length transgenes were expressed pan-neuronal using the Elav-GAL4 gene driver. **(B)** Average locomotor activity of 20 days old male flies. **(C)** Quantification of average locomotor activity of five days old flies. Relative activity is displayed as area under the curve normalized to HTTflQ23 flies. Error bars represent mean ± SEM; one-way ANOVA Dunnett's post hoc test compared to HTTflQ23 flies; n.s. means not statistically significant. **(D)** Quantification of average locomotor activity of 20 days old flies. Error bars represent mean ± SEM; one-way ANOVA Dunnett's post hoc test compared to HTTflQ23; * p <0.05. **(E)** Mean daybreak activity peak calculated by the mean of beam breaks between 7:00 and 7:30 am for each day.

All full-length HTT expressing flies showed normal crepuscular behavior with a clear activity peak at daybreak at 7 am and during the twilight activity period at 9 pm (Fig. 2.3 A). The relative activity, calculated from the area under the curve, showed no significant difference in young five days old flies expressing the HTTflQ23, HTTflQ73 and HTTflQ145 proteins (Fig. 2.3 C). In comparison, in 20 days old flies the expression of the HTTflQ145 protein led to a significant reduction in locomotion activity compared to HTTflQ23 flies (Fig. 2.3 B and D). The relative activity of HTTflQ73 flies is slightly reduced, but shows no significant difference to HTTflQ23 flies (Fig. 2.3 D). In addition, the morning activity quantified by the mean of the daybreak activity monitored over time exhibit similar results (Fig. 2.3 E). Flies expressing HTTflQ23 showed the highest activity performance, followed by HTTflQ73 flies. Young HTTflQ145 flies have a similar daybreak activity as HTTflQ23 control flies (during the first 15 days). With increasing age, however, the HTTflQ145 flies exhibit a decreased locomotor activity, which is reduced to half (Fig. 2.3 D) compared to HTTflQ23 and HTTflQ73 flies.

To evaluate whether the expression of pathogenic full-length HTT also affects the longevity of transgenic flies, life span analysis [153] was performed with flies expressing HTTflQ23, HTTflQ73 or HTTflQ145 pan-neuronal. Flies, which were raised from cross-breeding of Elav-GAL4 and w^{1118} flies, were used as a negative control group. For life span analysis, ten flies per vial and a total number of 200 flies were kept on standard food, the survivors were transferred every two – three days to fresh food and dead flies were recorded.

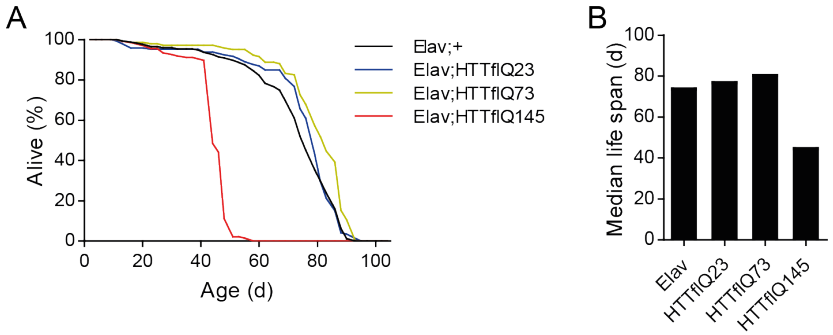

Figure 2.4: Pan-neuronal expression of HTTflQ145 reduces *Drosophila* life span.
(A) Life span analysis of HTTflQ23, HTTflQ73 and HTTflQ145 flies, plotted as the percentage of surviving flies of one replicate (Elav n = 175, HTTflQ23 n = 146; HTTflQ73 n = 143; HTTflQ145 n = 114). The gene-driver control Elav indicated in black arises from cross-breeding of Elav-GAL4 and w^{1118} flies. **(B)** Median life span displays the time when 50 % of the flies died.

Based on the survival curves the median life span was calculated, representing the age at which half of the analyzed flies have died. Flies of the gene-driver control Elav;+ displayed a median

survival of 78 days (Fig. 2.4 A and B). HTTflQ23 flies showed a median of 77 days and HTTflQ73 of 81 days. Strikingly, flies with pan-neuronal expression of HTTflQ145 displayed a much shorter median life span of 45 days. In summary, the expression of HTTflQ145 caused a dramatic reduction in life span compared to flies expressing the proteins HTTflQ23 and HTTflQ73. Flies expressing HTTflQ23 or HTTflQ73 cannot be clearly distinguished from flies that do not express a transgene (Elav;+). This result is consistent with previous findings, which showed that expression of pathogenic full-length huntingtin ($128Qhtt^{FL}$) leads to a reduced survival [88]. In conclusion, the pan-neuronal expression of pathogenic full-length HTT with 145 glutamines causes an impaired activity phenotype and reduces the life span of flies, while such an effect was not observed when full-length HTT proteins with 73 or 23 glutamines were expressed in flies.

2.2.3 Full-length HTT have no influence on retinal structure

In order to analyze the effects of HTT expression on the cellular level, the proteins HTTflQ23, HTTflQ73 and HTTflQ145 were expressed in flies using an eye-specific gene-driver and finally retinal tissues in young three days old flies were systematically analyzed. For this purpose, flies carrying the UAS-transgenes were crossed with GMR-GAL4 flies to reach a high-level of expression in the eye-imaginal disc posterior of the morphogenetic furrow [184]. The retinas of flies expressing HTTflQ23, HTTflQ73 and HTTflQ145 displayed no difference in the retinal structure compared to the GMR control flies (cross-breeding of GMR-GAL4 and w^{1118} flies). This indicates that the expression of HTTflQ145 in young flies does not induce significant retinal defects.

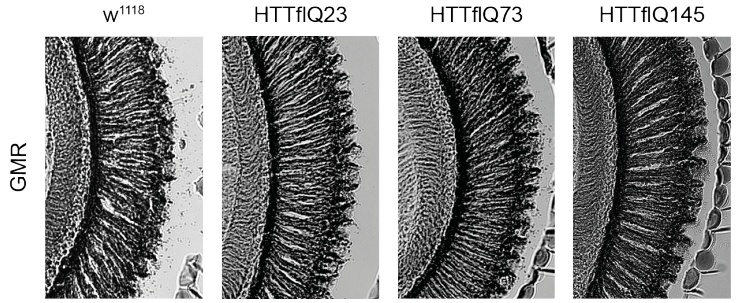

Figure 2.5: Mutant full-length HTT expression in young flies does not induce photoreceptor degeneration.
Shown are representative horizontal retina paraffin-sections from three days old female flies expressing HTTflQ23, HTTflQ73 or HTTflQ145 by the eye-specific GMR gene-driver. The GMR control arises from cross-breeding of GMR and w^{1118} flies. For each genotype at least 20 heads were analyzed and a representative retina is shown.

2.3 Analysis of transgenic *Drosophila* models expressing N-terminal HTT513 fragments

In order to confirm the genetic identity of the HTT513 fly lines (Table 2.1), PCR analysis was performed using the pUAST primer pair, which enables the amplification of the inserted cDNA. The analysis in the agarose gel revealed the expected size for the HTT513Q17 fragment with ~1.8 kb, for the HTT513Q68 fragment with ~1.9 kb and for the HTT513Q145 fragment with ~2.1 kb (Fig. 2.6 A). The expression of HTT513Q68 results in a ~80 kDa protein (Fig. 2.6 B), which is comparable to the molecular weight of a HTT513Q72 protein (80 kDa) produced in a transgenic YAC73 mice. The HTT513Q17 and HTT513Q145 proteins appear according their specific polyQ length (Fig. 2.6 B). The HTT513Q68 and HTT513Q145 fragments were not investigated further. Exclusively flies expressing the HTT513Q17 fragment were further used in control experiments, when HTT exon-1 proteins with short and long polyQ sequences were investigated in depth (see below).

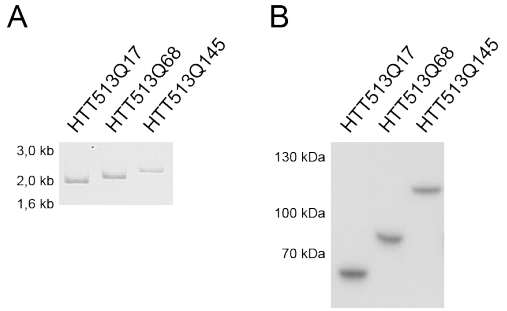

Figure 2.6: PCR and Western blot analysis of the HTT513 transgenes.
(A) PCR analysis of flies containing human cDNAs expressing HTT fragments with 513 amino acids using the pUAST primer pair. The expected PCR products of 1786 bp (HTT513Q17), 1939 bp (HTT513Q68) and 2170 bp (HTT513Q145) were obtained. **(B)** Western blot analysis of the HTT513 proteins produced in HD transgenic flies using the C-terminal specific MAB2166 antibody.

2.4 Characterization of transgenic *Drosophila* models expressing HTT exon-1 fragments with pathogenic and non-pathogenic polyQ lengths

2.4.1 Verification of HTT exon-1 models

The transgenic flies expressing the exon-1 HTT fragments were genotyped by PCR analysis of genomic DNA using the pUAST primer pair. PCR products of the exon-1 fragments appear in accordance to their specific size in the agarose gel (Fig. 2.7 A). In detail, the PCR amplification obtained expected PCR products with ~500 bp for HTTex1Q0, ~550 bp for HTTex1Q17, ~600 bp for HTTex1Q49 and ~750 bp for HTTex1Q97.

To confirm the expression of the exon-1 proteins, the fragments were expressed pan-neuronal and fly heads were collected. First, I tested various anti-HTT antibodies (including MW1, MW8, MAB1574, MAB5473, 3B5H10, MAB5492, anti-CAG, HD1 and anti-Agg53; data not shown) to select a suitable antibody that can detect the different HTT exon-1 proteins in brain extracts. Interestingly, I found that only the 2B7 antibody is suitable to detect the HTT513Q17 protein in fly brain lysates (Fig. 2.6 B). Then, with this antibody, fly head lysates of HTTex1Q0, HTTex1Q17, HTTex1Q49 and HTTex1Q97 flies were examined by Western blotting. For the analysis, 7.5 μg fly head lysate from HTT513Q17 flies and respectively 75 μg fly head lysate from HTTex1Q0, HTTex1Q17, HTTex1Q49 and HTTex1Q97 flies were loaded into a SDS-Page. Beside the HTT513Q17 protein, no protein bands for HTTex1Q0, HTTex1Q17, HTTex1Q49 or HTTex1Q97 were detectable (Fig. 2.7 B). The HTTex1Q97 sample showed a smear near the gel pockets, which indicates the formation of insoluble high molecular weight HTT protein aggregates in flies expressing the pathogenic HTT fragment. As soluble HTT exon-1 proteins were not detectable by the Western blotting (Fig. 2.7 B), the transcription of the exon-1 transgenes were evaluated. Total RNA was extracted from *Drosophila* heads, to perform cDNA synthesis and subsequent RT-PCR analysis. The data from the RT-PCR analysis indicates that the HTTex1Q0, HTTex1Q17, HTTex1Q49 and HTTex1Q97 fragments are transcribed in the fly brain (Fig. 2.7 C).

These results suggest that soluble HTT exon-1 proteins (HTTex1Q0, HTTex1Q17, HTTex1Q49 and HTTex1Q97) are indeed produced in the different HD fly lines. However, their abundance in brain lysates is too low in order to be detected on immunoblots with the 2B7 antibody. Interestingly, I found that high molecular weight HTTex1Q97 aggregates are detectable in fly extracts with the 2B7 antibody, indicating that HTT aggregates, which are less efficiently degraded than soluble, can accumulate in HD fly brains.

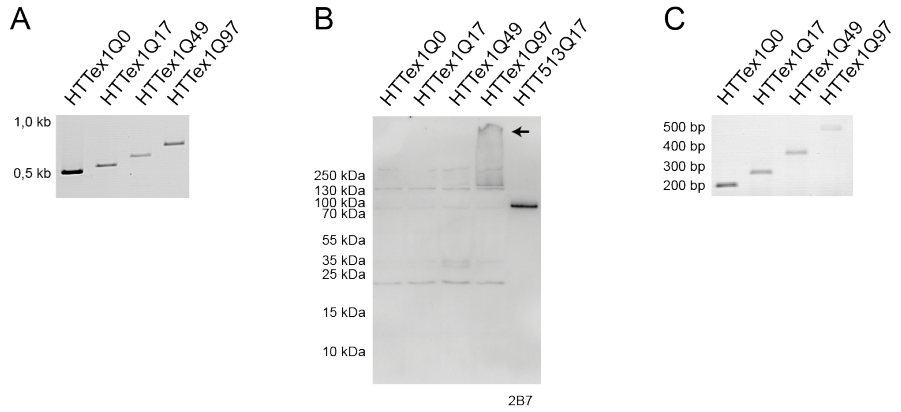

Figure 2.7: Analysis of the CAG repeat sequence size and of the protein expression in transgenic HTTex1 flies.
(A) PCR analysis of flies containing HTT exon-1 cDNAs using the pUAST primer pair. The expected PCR products of 475 bp (HTTex1Q0), 526 bp (HTTex1Q17), 619 bp (HTTex1Q49) and 766 bp (HTTex1Q97) were obtained. **(B)** Western blot analysis of transgenic flies expressing the HTT513Q17 protein and the different exon-1 proteins. 75 μg total protein of the head lysates from the various HTTex1 fly lines was loaded onto a polyacrylamide gel. From the HTT513Q17 head lysate, only 7.5 μg of total protein was applied. The membrane was probed with the 2B7 antibody. The arrow indicates high molecular weight HTT aggregates. **(C)** RT-PCR analysis of HTT exon-1 transcripts, which were extracted from fly heads and analyzed using the HTT-ex1 primer pair. The fragments with expected sizes of 204 bp (HTTex1Q0), 255 bp (HTTex1Q17), 348 bp (HTTex1Q49) and 495 bp (HTTex1Q97) were amplified.

2.4.2 Phenotypic analysis of the HTT exon-1 *Drosophila* models

With the intention to investigate the phenotypic effects of pan-neuronal expressed HTTex1 fragments (HTTex1Q0, HTTex1Q17, HTTex1Q49 and HTTex1Q97) in the *Drosophila* models, I first studied the circadian locomotor behavior and movement of transgenic flies using the *Drosophila* Activity Monitors. All transgenic HTTex1 flies display a normal crepuscular behavior with distinct activity peaks at daybreak and twilight periods (Fig. 2.8 A). However, HTTex1Q97 expressing flies compared to HTTex1Q0, HTTex1Q17 and HTTex1Q49 flies showed an overall reduced activity (Fig. 2.8 A and B).
To resolve this observation, the daybreak activity between 7:00 and 7:30 am was analyzed over a period of 35 days (Fig. 2.8 C). HTTex1Q97 expressing flies compared to HTTex1Q0, HTTex1Q17 and HTTex1Q97 showed a significantly reduced locomotor activity directly after hatching, supporting the initial result (Fig. 2.8 A). The activity of HTTex1Q97 flies decreased over time until the flies showed no activity anymore at an age of 20 days (Fig. 2.8 C). The relative activity of HTTex1Q0, HTTex1Q17 and HTTex1Q49 flies was very similar, indicating that these proteins have no influence on the fly behavior.

Next, the locomotor abilities of flies expressing the HTT exon-1 fragments were analyzed using

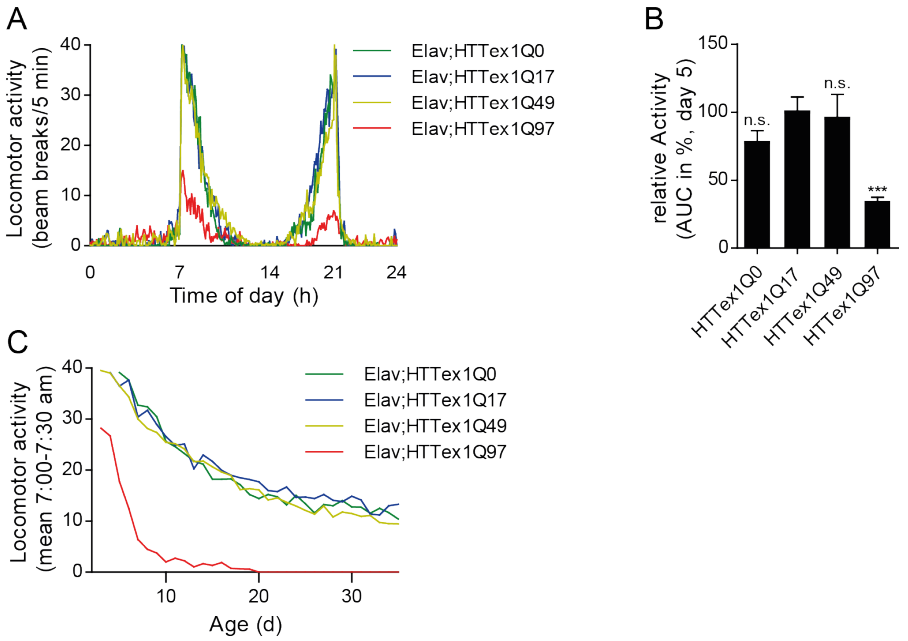

Figure 2.8: Effect of pan-neuronal expression of HTTex1Q0, HTTex1Q17, HTTex1Q49 or HTTex1Q97 on *Drosophila* circadian locomotor behavior.
(A) Average locomotor activity of 5 days old male flies (HTTex1Q0 n = 14; HTTex1Q17 n = 15; HTTex1Q49 n = 15; HTTex1Q97 n = 14) under 12:12 light-dark cycle (light switching-on 7 am, light switching-off 7 pm). The HTT exon-1 transgenes were expressed pan-neuronal using the Elav-GAL4 gene driver. **(B)** Quantification of average locomotor activity of 5 days old flies. Relative activity is displayed as area under the curve normalized to HTTex1Q17. Error bars represent mean ± SEM; one-way ANOVA Dunnett's post hoc test compared to HTTex1Q17; n.s. means not statistically significant; *** p <0.001. **(C)** The daybreak activity calculated by the mean of beam breaks between 7:00 and 7:30 am for each day.

the negative geotaxis (climbing) assay [185]. With this assay, the percentage of flies is recorded that climbs above the 8 cm mark within 15 seconds after trapping the flies to the bottom of the measuring vial. The Elav,+ flies, which have been used as a control group show a progressive decline in climbing abilities during the measurement period. It was demonstrated previously that this decline in locomotor activity is age-related and a normal behavior of wild-type flies [186]. The wild-type HTT flies expressing the HTTex1Q17 protein performed comparable to the Elav;+ control flies (Fig. 2.9 A). HTTex1Q0 flies showed a slight but no significant decrease in climbing abilities compared to the wild-type HTTex1Q17 and the control flies. The locomotor performance of HTTex1Q49 flies was comparable to the performance of the HTTex1Q17 flies during the first 25 days. However, after 30 days the locomotor activity of HTTex1Q49 flies was significantly decreased compared to HTTex1Q17 flies. The most severely impaired climbing performance was observed with flies expressing the HTTex1Q97 protein. After the first measurement at day three a very rapid decline of climbing abilities was observed and finally HTTex1Q97

expressing flies were incapable of climbing at an age of 25 days. In summary, the generated mHTT exon-1 *Drosophila* models exhibit strong locomotor impairments that exacerbate in a polyQ-length dependent manner.

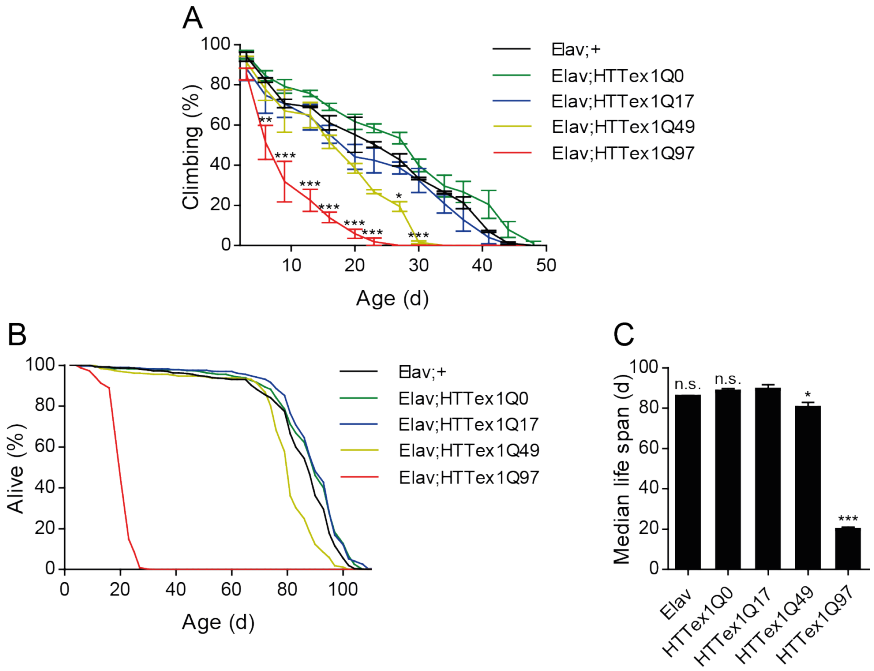

Figure 2.9: Pan-neuronal expression of HTT exon-1 proteins in transgenic flies causes a polyQ-length dependent impairment of climbing and survival.
(A) Climbing abilities of HTT exon-1 fly lines depicted as average of three independent experimental replicates. For one replicate 100 flies were analyzed per genotype. Error bars represent mean ± SEM; two-way ANOVA; * p <0.05; ** p <0.01; *** p <0.001. **(B)** Life span analysis of flies expressing the exon-1 transgenes plotted as the percentage of surviving flies of three independent replicates (Elav n = 143, 94, 85; HTTex1Q0 n = 160, 91, 87; HTTex1Q17 n = 163, 89, 86; HTTex1Q49 n = 148, 85, 85; HTTex1Q97 n = 141, 95, 99). **(C)** Median life span displays the time when 50 % of the flies survived. Error bars represent mean ± SEM from three independent replicates; one-way ANOVA Dunnett's post hoc test compared to HTTex1Q17; n.s. means not statistically significant.

Previously generated *Drosophila* models that were produced by p-element mutagenesis and that express a pathogenic HTT exon-1 fragment showed a significantly reduced longevity [187]. To confirm this phenotype in our HTT exon-1 *Drosophila* models, life span assays were performed. Ten flies per vial and a total number of 100 flies were recorded. Pan-neuronal expression of HTTex1Q0 and HTTex1Q17 caused no difference in survival compared to Elav;+ control flies (Fig. 2.9 B). These fly lines show a median life span of 85 – 90 days (Fig. 2.9 C). In contrast, the expression of the pathogenic HTTex1Q49 protein caused a significant reduction of the life span

and even more severe phenotype was obtained when HTTex1Q97 expressing flies were analyzed. HTTex1Q97 expressing flies showed a median survival of 20 days.

To examine potential effects of mutant HTT expression on sensory and olfactory processing, Elav;HTTex1Q97 flies were finally analyzed in a T-maze. The T-maze is a teaching machine developed by Tully and Quinn [188] and is used to measure Pavlovian learning and memory in flies [189]. In this assay, flies have the choice between a favorable (empty vial) and an unfavorable (electric shock / limonene) situation. The avoidance of the unfavorable situation is measured by a performance index (PI) calculated as the fraction of flies that avoid the situation minus the fraction of flies that do not. The control flies (+;HTTex1Q97: obtained from cross-breeding of w^{1118} with UAS-HTTex1Q97 flies; and Elav;+ flies) display the genetic background of the transgenic Elav;HTTex1Q97 flies without expression of the transgene. Both fly lines show normal avoidance of 200 V electric shocks (Fig. 2.10 A). However, a significantly reduced shock avoidance was observed with Elav;HTTex1Q97 flies.

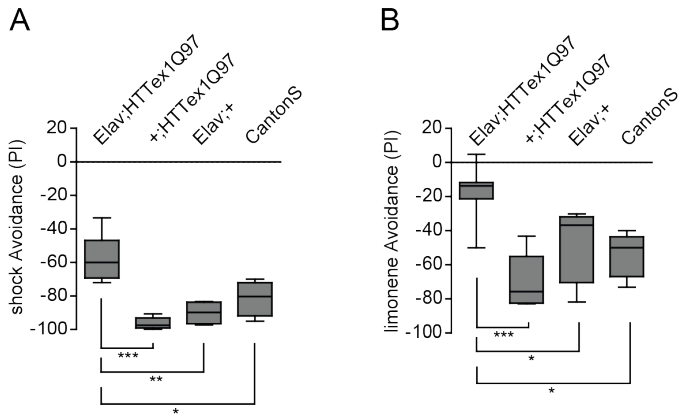

Figure 2.10: Electric shock and odor avoidance of Elav;HTTex1Q97 flies.
(A) Electric shock avoidance of three days old flies expressing HTTex1Q97 (Elav;HTTex1Q97) panneuronal and genetic controls (Elav;HTTex1Q97 n = 5; HTTex1Q97 n = 5; Elav;+ n = 4; CantonS n = 4) was measured in a T-maze. Box-whisker plots show performance index, negative values indicate shock avoidance; one-way ANOVA Dunnett's post hoc test compared to Elav;HTTex1Q97; * p <0.05; ** p <0.01; *** p <0.001. **(B)** Limonene avoidance of three days old Elav;HTTex1Q97 flies and genetic controls (Elav;HTTex1Q97 n = 6; +;HTTex1Q97 n = 6; Elav;+ n = 6; CantonS n = 5).

A similar result was obtained when the avoidance of the odor limonene was assessed (Fig. 2.10 B). Two genetic controls and CantonS wild-type flies show normal avoidance behavior towards limonene, whereas Elav;HTTex1Q97 flies do not avoid the presented odor. Together, these results suggest an impairment of sensory pathways of HTTex1Q97 expressing flies, which are responsible for transmission and processing of odor and pain stimuli.

2.4.3 Mutant HTTex1 protein disrupts retina structure in transgenic HD flies

To investigate the potential degeneration at the cellular level, the effects of the expression of the exon-1 fragments in retinal tissue in young three days old flies was analyzed. The expression of the mutant exon-1 fragment HTTex1Q97 causes a neurodegenerative eye phenotype evident in the retinal histology (Fig. 2.11). Retinal sections prepared from flies expressing the HTTex1Q97 protein exhibited a reduction and loss of photoreceptor cells and the formation of holes indicated with yellow arrows. Furthermore, the photoreceptor cells partially detached from the retinal floor indicated with red arrows. In comparison, expression of the proteins HTTex1Q0, HTTexQ17 and HTTexQ49 showed no disruption of photoreceptor cells. A similar result was also obtained when GMR control flies (cross-breeding of GMR-GAL4 and w^{1118} flies) were analyzed.

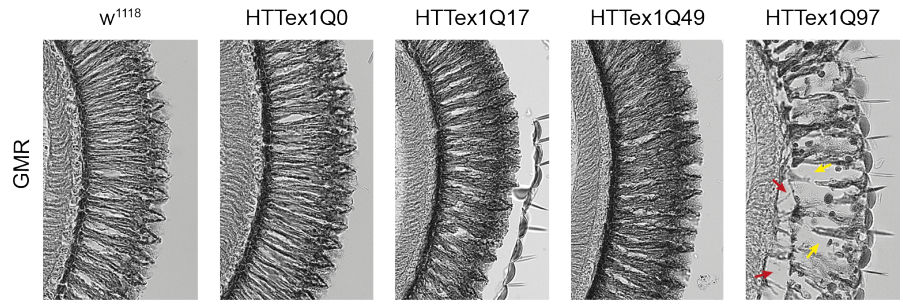

Figure 2.11: Expression of mutant HTTex1Q97 protein causes damaged photoreceptor cells in *Drosophila*.
Shown are representative horizontal retina paraffin-sections from three days old female flies expressing HTTex1Q0, HTTex1Q17, HTTex1Q49 or HTTex1Q97 by the eye-specific GMR gene-driver. Flies containing the GMR gene driver were crossed with flies containing the different HTT exon-1 transgenes and with w^{1118} flies as a negative control. For each genotype at least 20 heads were analyzed and a representative retina is shown. Yellow arrows indicate loss of retinal integrity and red arrows show detachment of retinal floor and photoreceptor cells.

2.4.4 Detection of HTTex1Q97 aggregates in *Drosophila* salivary glands

Western blot analysis of HTT exon-1 proteins using the 2B7 antibody showed the presence of higher molecular weight HTT aggregates in flies expressing the HTTex1Q97 protein. To examine whether HTT aggregates are formed in HTTex1Q97 flies, an immunofluorescence staining of salivary glands from wandering third-instar larvae was performed with several HTT aggregate-specific antibodies. Salivary glands contain giant polytene chromosomes that harbor multiple copies allowing high level of expression. Due to the high expression level, the formation of HTT aggregates is expected. In addition, salivary glands can be easily dissected. For systematic analysis, the antibodies MAB5492, MW8, MAB5374, anti-Agg53, HD1 and 3B5H10 were applied (Fig. 2.12). The MAB5492 antibody is specific for amino acids 1 – 82 in HTT, while MW8 binds the C-terminus of exon-1 [190, 191]. The MAB5374 antibody was raised against the first 250 amino acids of the human HTT [192]. The antibodies anti-Agg53 and HD1 have a high preference for HTT in its aggregates state and were produced in our group by former colleagues. The 3B5H10 antibody is specific for soluble mutant HTT and preferentially detects monomeric protein [193].

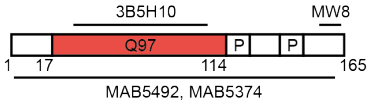

Figure 2.12: Schematic representation of antibody epitopes within the pathogenic HTT exon-1 protein.

HTT proteins were expressed using the salivary gland-specific gene driver 14-3fkh-GAL4 [194]. HTT staining was not detectable in HTTex1Q0, HTTex1Q17 or HTTex1Q49 expressing flies, but was observed in HTTex1Q97 flies in form of distinct puncta using the antibodies MAB54892, MW8, MAB5374, anti-Agg53 and HD1 with a preference for HTT aggregates (Fig. 2.13 A). The antibody 3B5H10, which preferentially recognizes monomeric HTT fragments exhibited no signal. Thus, HTTex1Q97 aggregates are located in the cytoplasm and the nucleus of salivary gland cells. Whereby, the HTT aggregates in cytoplasm display a peripheral staining pattern. The reason for this staining pattern may be due to the dense organization of the aggregates, which potentially masks epitopes for antibody binding in the center of inclusion bodies with HTT aggregates. The expression of HTTex1Q0, HTTex1Q17 and HTTex1Q49 does not lead to the formation of HTT aggregates. The negative control (w^{1118} / HTTex1Q97) flies also show no aggregate-specific antibody signal. To examine whether aggregate formation is HTT-specific, the fluorescent protein GFP was expressed under the same conditions (Fig. 2.13 B). A diffuse and ubiquitous GFP staining was observed in cells, indicating that HTT aggregates are only formed when an exon-1 fragment with an elongated polyQ tract is expressed.

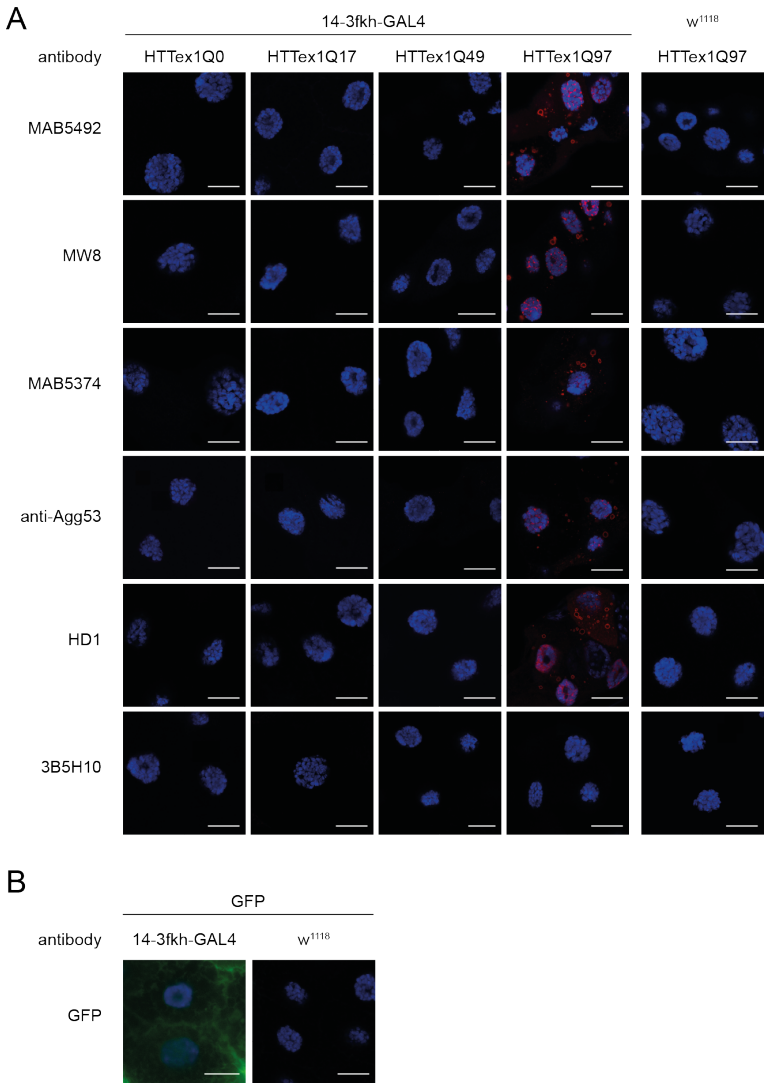

Figure 2.13: Expression of HTTex1Q97 causes the formation of aggregates in salivary glands.
(A) Immunostaining of salivary glands from third-instar larvae dissected from flies that were obtained from cross-breeding between 14-3fkh-GAL4 or w^{1118} flies and flies containing HTTex1Q0, HTTex1Q17, HTTex1Q49 or HTTex1Q97 using the antibodies MAB5492, MW8, MAB5374, anti-Agg53, HD1 and 3B5H10. HTT-specific antibody signals are indicated in red and DAPI signal in blue. Scale bars: 20 μm. **(B)** Immunostaining of salivary glands dissected from flies that evolved from cross-breeding between 14-3fkh-GAL4 or w^{1118} flies and flies expressing GFP. A GFP-specific antibody was used. GFP signal is indicated in green and DAPI signal in blue. Scale bars: 20 μm.

2.4.5 The pathogenic HTTex1Q97 protein forms SDS-stable aggregates in *Drosophila* brains

In order to examine whether aggregated HTT protein can be detect in *Drosophila* brains they were systematically analyzed with dot blot (DB) assays, filter retardation assays (FRAs) and immunohistological methods. With DB assays, protein contained in the fly head lysates are detected after filtration on nitrocellulose membranes independent of their size using specific antibodies [195]. The preparation of the lysates takes place under native conditions (tris-lysis buffer), allowing the detection of native proteins that are retained on nitrocellulose membranes. For the analysis of proteins with FRAs, head lysates were prepared under denaturing conditions (protein extraction buffer) and subsequently filtered through a cellulose acetate membrane with a pore size of 0.2 μm [196]. Under these conditions, small protein complexes can pass the pores of the membrane, whereas larger particles will stick to the membrane. This allows the selection of aggregated HTT structures of high molecular weight.

Fly heads of young three days old Elav;HTTex1Q97 and +;HTTex1Q97 flies were collected and analyzed using the MAB5492, MW8, MAB5374, anti-Agg53 and HD1 antibodies to select a suitable antibody for the DB assay and FRA (Fig. 2.14 A). The MAB5492 antibody exhibits a strong signal in the filter assay and an alleviated signal in the dot blot assay for the Elav;HTTex1Q97 sample compared to the negative control, indicating the presence of SDS-insoluble aggregates. The MW8 antibody detects HTT aggregates in the DB assay and FRA. In contrast, the MAB5374 antibody exclusively detects aggregates in the FRA. The anti-Agg53 and HD1 antibodies also detect the HTTex1Q97 aggregates in the filter retardation assay. However, both antibodies also show a signal in the DB assay of head lysates from +;HTTex1Q97 flies. These flies carry the cDNA encoding the HTTex1Q97 protein, but are unable to express the protein due to the missing GAL4 protein. This suggests that these antibodies unspecifically detect proteins in the fly head lysates and therefore are unsuitable for the specific detection of HTT exon-1 proteins in DB assays. To summarize, the antibodies MAB5492 and MW8 achieved the most promising results for the detection of HTTex1Q97 aggregates in fly brains. Thus, they were subsequently used in further experiments.

After the selection of suitable anti-HTT aggregate-specific antibodies, young and middle-aged flies expressing different exon-1 fragments were analyzed for the presence of HTT aggregates (Fig. 2.14 B-D). As expected, in flies expressing the wild-type HTT exon-1 fragments (Q0 or Q17), no aggregates are detectable at different ages in the DB assays and FRAs. Solely at an age of 50 days, flies expressing HTTex1Q49 show a low amount of aggregates in the fly brain. However, at this time no SDS- and heat-stable HTTex1Q49 aggregates are detectable in the FRAs.

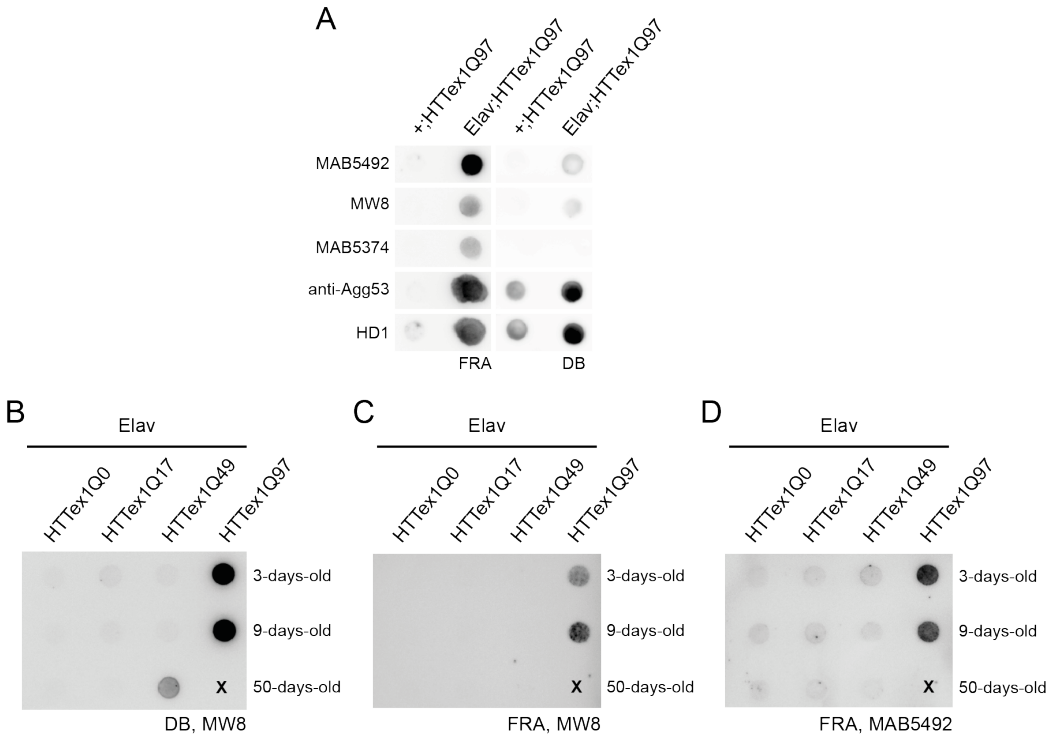

Figure 2.14: Mutant HTT exon-1 expression leads to the formation of SDS-insoluble aggregates.
(A) Analysis of three days old Elav;HTTex1Q97 and +;HTTex1Q97 (negative control) flies by filter retardation assays (FRA) and dot blot (DB) assays. Heads were homogenized in protein extraction buffer (FRA) and tris-lysis buffer (DB). Equal amounts of total protein (corresponding to ten fly heads) were loaded. The antibodies MAB5492, MW8, MAB5374, anti-Agg53 and HD1 were applied at a dilution of 1:1000. **(B)** Analysis of HTT aggregate load in flies after pan-neuronal expression of HTTex1Q0, HTTex1Q17, HTTex1Q49 and HTTex1Q97 in 3, 9 and 50 days old flies with DB assays using the MW8 antibody (15 μg protein was loaded). Heads were homogenized in RIPA-buffer. **(C)** Analysis of aggregate load in the same samples as in B using FRA. Immunodetection was performed using the MW8 antibody (75 μg protein was loaded). **(D)** Analysis of samples using the MAB5492 antibody (75 μg protein was loaded). Same samples as in C.

This late occurrence of HTT aggregates explains why no aggregates were detected in the salivary glands (Fig. 2.13), indicating that the expression time is not sufficient for the formation of visible aggregates. The pan-neuronal expression of the HTTex1Q97 protein was associated with appearance of a large quantity of SDS- and heat-stable aggregates already in three and nine days old flies. Because HTTex1Q97 overproducing flies have a median life span of only 20 days, an analysis of 50 days old animals was not possible. Since the signals in the FRAs were considerably weaker than in the DB assays although more head lysate was loaded, it can be assumed that only a fraction of the HTTex1Q49 aggregates formed in the fly brains are SDS- and heat-stable.

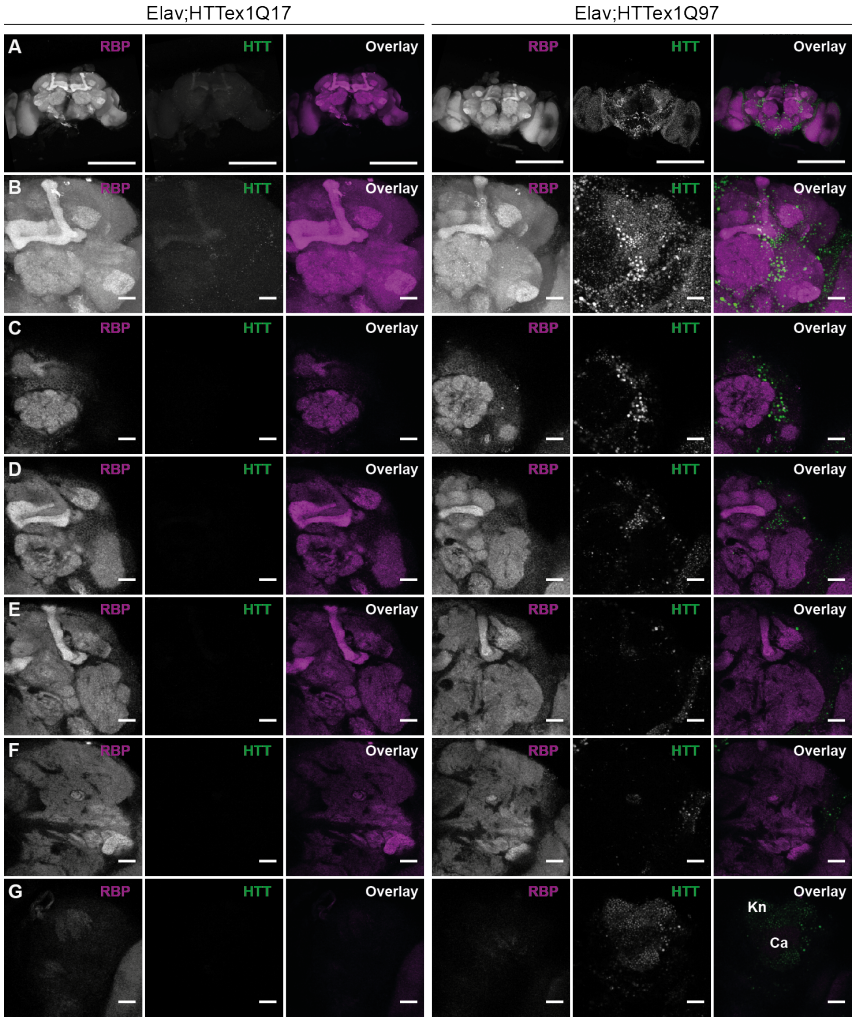

Figure 2.15: Visualization of HTTex1Q97 aggregates in *Drosophila* brains.
Immunostaining of the whole brain from three days old HTTex1Q17 and HTTex1Q97 flies. In the overlay the RIM-binding protein (RBP) signal is indicated in magenta and the MAB5492 signal in green. **(A)** Representative confocal images of the whole brain (left, scale bars: 200 μm) and **(B)** a magnification of the right central brain region (right, scale bars: 20 μm) are shown for each genotype. Shown is an enlargement of the right central brain region with the **(C)** detail of the antennal lobe, **(D)** anterior frontal section with antennal lobe and MB γ and β lobe, **(E)** MB α lobe, **(F)** MB peduncles and **(G)** posterior dorsal detail with MB calyx. Ca = Calyx, Kn = Kenyon cell bodies.

To analyze the location of HTT aggregates in *Drosophila* brains, whole brains were dissected and stained with antibodies against the RIM-binding protein (RBP) and the aggregate-specific HTT antibody MAB5492. The RBP is enriched in the active zones of synapses [197] and visualizes the neuropil. Pan-neuronal expression of HTTex1Q97 (Elav;HTTex1Q97) leads to an accumulation and subsequent deposition of the protein in different brain areas and in the mushroom body calyx (Fig. 2.15). There is no co-localization of RBP staining with the HTT staining, indicating

that the HTT aggregates are located in the cell bodies of neurons and Kenyon cells in the calyx. The expression of the wild-type fragment (Elav;HTTex1Q17) shows no HTT aggregates as shown before in the staining of *Drosophila* salivary glands (Fig. 2.15 A-G).

2.4.6 HTTex1Q97 aggregates formed in *Drosophila* brains are seeding competent structures

Self-propagation of pathogenic protein aggregates is a hallmark of neurodegenerative diseases including HD [198]. To investigate to which extent seeding and spreading of HTT aggregates is critical for disease development in flies, I assessed whether the HTT aggregates formed in fly brains possess seeding activity. For this purpose, fly head lysates were analyzed in the FRASE (FRET-based aggregate seeding) assay that was recently established in our lab. For this assay recombinant huntingtin (HTTex1Q48) was fused to the donor CyPet and the acceptor YPet, respectively (Fig. 2.16 A). To prevent the immediate formation of HTT co-aggregates, a GST-tag was fused to the N-terminus of the HTTex1Q48-CyPet / -YPet fusion proteins, which reduces the propensity of HTTex1Q48 to spontaneously form aggregates.

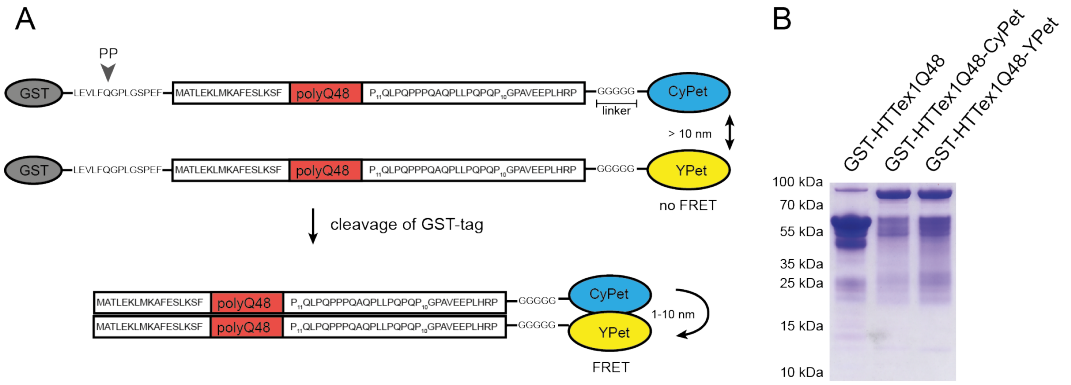

Figure 2.16: Purification of CyPet- and YPet-tagged and untagged huntingtin proteins. **(A)** Proteins of interest expressed as CyPet and YPet fusion proteins. The fluorescent emission peak of CyPet overlaps the excitation peak of YPet. In case of aggregation after PreScission protease (PSP) cleavage, CyPet an YPet get in close proximity and an energy transfer is possible. **(B)** Analysis of expressed and purified fusion proteins in a Coomassie stained gel. For each protein 10 μl of the protein preparation was loaded.

The recombinant fusion proteins GST-HTTex1Q48-CyPet / -YPet and the untagged huntingtin protein GST-HTTex1Q48 were expressed in *E.coli*, purified using glutathione-agarose beads and were visualized in a polyacrylamide gel stained with Coomassie brilliant blue (Fig. 2.16 B). The untagged GST-HTTex1Q48 protein shows a band at around ~60 kDa whereby the theoretical size of the protein is 42 kDa. This indicates that the fusion protein migrates slower than expected in

SDS gels as observed previously [199]. This effect is probably due to the weak binding of SDS to the polyQ tract. The GST-HTTex1Q48-CyPet and -YPet fusion proteins display a dominant band at ~90 kDa and show also a higher molecular weight in the SDS gels.
For the analysis of fly head lysates in the FRASE assay, they were homogenized in brain lysis buffer and equal amounts were added to the aggregation reaction mix (Fig. 2.17 A). The GST-HTTex1Q48-CyPet and -YPet proteins were treated with the PSP and the spontaneous formation of HTTex1Q48-CyPet / -YPet co-aggregates was quantified through repeated FRET measurements. A time-dependent increase of the FRET efficiency was observed (Fig. 2.17 B).

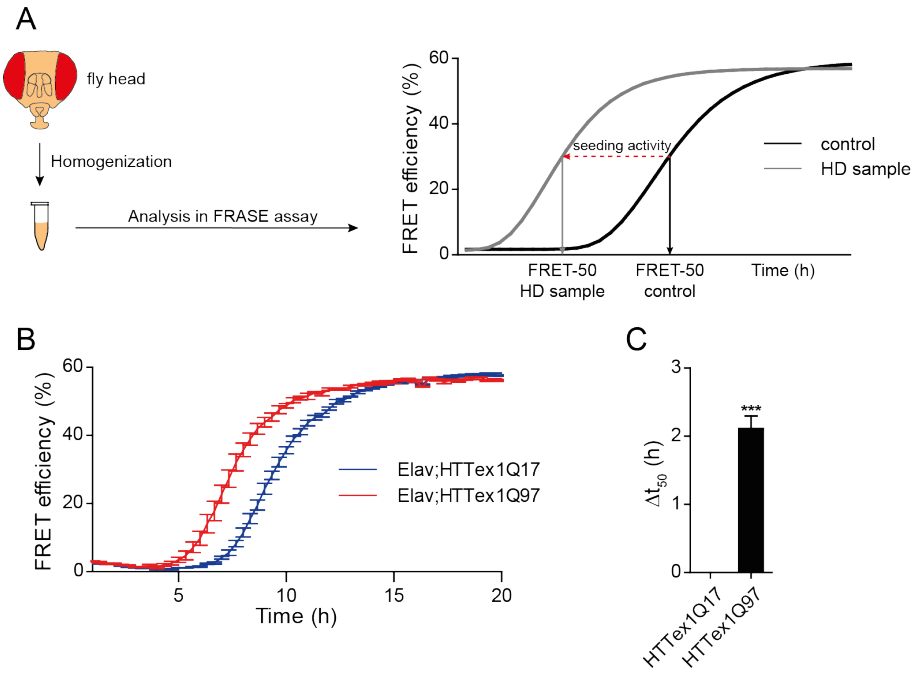

Figure 2.17: Analysis of HTTex1Q97 aggregates prepared from *Drosophila* brains in FRASE assays.
(A) Schematic representation of the FRASE assay. Fly heads were homogenized in brain lysis buffer and equal amounts were added to the HTT aggregation reactions. **(B)** Fly head lysates of Elav;HTTex1Q17 and Elav;HTTex1Q97 flies were analyzed in the FRET-based aggregation assay. Values are means ± SEM of three biological replicates each performed in triplicates. **(C)** Seeding activity was quantified by subtracting the t_{50} value of the sample from the control (Elav;HTTex1Q17). Error bars represent mean μ SEM; unpaired t-test; *** p <0.001.

The addition of head lysates from Elav;HTTex1Q97 flies to the FRASE aggregation reaction resulted in a significantly decreased lag phase compared to lysates from Elav;HTTex1Q17 flies, which served as a control (Fig. 2.17 C). The head lysates prepared from Elav;HTTex1Q97 flies reduced the lag phase for ~2 hours, indicating that the lysates contain seeding-competent HTT aggregates.

In summary, the analysis of the full-length *Drosophila* models revealed in Elav;HTTflQ145 flies an impaired locomotor behavior and reduced survival. The Elav;HTTflQ73 flies showed no significant difference to flies expressing the wild-type fragment, HTTflQ23. The characterization of the different HTT exon-1 fragments revealed an more severed HD-like phenotype with increasing polyQ length of the expressed protein. This polyQ length-dependency was evident in the locomotion activity, climbing behavior and survival phenotype. Pan-neuronal expression of the pathogenic HTT fragment (HTTex1Q97) caused a reduced activity and degenerated sensory and olfactory processing (Fig. 2.10). Moreover, the expression of the protein in *Drosophila* resulted in the formation of SDS- and heat-stable aggregates in neuronal and non-neuronal tissue. When expressed in *Drosophila* brains, the HTT aggregates are located in the cell bodies and are seeding competent.

2.5 Analysis of long-time adult-onset expression of wild-type and mutant HTT fragments

The conventional UAS-GAL4 expression system allows spatially controlled expression of the transgene. However, a limitation of the system is the lack of temporal control. The expression of the HTT transgenes begins during the embryonic developmental stage 12 [182] and results in neurodegeneration in young three days old flies as shown. In order to investigate early changes in the disease, inducible expression of the transgene is required. One possibility for temporal control of gene expression is the TARGET system [177], which depends on the temperature sensitive mutant GAL80^{ts}. In proof of principle experiments, I have shown that behavioral differences are caused by the temperature shift alone. I found that experimental and control groups are affected similarly by the temperature increase (data not shown). Thus, the TARGET system was not used for the measurements of behavioral defects. To overcome these limitations, the inducible GeneSwitch expression system, which is based on a ru-486-dependent GAL4-progesterone-receptor fusion protein [177] was used to analyze flies before the onset of neurodegeneration.

2.5.1 Dynamics of inducible HTT expression in adult *Drosophila* neurons

To generate an adult-onset *Drosophila* model of HD, the pathogenic HTT exon-1 fragment HTTex1Q97 was expressed using the inducible pan-neuronal gene driver Elav-Gene-Switch (referred to as "GSelav") (Fig. 2.18 A). This driver line was previously used to develop an adult-onset *Drosophila* model of spinocerebellar ataxia 7 (SCA 7) and Alzheimer's disease. It is able to control the expression of HTT fragments spatially and temporally, which enables the expression specifically in neurons of adult flies [200, 201].

Transgene expression under the control of the Elav-Gene-Switch system needed to be optimized in order to obtain sufficient transgene expression but simultaneously avoid toxic effects by high doses of the hormone. As the genomic landing site is equal in all of the generated fly lines, it can be assumed that the ru486 response and transgene expression is similar in lines expressing different HTT exon-1 proteins. For the expression test, HTT513Q17 flies were used and treated with increasing concentrations of ru-486. Therefore, flies containing the UAS-HTT513Q17 transgene were crossed with GSelav flies and the resulting offspring was raised on normal fly food to prevent gene expression. The offspring was treated with different concentrations of the hormone, which was added after cooking the food. The fly heads were collected after four days of treatment and the head lysates were analyzed by Western blotting.

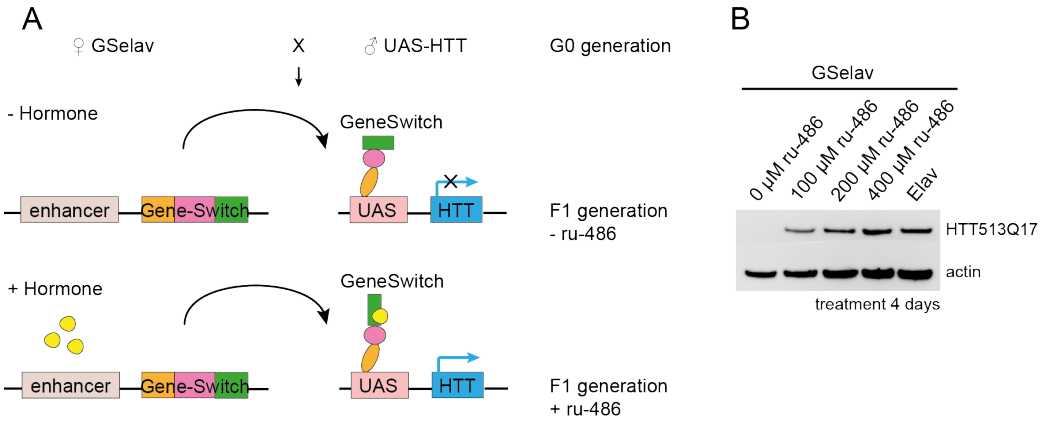

Figure 2.18: Adult-onset induction of HTT expression in the *Drosophila* nervous system. **(A)** A schematic representation of the Gene-Switch expression system is shown. The gene-driver line GSelav was crossed with flies containing the HTT cDNA fragment fused to an upstream activation (UAS) sequence. The expression is repressed in the absence of the hormone ru-486 and activated in the presence of the hormone. **(B)** Western blot analysis of the expression in treated GS;HTT513Q17 flies (0 μM, 100 μM, 200 μM and 400 μM ru-486) and Elav;HTT513Q17. Equal amounts (~ten heads per lane) were loaded and immunodetected with the MAB2166 and anti-actin antibodies.

I observed no gene expression in flies that were cultivated on normal food. In comparison, the hormone treated flies showed a dose-dependent expression of the HTT513Q17 protein. For further studies, a level of expression comparable to the conventional expression system (GAL4 / UAS) will be utilized to ensure comparability between both expression systems. A concentration of 400 μM ru-486 showed a similar gene expression in comparison to the conventional expression system (Elav;HTT513Q17) and has been used in previous studies [202]. Thus, this concentration was chosen for all further experiments.

In order to verify the expression of the gene encoding the HTTex1Q97 protein, the transcription of the transgene was analyzed. For this purpose, the GS;HTTex1Q97 and GS;HTTex1Q17 flies

were treated with the hormone ru-486 for different days as indicated in Figure 2.19 A. As negative controls, flies were used that contain only the UAS-HTTex1Q17 or UAS-HTTex1Q97 transgenes but were not crossed to GSelav flies. Thus, the expression of the transgenes should not be induced upon ru-486 treatment. Without hormone treatment the mRNA levels encoding HTTex1Q17 and HTTex1Q97 were comparable to the negative controls where no HTT is expressed (Fig. 2.19 B and C). I observed a significant increase in the mRNA levels after 24 hours of treatment in the HTTex1Q97 flies. After three days of expression, the maxima of HTTex1Q17 and HTTex1Q97 mRNA levels were reached and remained stable also when samples were analyzed after six and twelve days.

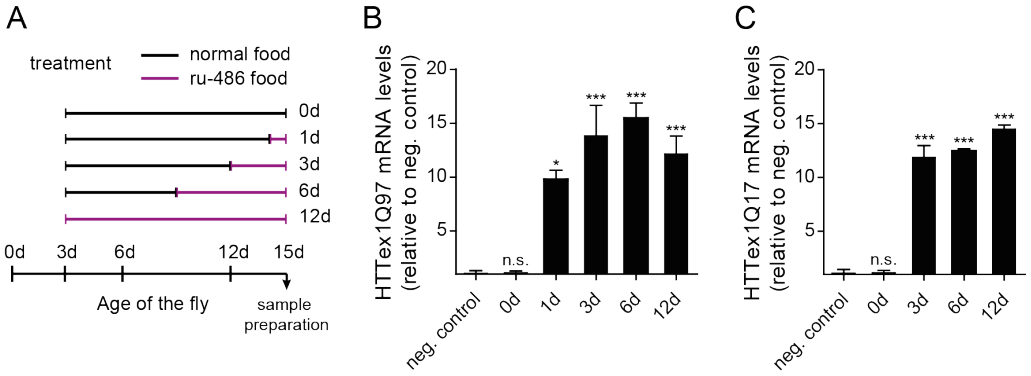

Figure 2.19: Induction of HTT exon-1 mRNA expression in the *Drosophila* nervous system. **(A)** Scheme of temporal sequences of the ru-486 treatment. The black line indicates no treatment, the purple line indicates ru-486 treatment. **(B)** Quantification of HTTex1Q97 mRNA levels of different treated GS;HTTex1Q97 flies by qRT-PCR. The rp49 gene was used as reference gene. Error bars represent mean ± SEM of three biological replicates performed each as technical triplicates; values are normalized to the negative control (+;UAS-HTTex1Q97, fly strain which contains only the UAS-HTT transgene); one-way ANOVA Dunnett's post hoc test compared to negative control; n.s. means not statistically significant; * p <0.05; *** p <0.001. **(C)** Quantification of HTTex1Q17 mRNA levels of different treated GS;HTTex1Q17 flies by qRT-PCR. Values are normalized to the negative control (+;UAS-HTTex1Q17).

2.5.2 Long-time expression of HTTex1Q97 causes behavioral impairments

The presented studies have shown that constitutive expression of the HTTex1Q97 in fly neurons shortens the life span of flies and reduces their locomotion (Fig. 2.9). To determine whether expression of the protein in adult flies causes similar impairments, the survival and climbing abilities were examined. Flies were treated with the hormone (ru-486) to induce transgene expression in three days old flies post-eclosion (Fig. 2.20 A). For comparison, a control group with the same genetic background was cultured as well on hormone food. These control flies are obtained from a crossing of GSelav flies with w^{1118} flies. The resulting flies (GS;+) were

treated identical to the experimental group of GS;HTTex1Q97 flies. For a better understanding, the chronically treated flies (ru-486 food) were labeled with ON and the untreated (normal food) flies were labeled with OFF. Consequently, the long-time treated GS;HTTex1Q97 flies are called GS;HTTex1Q97^{ON} flies and untreated flies are called GS;HTTex1Q97^{OFF} flies.
The treated control GS;+^{ON} flies behaved comparable to the untreated GS;+^{OFF} flies as expected, suggesting that ru-486 hormone treatment does not affect the climbing behavior in flies (Fig. 2.20 B). The GS;HTTex1Q97^{OFF} flies exhibited a similar climbing performance, supporting the assumption that the pathogenic HTTex1Q97 protein is not expressed in these flies. However, the GS;HTTex1Q97^{ON} flies after chronic hormone treatment showed a dramatically reduced climbing performance in comparison to the GS;HTTex1Q97^{OFF}, GS;+^{ON} and GS;+^{ON} flies. In detail, the chronic expression of the HTTex1Q97 fragment in flies during the first 25 days did not influence the climbing performance compared to the controls. However, the climbing abilities declined rapidly after 25 days and flies were unable to climb when they reached an age of ~30 days.
To determine the effect of adult-onset expression of the HTTex1Q97 fragment on survival, additionally a life span assay was performed (Fig. 2.20 C and D). In this case, as an additional control, flies expressing the HTTex1Q17 fragment were also incorporated into the analysis. I found that the GS;HTTex1Q17^{ON} flies displayed a median life span of 89 days and the GS;HTTex1Q17^{OFF} flies of 91 days (Fig. 2.20 C and D). The median life span of the control GS;+^{ON} flies and GS;+^{OFF} flies was 88 days and 89 days, respectively. The median life span of both treated and untreated control groups (GS;+ and GS;HTTex1Q17) was similar to GS;HTTex1Q97^{OFF} flies, which showed a median life span of 85 days (Fig. 2.20 D). The chronic, adult-onset expression of the HTTex1Q97 fragment dramatically reduced the survival of flies (Fig. 2.20 D). The GS;HTTex1Q97^{ON} flies showed a significantly reduced life span with a median life span of ~30 days. Together these data indicate that ru-486 treated GS;HTTex1Q97 flies show decreased climbing abilities shortly before they start to die.

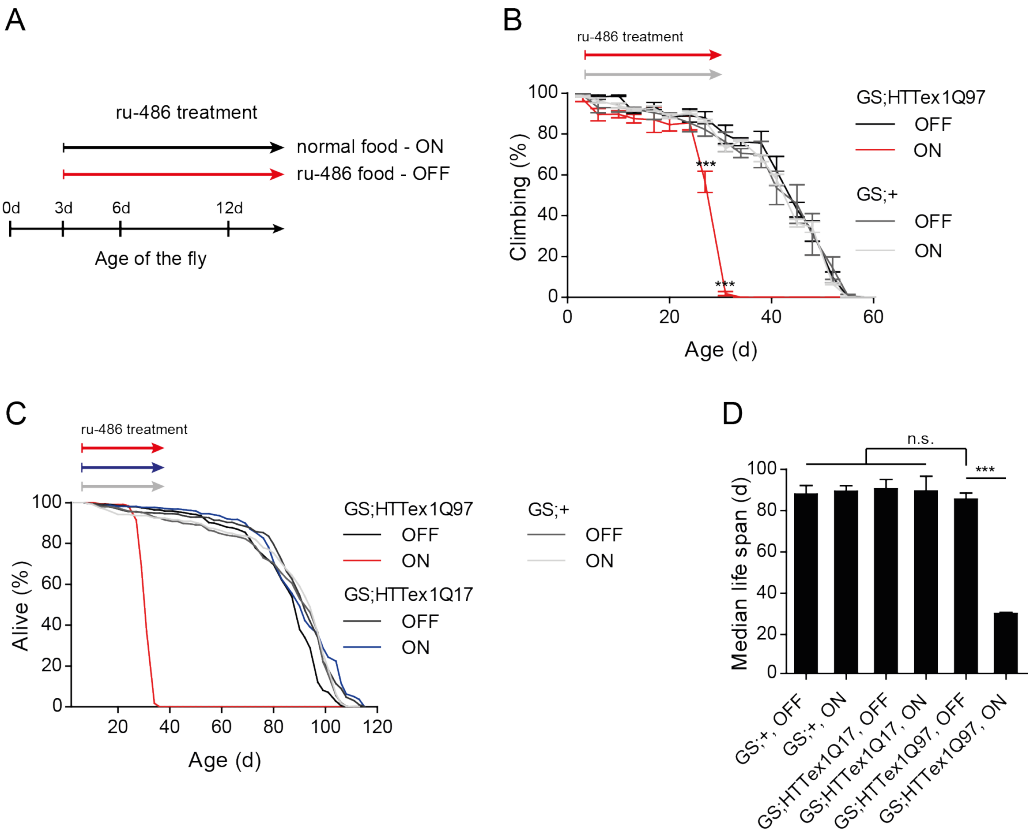

Figure 2.20: Chronic adult-onset expression of HTTex1Q97 leads to decreased climbing abilities and reduced survival of flies.
(A) Scheme of temporal sequences of the ru-486 treatment. The black line indicates no treatment and the red line indicates ru-486 treatment started from day three post-eclosion. **(B)** Climbing abilities of GS;HTTex1Q97^{ON} (red), GS;HTTex1Q97^{OFF} (black), GS;+^{ON} (light gray) and GS;+^{OFF} (middle gray) flies. The GS;+ flies arised from the cross-breeding of GSelav-GAL4 and w^{1118} flies. Results of three independent replicates, started with 100 flies per group for one replicate, are shown. Error bars represent mean ± SEM; two-way ANOVA Dunnett's post hoc test compared to GS;HTTex1Q97^{OFF}; *** p <0.001. **(C)** Life span analysis of GS;+^{ON}, GS;+^{OFF}, GS;HTTex1Q97^{ON}, GS;HTTex1Q97^{OFF}, GS;HTTex1Q17^{ON} (blue) and GS;HTTex1Q17^{OFF} (dark gray) flies. Life span is plotted as the percentage of surviving flies of three replicates (GS;HTTex1Q97^{ON} n = 102, 98, 106; GS;HTTex1Q97^{OFF} n = 99, 96, 107; GS;HTTex1Q17^{ON} n = 100, 109, 101; GS;HTTex1Q17^{OFF} n = 107, 102, 100; GS;+^{ON} n = 87, 106, 106; GS;+^{OFF} n = 97, 96, 100). **(D)** The analysis of the median life span displays the time when 50 % of the flies survived. Error bars represent mean ± SEM from three independent experiments; one-way ANOVA Tukey's post hoc test; n.s. means not statistically significant.

2.5.3 Chronic expression of mutant HTTex1Q97 in flies leads to the formation of SDS-stable aggregates.

To survey, if the amount of HTT aggregates in the fly heads increases with sustained protein expression, I quantified the formation of HTT aggregates using DB assays, FRAs and histological methods. Therefore, heads from GS;+, GS;HTTex1Q17 and GS;HTTex1Q97 flies were collected before the treatment (labeled as 0d) and after ru-486 treatment for 24 days. Treatment started three days post-eclosion of flies (labeled as 24d) (Fig. 2.21 A). This time point was selected because after 24 days of treatment, only ~50 % of the flies were able to climb up the glass vial. However, after 24 days of treatment most flies were still alive in life span assays (Fig. 2.20 C). I found that the treated and untreated GS;HTTex1Q17 flies contain no insoluble HTT aggregates, when brains were analyzed in FRAs (Fig. 2.21 B). The GS;+$^{24d\text{-}ON}$ flies also showed no antibody signal in the DB assays and the FRAs (Fig. 2.21 C). In comparison, in the head lysates of GS;HTTex1Q97$^{24d\text{-}ON}$ flies, a high amount of SDS-insoluble and heat-stable HTT aggregates were detectable with FRAs and DB assays using the aggregate-specific antibodies MW8 and MAB5492 (Fig. 2.21 C).

To confirm these observations, whole-brains of treated and untreated flies were also immunoassayed using the MAB5492 antibody. This analysis revealed that in ru-486 treated flies HTTex1Q97 aggregates are detectable in all brain regions, whereas they were not observed in untreated flies (Fig. 2.21 D).

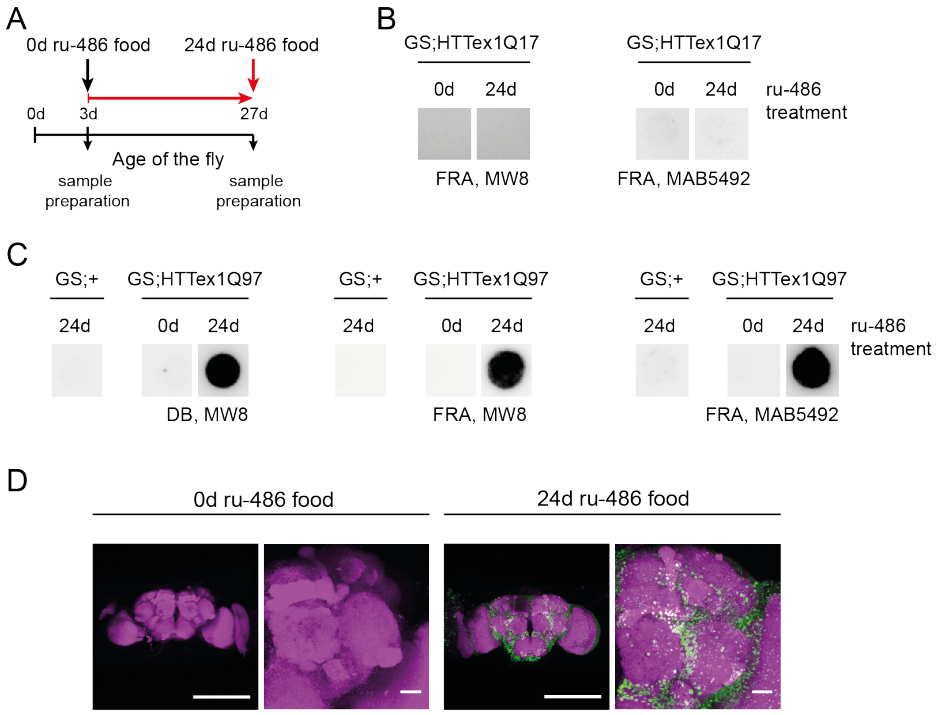

Figure 2.21: Adult-onset expression of HTTex1Q97 for 24 days leads to the formation of insoluble HTT aggregates in *Drosophila* brains.
(A) Scheme of the temporal sequences of ru-486 treatment. The untreated flies were collected three days after hatching (black arrow). The red line indicates ru-486 treatment starting from day three post-eclosion for 24 days. The flies were collected at an age of 27 days (red arrow). **(B)** Aggregate load of treated and untreated GS;HTTex1Q17 flies analyzed with the FRA assay using the MW8 and MAB5492 antibodies. Equal amounts were loaded (75 μg protein). **(C)** Aggregate load of treated and untreated GS;+ and GS;HTTex1Q97 flies. Brain extracts were analyzed by DB assays (15 μg protein) and FRAs (75 μg protein) using the MW8 and MAB5492 antibodies. **(D)** Confocal images of the whole-brain of treated and untreated GS;HTTex1Q97 flies. The RBP staining is shown in magenta and the MAB5492 staining in green. For each group a representative whole brain (left, scale bars: 200 μm) and a magnification of the right central brain region is displayed (right, scale bars: 20 μm).

2.5.4 Short-time expression of mutant HTTex1Q97 protein in transgenic flies is sufficient to detect insoluble HTT aggregates in adult neurons

To monitor the kinetics of mutant HTT aggregation in fly brains, HTTex1Q97 expression was induced in three days old flies and samples were analyzed at different time points after induction using DB assays and FRAs. The selected time points and the exact treatment periods are shown in Figure 2.22 A. I found that amount of insoluble HTTex1Q97 aggregates steadily increases over time in fly heads (Fig. 2.22 A-C). Analysis of head lysates with DB assays and FRAs showed the first appearance of HTT aggregates after six days of expression and high amounts of aggregates were detectable after 12 days. Interestingly, the abundance of HTTex1Q97 aggregates did not

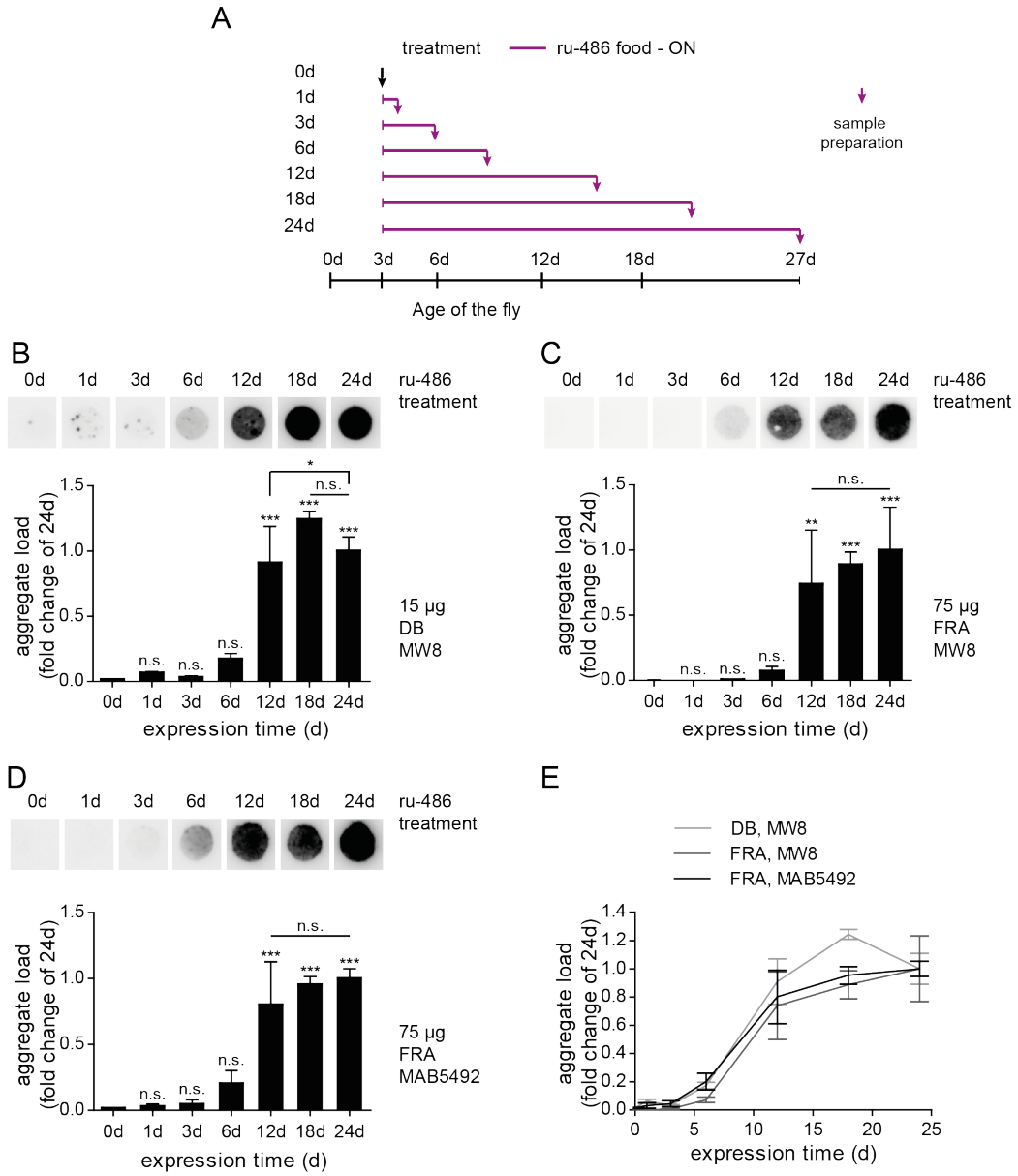

Figure 2.22: Time-dependent accumulation of HTTex1Q97 aggregates in HD fly brains. **(A)** Scheme of the temporal sequences of ru-486 treatment. The purple line indicates time periods of ru-486 treatment. The flies were collected after the indicated times (arrows). **(B)** Aggregate load in brains of GS;HTTex1Q97 flies after expression of the recombinant HTT protein for different time periods. The heads were lysed in RIPA buffer and 15 μg of total protein were analyzed in the DB assays using the MW8 antibody. Shown is a representative dot blot of multiple independent biological replicates (n = 3, 3, 3, 3, 3, 3, 2) and the quantification of the dots. Error bars represent mean $\pm$ SEM from replicates; one-way ANOVA Dunnett's post hoc test compared to 0d and Tukey's post hoc test; n.s. means not statistically significant; ** p <0.01; *** p <0.001. **(C)** HTT aggregate load in brain samples similar to B. Samples in this case, were analyzed by FRAs (75 μg protein) using the MW8 antibody. **(D)** HTT aggregate load in brain samples similar to B. Samples were analyzed by FRAs using the MAB5492 antibody. **(E)** Quantified data from the bar charts in B-D were plotted in a line chart. Light grey indicates data from B, dark grey from C and black from D. Error bars represent mean $\pm$ SEM.

significantly change between 12 days and 24 days of expression, indicating that a maximum amount of large SDS-stable HTT aggregates is reached after ~12 days which does not increase further over time.

Overall these results confirm that the Gene-Switch system is sufficient to induce the expression of the pathogenic HTTex1Q97 protein in the fly nervous system. Furthermore, I found that the HTT protein accumulates over time in ru-486 treated flies.

2.5.5 The HTTex1Q97 aggregates formed in *Drosophila* brains are seeding-competent structures

In order to analyze whether the HTT aggregates that are detected after 24 days of expression in fly brains are seeding-competent structures, head protein lysates were examined using the established FRASE assay. In addition, brain extracts of untreated control flies aged for 24 days were also analyzed (Fig. 2.23 A). The head lysates prepared from ru-486 treated flies significantly reduced the lag phase of the spontaneous HTTex1Q48 fusion protein polymerization (Fig. 2.23 A and B). This indicates that after 24 days of HTTex1Q97 expression, seeding-competent HTT aggregates are formed in *Drosophila* brains, which can shorten the lag phase of the reporter proteins GST-HTTex1Q48-CyPet / -YPet in cell-free FRASE assays.

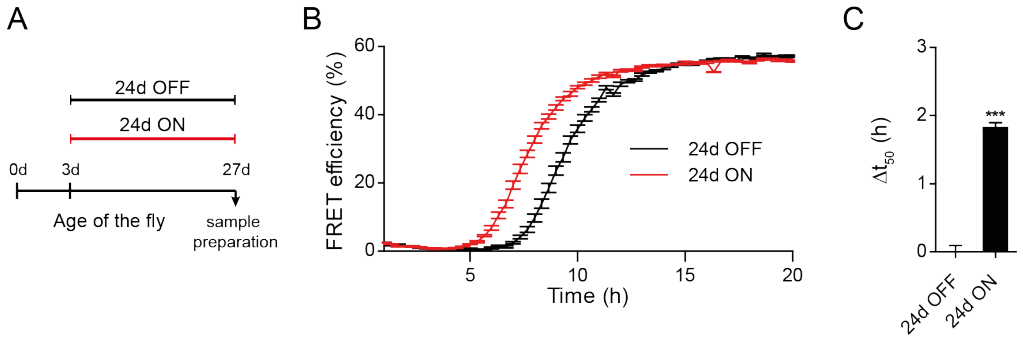

Figure 2.23: Analysis of the seeding-activity of HTTex1Q97 aggregates in fly brains using the FRASE assay.

(A) Scheme of hormone treatment. GS;HTTex1Q97 flies were kept on normal food for 24 days (black line) or were fed for 24 days with hormone-treated food (red line). **(B)** Fly head lysates of treated and untreated GS;HTTex1Q97 flies were analyzed in the FRET-based HTT aggregate seeding (FRASE) assay. Values are means ± SEM of three biological replicates each performed in triplicates. **(C)** Seeding activity was quantified by subtracting the t_{50} value of the sample from the control (GS;HTTex1Q97$^{24d\text{-}ON}$. Error bars represent mean ± SEM; unpaired t-test; *** p <0.001.

2.6 Analysis of the effects of short-time adult-onset expression of wild-type and mutant HTT fragments in HD transgenic flies

In previous experiments, I found that long-time expression of mutant HTT fragments in adult flies with the Gene-Switch expression system causes behavioral impairments that are comparable to the constitutive expression with the GAL4 / UAS system. To examine whether the observed HTT induced phenotypes are require long time expression of the pathogenic protein, I next analyzed the effects of short-time expression of HTT fragments in young adult animals. Therefore, in the following experiments the inducible flies were treated for short periods of time with the hormone ru-486 and subsequently flies were transferred to normal food in order to turn off the expression of the transgene.

2.6.1 Transfer of transgenic flies to food lacking the hormone ru-486 is sufficient to turn off HTT expression

First, I investigated the capability of the Gene-Switch system to turn off the expression of mutant HTT in transgenic flies. For this purpose, GS;HTTex1Q97 flies were treated for three days with ru-486 and then cultivated on normal food for various time periods as shown in Figure 2.24 A. After six hours on normal food following the expression period, I observed a slight but not significant decrease of the HTTex1Q97 mRNA levels in transgenic flies (Fig. 2.24 B). However, after twelve hours on normal food a ~50 % decrease of the HTT mRNA was detectable in the fly heads and after 24 hours HTT mRNA was undetectable by qRT-PCR analysis, indicating that HTT expression is turned off effectively when flies transferred to food lacking the ru-486 hormone. In an independent experiment, I also investigated whether HTT expression can be turned off after the transgenic flies were incubated for six days on ru-486 food. I found that mutant HTT mRNA levels were almost undetectable after 24 hours on normal food (Fig. 2.24 C), confirming the results obtained with 3d hormone treated flies (Fig. 2.24 B). Thus, these studies indicate that HTT mRNAs are undetectable with qRT-PCR in HD transgenic flies when they are transferred for ~one day to food lacking the hormone ru-486 (Fig. 2.24 D).

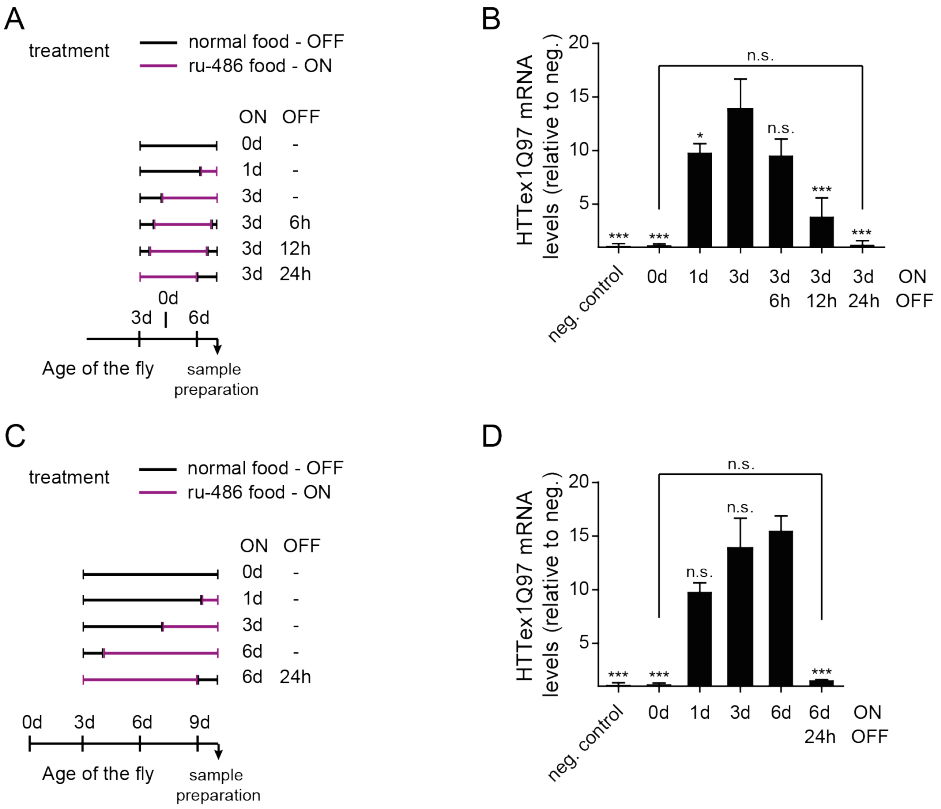

Figure 2.24: Analysis of HTTex1Q97 expression in the absence of the hormone ru-486. **(A)** Scheme for the hormone treatment of GS;HTTex1Q97 flies. Black lines indicate untreated time periods and purple lines indicate time periods during which flies were treated with ru-486. Flies were collected at an age of seven days and were then analyzed. **(B)** Quantification of HTTex1Q97 mRNA levels in GS;HTTex1Q97 flies by qRT-PCR. Error bars represent mean ± SEM of three biological replicates; values are normalized to the negative control; one-way ANOVA Dunnett's post hoc test compared to 3d-ON; n.s. means not statistically significant; * p <0.05; *** p <0.001. **(C)** Hormone treatment scheme for GS;HTTex1Q97 flies. Flies were collected at an age of ten days and were analyzed. **D** Quantification of HTTex1Q97 mRNA levels in GS;HTTex1Q97 flies by qRT-PCR. One-way ANOVA Dunnett's post hoc test compared to 6d-ON.

2.6.2 Analysis of the effects of short-time HTTex1Q97 expression on behavioral phenotypes

Since ru-486 induced gene expression in transgenic flies can be effectively turned off through transfer of flies to food lacking the hormone (Fig. 2.24), I next investigated the effects of short-time HTTex1Q97 expression on the climbing abilities and the life span of flies. To ensure comparability to the long-time induction experiments (Fig. 2.20), three days old flies treated for three or six days with the hormone were transferred to normal food (lacking ru-486) and subsequently cultivated under these conditions until a climbing phenotype was detectable (Fig. 2.25

A). The three and six days hormone treated flies were termed GS;HTTex1Q97$^{3d\text{-}ON/OFF}$ and GS;HTTex1Q97$^{6d\text{-}ON/OFF}$, respectively. In addition, control flies that do not express the HTT gene treated for short periods of time with the hormone (GS;+$^{3d\text{-}ON/OFF}$ and GS;+$^{6d\text{-}ON/OFF}$) were systematically analyzed concerning the climbing phenotype.
I found that climbing behavior of GS;+$^{3d\text{-}ON/OFF}$, GS;+$^{6d\text{-}ON/OFF}$ and GS;HTTex1Q97^{OFF} flies was very similar. However, both short-time and long-time expression of HTTex1Q97 decreased the climbing performance of flies (Fig. 2.25 B). At the beginning, all treated fly lines (GS;HTTex1Q97$^{3d\text{-}ON/OFF}$, GS;HTTex1Q97$^{6d\text{-}ON/OFF}$ and GS;HTTex1Q97^{ON}) showed a very similar behavior than the control fly lines (GS;+$^{3d\text{-}ON/OFF}$, GS;+$^{6d\text{-}ON/OFF}$ and GS;HTTex1Q97^{OFF}). However, after 21 – 24 days the HTTex1Q97 expressing flies lost very rapid their climbing abilities. I found that chronic hormone treatment resulted in a reduction of the climbing abilities by half at an age of 27 days (Fig. 2.25 B). In comparison, in GS;HTTex1Q97$^{3d\text{-}ON/OFF}$, GS;HTTex1Q97$^{6d\text{-}ON/OFF}$ flies a 50 % loss of climbing abilities was observed after 31 and 34 days, respectively. Since the climbing abilities of chronically and short-time treated transgenic flies (6d-ON/OFF) are very similar, it can be concluded that the duration of HTTex1Q97 expression is not correlated to the observed climbing phenotype.

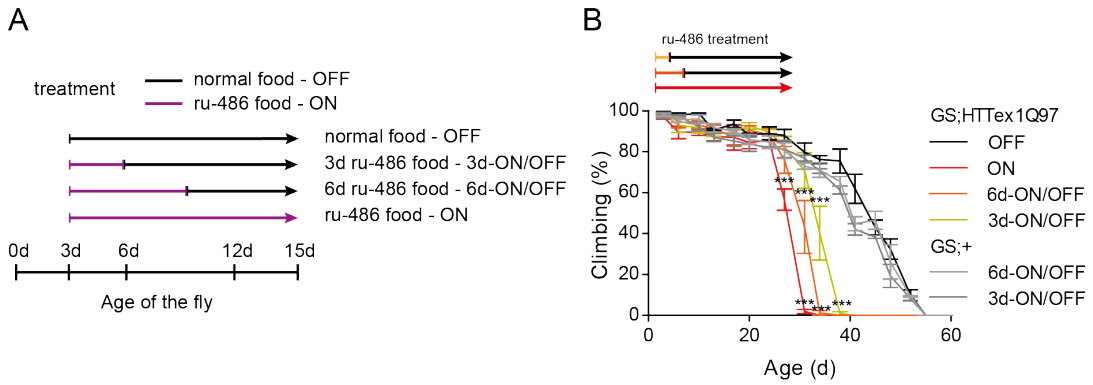

Figure 2.25: Behavioral analysis of short-time expression of HTTex1Q97 in the nervous system of HD transgenic flies.
(A) Scheme of the temporal hormone treatment strategy. The black lines indicate the time period where flies were not treated with hormone (normal food) and the purple lines indicate the time where flies were hormone treated. Treatment started at day three post-eclosion. **(B)** Analysis of climbing abilities of GS;+$^{3d\text{-}ON/OFF}$ (middle grey), GS;+$^{6d\text{-}ON/OFF}$ (light grey), GS;HTTex1Q97^{ON} (red), GS;HTTex1Q97$^{6d\text{-}ON/OFF}$ (orange), GS;HTTex1Q97$^{3d\text{-}ON/OFF}$ (yellow) and GS;HTTex1Q97^{OFF} (black) flies. Results of three independent replicates,. Experiments were started with 100 flies per group for one replicate. Error bars represent mean ± SEM; two-way ANOVA Dunnett's post hoc test compared to GS;HTTex1Q97^{OFF} flies; *** p <0.001.

The same fly lines were also analyzed in the life span assay using the same treatment procedure. In addition, GS;HTTex1Q97 flies were investigated where the HTT transgender was expressed

for only one day (Fig. 2.26 A).

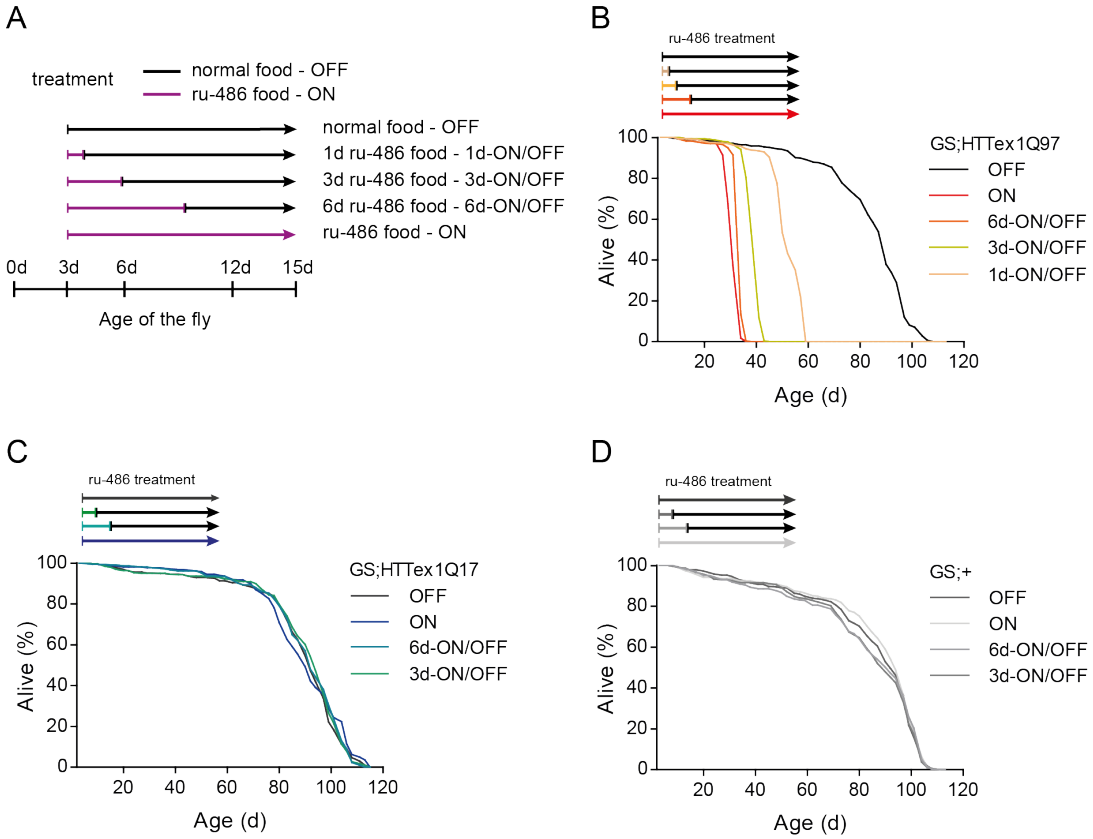

Figure 2.26: Life span analysis of transgenic flies after short-time expression of HTTex1Q97 in the nervous system.
(A) Scheme of temporal hormone treatment. The black lines indicate time periods without hormone treatment (normal food) and the purple lines indicate time periods with hormone treatment. Treatment started at day three post-eclosion. **(B)** Life span analysis of GS;HTTex1Q97^{ON} (red), GS;HTTex1Q97$^{6d\text{-}ON/OFF}$ (orange), GS;HTTex1Q97$^{3d\text{-}ON/OFF}$ (yellow), GS;HTTex1Q97$^{1d\text{-}ON/OFF}$ (rose),and GS;HTTex1Q97^{OFF} (black) flies. Life span is plotted as the percentage of surviving flies of three replicates (GS;HTTex1Q97$^{1d\text{-}ON/OFF}$ n = 107, 110, 106; GS;HTTex1Q97$^{3d\text{-}ON/OFF}$ n = 107, 108, 107; GS;HTTex1Q97$^{6d\text{-}ON/OFF}$ n = 108, 105, 94). **(C)** Life span analysis of GS;HTTex1Q17^{ON} (blue), GS;HTTex1Q17$^{6d\text{-}ON/OFF}$ (cyan), GS;HTTex1Q17$^{3d\text{-}ON/OFF}$ (green) and GS;HTTex1Q17^{OFF} (dark grey) flies. The mean of three independent replicates are shown (GS;HTTex1Q17$^{3d\text{-}ON/OFF}$ n = 109, 96, 97; GS;HTTex1Q17$^{6d\text{-}ON/OFF}$ n = 110, 97, 100). **(D)** Survival analysis of GS;+^{ON} (very light grey), GS;+$^{6d\text{-}ON/OFF}$ (light grey), GS;+$^{3d\text{-}ON/OFF}$ (middle grey) and GS;+^{OFF} (dark grey) flies. The mean of three independent replicates are shown (GS;+$^{3d\text{-}ON/OFF}$ n = 90, 100, 105; GS;+$^{6d\text{-}ON/OFF}$ n = 93, 85, 98).

Interestingly, I found that the GS;HTTex1Q97$^{6d\text{-}ON/OFF}$ flies display with a median life span of 33 days, which is not significantly different to GS;HTTex1Q97^{ON} flies with a median life span of 30 days (Fig. 2.26 B and 2.27 B). In comparison, the GS;HTTex1Q97$^{3d\text{-}ON/OFF}$ flies exhibited a median life span of 38 days, which was significantly different to GS;HTTex1Q97$^{6d\text{-}ON/OFF}$ flies. Strikingly, the GS;HTTex1Q97$^{1d\text{-}ON/OFF}$ flies showed a median life span of 51 days, indicating that even a very short period of HTTex1Q97 expression is sufficient to decrease the survival of flies. Overall, a longer survival with shorter HTT expression times is observed. However, the similarity between the chronically treated flies and the flies treated for six days suggests that there is no correlation between the mutant HTT-induced toxicity and the time of HTTex1Q97 expression in flies.

In control, transgenic flies expressing the wild-type protein HTTex1Q17 were also investigated in survival assays. I found that GS;HTTex1Q17$^{3d\text{-}ON/OFF}$ and GS;HTTex1Q17$^{6d\text{-}ON/OFF}$ flies display a median life span of 91 days (Fig. 2.26 C and 2.27 A). A similar result was observed when GS;HTTex1Q17^{OFF} flies were analyzed. Finally, I also assessed the survival of the control flies GS;+$^{3d\text{-}ON/OFF}$ and GS;+$^{6d\text{-}ON/OFF}$ that were treated for short time with the hormone. These flies exhibited a median life span of 85 days similar to GS;+^{ON} and GS;+^{OFF} flies (Fig. 2.26 D and 2.27 A). Thus, the short-time expression of the wild-type HTTex1Q17 fragment has no significant impact on the survival of flies.

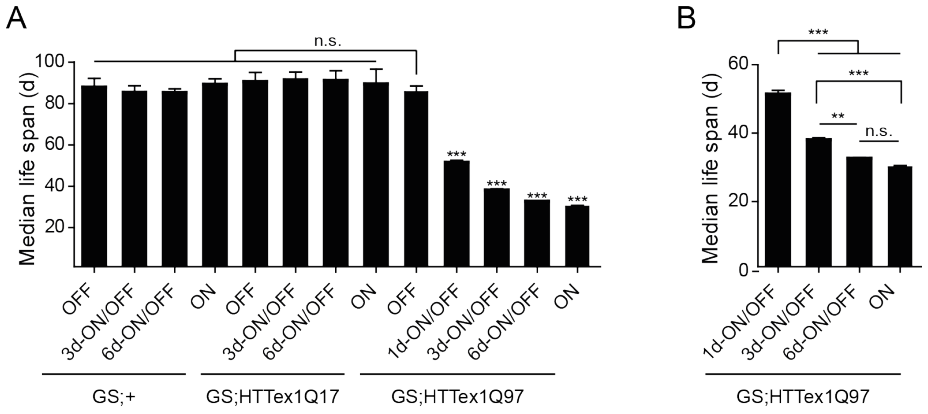

Figure 2.27: Comparison of the effects of HTT exon-1 expression for different periods of time on the survival of HD transgenic flies.
(A) Median life span of flies treated for different periods of time with the hormone ru-486 (GS;+, GS;HTTex1Q17 and GS;HTTex1Q97 flies). Error bars represent mean ± SEM from three independent replicates; one-way ANOVA Dunnett's post hoc test compared to untreated GS;HTTex1Q97; n.s. means not statistically significant; *** p <0.001. **(B)** Median life span of hormone treated GS;HTTex1Q97 flies. One-way ANOVA Tukey's post hoc test; n.s. means not statistically significant; ** p <0.01.

2.6.3 Investigation of HTTex1Q97 aggregation after short-time gene expression in HD transgenic flies

Long-time induction of HTTex1Q97 expression resulted in the time-dependent formation of insoluble protein aggregates in fly brains (Fig. 2.22). To analyze the HTT aggregate load after short-time gene induction, flies were treated for three or six days with the hormone and then cultured on normal food until they reached the treatment end point after 24 days (3d-ON/21d-OFF or 6d-ON/18d-OFF). Analysis of brain extracts with DB assays showed that no HTTex1Q97 aggregates are detectable after three days of expression using the MW8 antibody (Fig. 2.28 A). However, after further cultivation of flies on normal food without HTT expression for 21 days a significant amount of HTTex1Q97 aggregates was detectable with DB assays and FRAs (Fig. 2.28 A-C).

After six days of expression relatively small amounts of HTTex1Q97 aggregates were detectable by DB assays and FRAs (Fig. 2.28 A-C). Interestingly, in 6d-ON/18d-OFF treated flies the amount of the HTT aggregates was increased compared to flies that were treated for six days with the hormone (Fig. 2.28 A-C).

The biochemical investigations with DB assays and FRAs exhibited a higher HTT aggregate load in fly brains after the expression was turned off for 18 or 21 days. In order to verify these results, I also performed a systematic immunohistological analysis of fly brains. Flies were treated as described in Figure 2.28 and whole brains were stained with the antibodies MAB5492 and RBP (Fig. 2.29 A). Although no HTT aggregates were detectable in the filter assays after three days of expression, a very small amount of HTTex1Q97 aggregates was detectable in fly brains with immunohistological methods (Fig. 2.29 C). According to their position in the fly brain, the aggregates are located in the cell bodies that are clustered laterally to the antennal lobes [203]. As expected a higher amount of HTTex1Q97 aggregates was detectable in fly brains when the protein was expressed for six days (Fig. 2.29 D). Interestingly, flies treated for three days with subsequent cultivation on normal food for 21 days contained higher amounts of HTT aggregates compared to flies in which the transgene was only expressed for three days (Fig. 2.29 F). A similar result was also obtained when GS;HTTex1Q97$^{\text{6d-ON/18d-OFF}}$ transgenic flies were analyzed (Fig. 2.29 G).

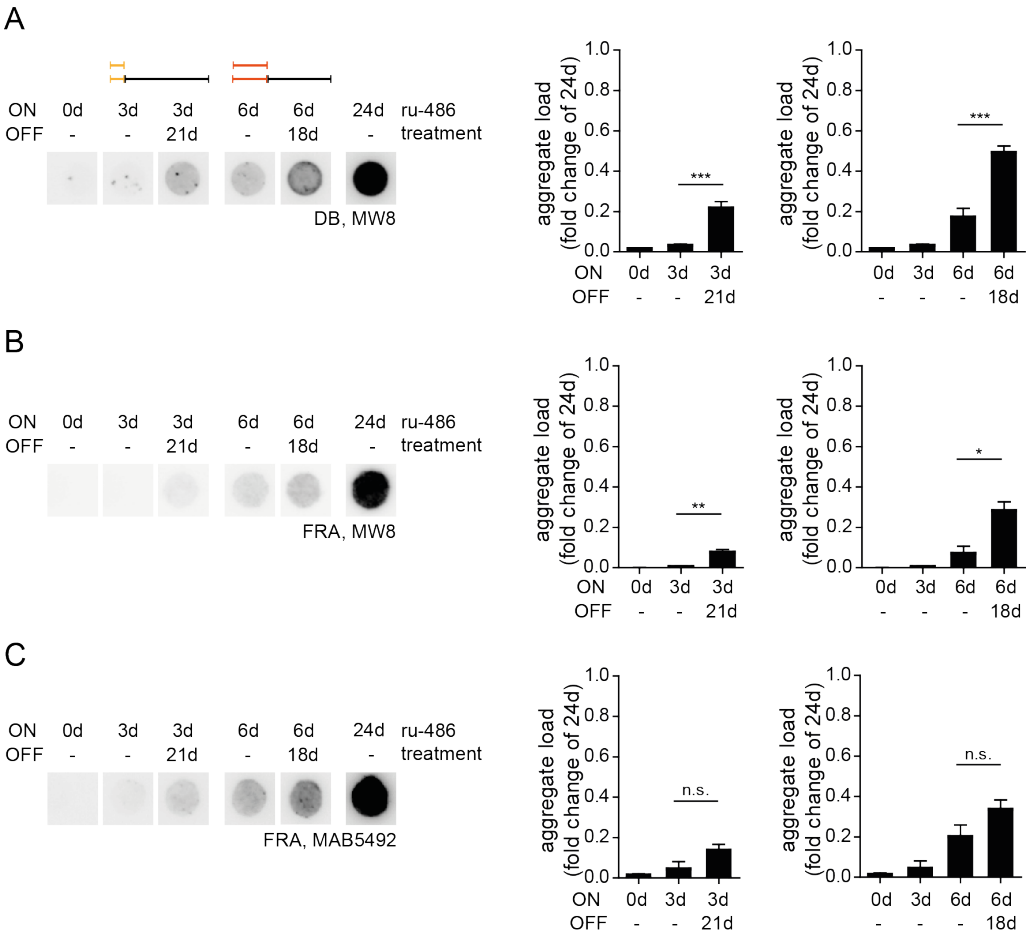

Figure 2.28: Analysis of HTTex1Q97 aggregate formation after short-time expression of the protein in neuronal cells.
(A) Analysis of HTTex1Q97 aggregate formation in hormone treated and untreated GS;HTTex1Q97 flies with DB assays (15 μg protein) using the MW8 antibody. Shown is a representative dot blot (left) of independent biological replicates (n = 3, 3, 3, 3, 3, 2) and the quantification of immunoreactive dots (right). Error bars represent mean $\pm$ SEM; unpaired t-test; *** p <0.001. **(B)** Analysis of HTT aggregate load in fly brains by FRAs (75 μg protein) using the MW8 antibody and quantification of immunoreactive dots; unpaired t-test; * p <0.05; ** p <0.01. **(C)** Analysis of HTT aggregate load in fly brains by FRAs (75 μg protein) using the MAB5492 antibody and quantification of immunoreactive dots; unpaired t-test; n.s. means not statistically significant.

In summary, the results indicate that the amount of HTTex1Q97 aggregates increases in fly brains over time even when the expression of the transgene was switched off for 18 or 21 days (Fig. 2.29 H). As an additional control, GS;HTTex1Q97 flies were cultured for 24 days on normal food. In these flies (24d-OFF), a slight antibody signal near the antennal lobes was detectable (Fig. 2.29 E and H).

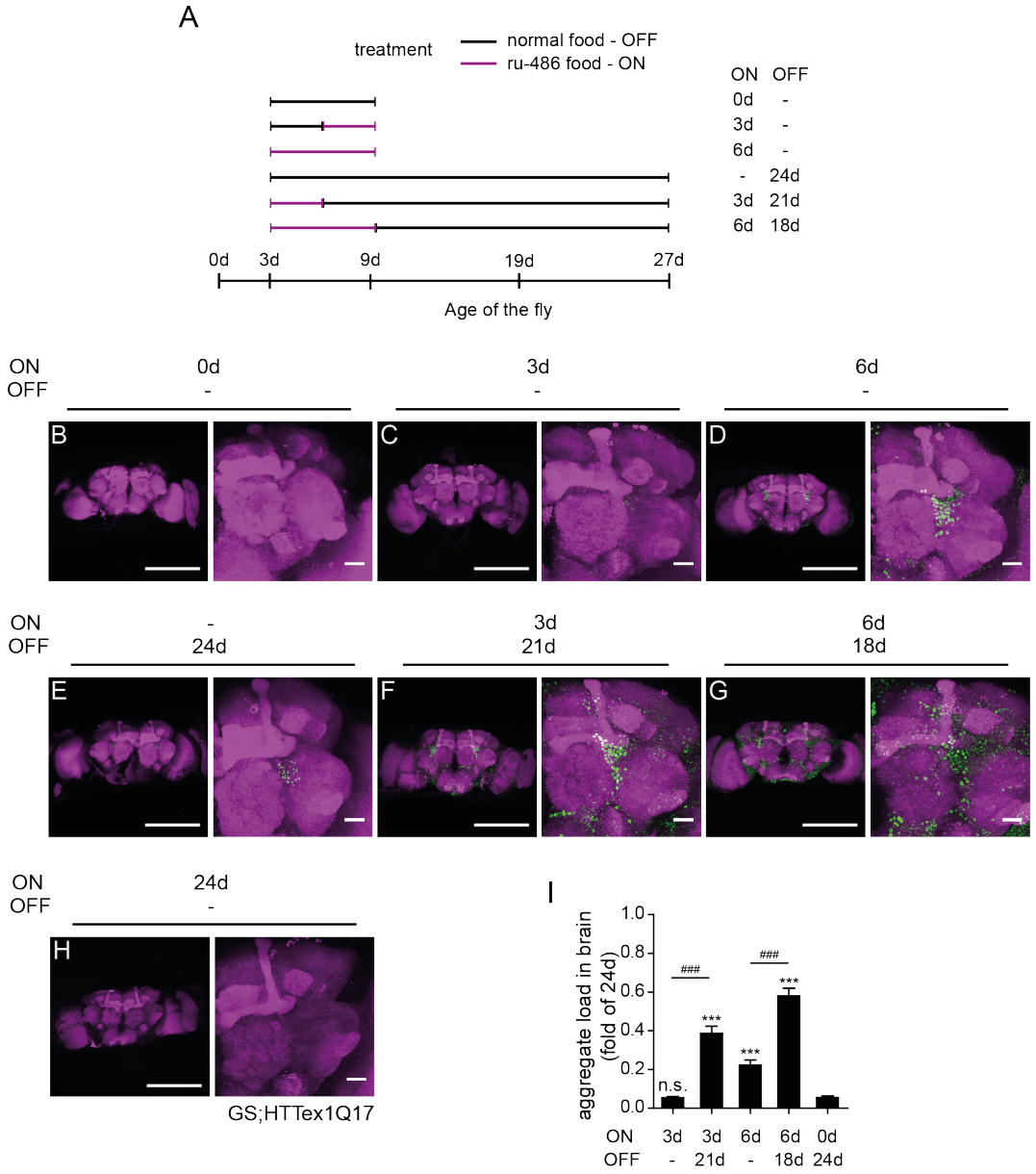

Figure 2.29: Analysis of HTT aggregate formation in *Drosophila* brains after short-time expression of the protein.
(A) Scheme of the hormone treatment strategy. **(B-G)** Representative confocal images of whole fly brains that were treated with and without hormone. The RBP staining is shown in magenta and the MAB5492 staining in green. For each group a representative whole brain (left, scale bars: 200 μm) and a magnification of the right central brain region (right, scale bars: 20 μm) is displayed. **(H)** Representative confocal images of the whole-brain of GS;HTTex1Q17$^{24d\text{-}OFF}$ flies. **(I)** Quantification of huntingtin antibody staining intensity measured over the whole brain. The HTT staining was normalized to GS;HTTex1Q97$^{24d\text{-}ON}$. Error bars represent mean $\pm$ SEM; one-way ANOVA Dunnett's post hoc test compared to GS;HTTex1Q97$^{24d\text{-}OFF}$; n.s. means not statistically significant; *** p <0.001. Unpaired t-test; ### p <0.001.

To exclude that the detected antibody signals are unspecific, the GS;HTTex1Q17 flies were cultured for 24 days on normal food and then analyzed using immunohistological methods. Since no aggregates were detectable in these flies, the signals in the GS;HTTex1Q97$^{24d\text{-}OFF}$ fly brains likely represents HTTex1Q97 aggregates. Although for 24 days no gene expression was induced in transgenic flies, HTT aggregates were reproducibly detected with immunihostological methods. Together these results indicate that the applied inducible Gene-Switch expression system is leaky and a low amount of HTT protein is produced also in non-induced flies. This very low background expression likely leads to a time-dependent accumulation of the HTT protein in fly brains. Interestingly, no phenotypic changes in climbing and survival were observed in these flies with an age of 27 days (Fig. 2.25 B and 2.26 A).

2.6.4 Short-time expression of HTTex1Q97 results in the formation of seeding-competent protein aggregates

Previous data showed that long-time induction of HTTex1Q97 leads to the formation of seeding-competent HTT aggregates in the fly heads (Fig. 2.23). In order to examine the seeding-competence of HTT aggregates that were produced by short-time expression, head lysates of GS;HTTex1-Q97$^{24d\text{-}ON}$, GS;HTTex1Q97$^{24d\text{-}OFF}$, GS;HTTex1Q97$^{3d\text{-}ON/21dOFF}$ and GS;HTTex1Q97$^{6\text{-}ON/18d\text{-}OFF}$ flies were analyzed using FRASE assays (Fig. 2.30 A).
I found that head lysates prepared from GS;HTTex1Q97$^{24d\text{-}OFF}$ flies show a similar kinetic in the FRASE assay than head lysates prepared from Elav;HTTex1Q17 flies that do not exhibit aggregates in the whole-brain stainings (Fig. 2.15, and 2.30 B). This indicates that the HTT aggregates, which are detectable in GS;HTTex1Q97$^{24d\text{-}OFF}$ flies by immunostaining analysis, are seeding-incompetent structures. In comparison, head lysates from long-time as well as the short-time induced flies showed a significant reduction of the lag phase, when the reporter proteins GST-HTTex1Q48-CyPet / -YPet were analyzed (Fig. 2.30 B and C). The head lysate of GS;HTTex1Q97$^{6d\text{-}ON/18d\text{-}OFF}$ flies shortens the lag phase more than head lysate of GS;HTTex1-Q97$^{3d\text{-}ON/21d\text{-}OFF}$ flies. Nevertheless, I did not observe a significant difference between the GS;-HTTex1Q97$^{6d\text{-}ON/18d\text{-}OFF}$ flies and GS;HTTex1Q97$^{24\text{-}ON}$ flies, although the long-time induced flies contain a substantial higher aggregate load in the brain as shown in DB assays and immunostainings (Fig. 2.28 and 2.29). This indicates that GS;HTTex1Q97$^{6d\text{-}ON/18d\text{-}OFF}$ flies already contain sufficient amount of HTT aggregates to accelerate the aggregation reaction similar than head lysates from GS;HTTex1Q97$^{24\text{-}ON}$ flies.

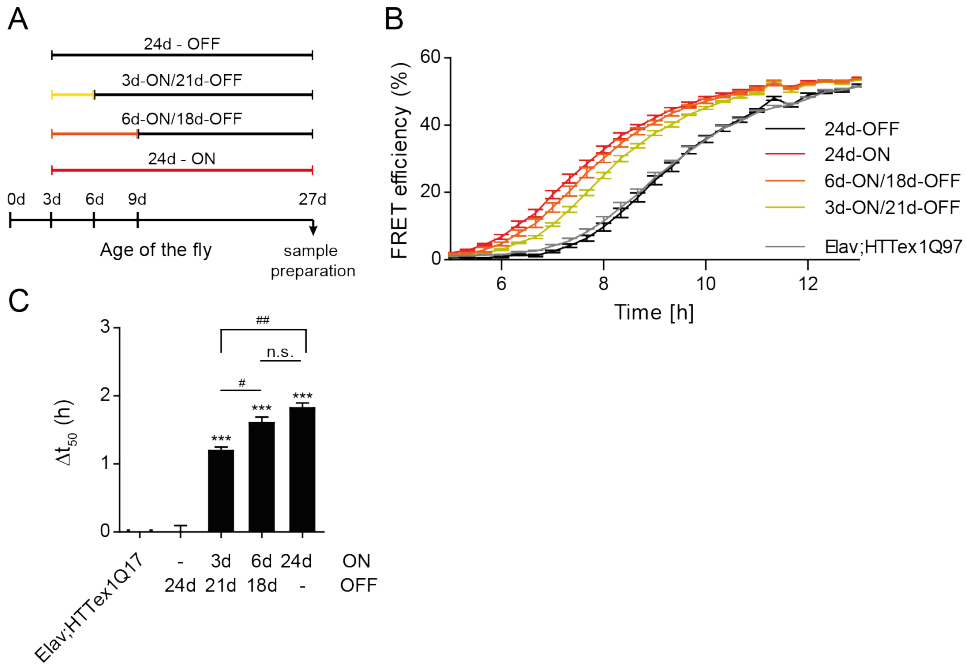

Figure 2.30: Short-time expression of HTTex1Q97 protein results in the formation of seeding-competent aggregates in fly brains.
(A) Scheme of hormone treatment of HD flies. The colors (red, orange and yellow) indicate treatment periods with the ru-486 hormone and black indicates the time where flies were cultivated on normal food. **(B)** Head lysates of GS;HTTex1Q97$^{24d\text{-}OFF}$ (black), GS;HTTex1Q97$^{24d\text{-}ON}$ (red), GS;HTTex1Q97$^{6d\text{-}ON/18d\text{-}OFF}$ (orange), GS;HTTex1Q97$^{3d\text{-}ON/21d\text{-}OFF}$ (yellow) and Elav;HTTex1Q97 flies were analyzed using the FRASE HTT seeding assay. Values are means ± SEM of three biological replicates each performed in triplicates. **(C)** Seeding activity was quantified by subtracting the t_{50} value of the sample from the control (GS;HTTex1Q97$^{24d\text{-}OFF}$). Error bars represent mean ± SEM; one-way ANOVA Dunnett's post hoc test compared to untreated flies; n.s. means not statistically significant; * p <0.05; ** p <0.01; *** p <0.001; One-way ANOVA Bonferroni's post hoc test; $^{\#}$ p <0.05; $^{\#\#}$ p <0.01.

2.6.5 Analysis of time-dependent HTTex1Q97 aggregation after short-time expression of the recombinant protein

To monitor the formation of HTTex1Q97 aggregates after short-time expression of the protein in flies, they were treated for six days with hormone and then cultivated for 2, 6, 10, 14, 18 and 22 days on normal food (Fig. 2.31 A). Analysis of head lysates with DB assays revealed that the amounts of HTT aggregates in the fly heads increases for ten days until steady state level is reached (Fig. 2.31 B).

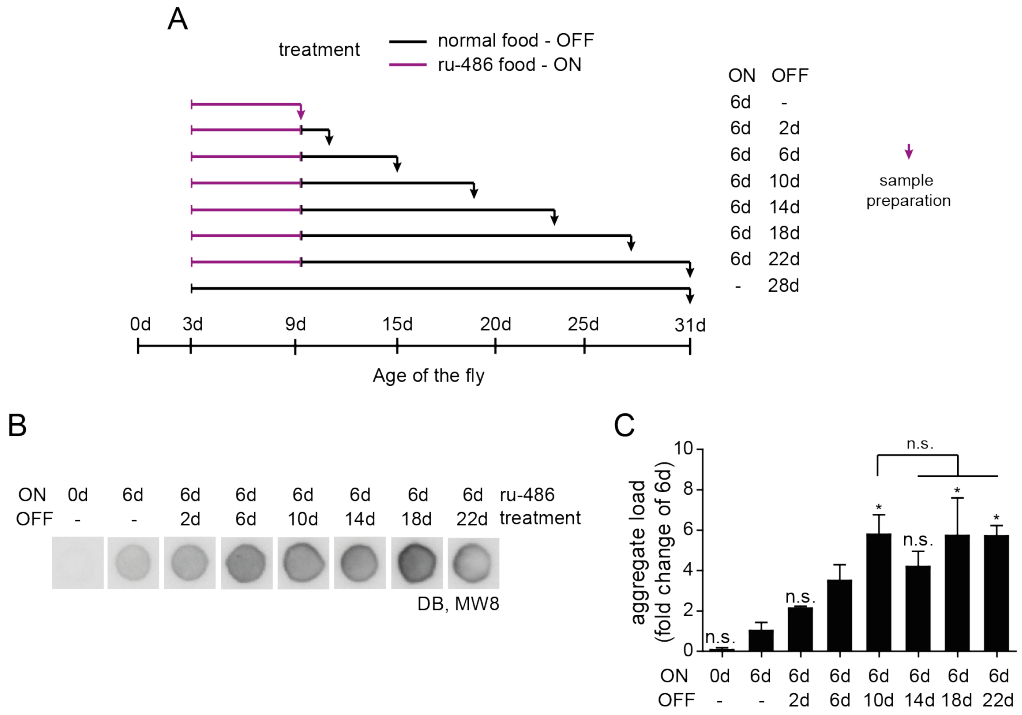

Figure 2.31: Time-dependent aggregation of the HTTex1Q97 protein after short-time expression in flies.
(A) Scheme of the hormone treatment of flies and the sample handling. The purple lines indicate the ru-486 treatment of flies, which started at day three post-eclosion and continued for six days. The black lines indicate untreated time periods. **(B)** Aggregate load in treated GS;HTTex1Q97 flies as analyzed by DB assays using the MW8 antibody. Shown is a representative dot blot of independent biological replicates (n = 3, 3, 3, 3, 3, 3, 3, 2). Equal amounts of protein were loaded (30 μg). **(C)** Quantification of the immunoreactive dots. Error bars represent mean $\pm$ SEM; one-way ANOVA Dunnett's post hoc test compared to 6d-ON or 6d-ON/10d-OFF treated GS;HTTex1Q97 flies; n.s. means not statistically significant; * p <0.05.

In order to verify these results, brains of hormone treated flies (similar to Fig. 2.31 A) were also systematically analyzed with immunohistological methods. A few brains are exemplarily shown (Fig. 2.32 A). As previously observed, HTT aggregates were found to be located in the cell bodies. The z-projection showed co-localization with the neuropil for a few HTT aggregates (white labeled huntingtin aggregates). The individual slices reveal no co-localization with the RBP signal. I found that the HTT aggregates in GS;HTTex1Q97$^{\text{6d-ON}}$ and GS;HTTex1Q97$^{\text{6d-ON/2d-OFF}}$ flies is not significantly different, but they have an altered localization in the brain (Fig. 2.32 A and B). After six days and ten days on normal food, the number of HTT aggregates was significantly increase compared to GS;HTTex1Q97$^{\text{6d-ON}}$ flies. Thus, similar to DB assays the immunohistological studies indicate that the amount of HTT aggregates increases over time in non-induced flies until a steady state level is reached after ten days (Fig. 2.32 B).

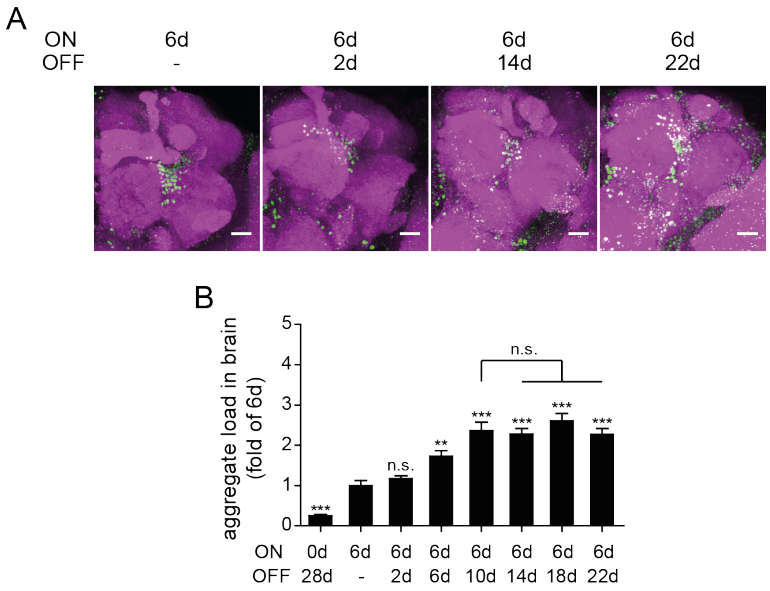

Figure 2.32: Analysis of HTT aggregation in HD flies after short-time expression of the protein in brains.
(A) Representative confocal images of whole brains of different GS;HTTex1Q97 flies after hormone treatment. The RBP signal is shown in magenta and the MAB5492 signal in green. For each group a representative magnification of the right central brain region (scale bars: 20 μm) is displayed. **(B)** Quantification of HTT antibody staining intensity measured over the whole brain. Error bars represent mean $\pm$ SEM; one-way ANOVA Dunnett's post hoc test compared to 6-ON or 6d-ON/10d-OFF treated GS;HTTex1Q97 flies; n.s. means not statistically significant; *** p <0.01; *** p <0.001.

2.6.6 The effect of short-time HTTex1Q97 expression on the life span of flies is age-independent.

Using an inducible *Drosophila* model of Alzheimer's disease, Iain Rogers and colleagues showed that aging increases the vulnerability of flies to Aβ42 aggregates. To analyze whether aging also influences HTTex1Q97 toxicity in HD flies, young (three days old) and old (30 days old) GS;HTTex1Q97 flies were treated for three days with the hormone ru-486 hormone and then flies transferred to non-hormone food were analyzed over time with the life span assay. I found that young treated flies display a median life span of 38 days, while old treated flies have a median life span of 63 days (Fig. 2.33 A and B). Thus, the time period between the turning-off of HTT expression and the death of the flies is very similar in both experimental paradigms. This suggests that age does not significantly influence the effect of the mutant HTT protein on the survival of flies (Fig. 2.33 C and D).

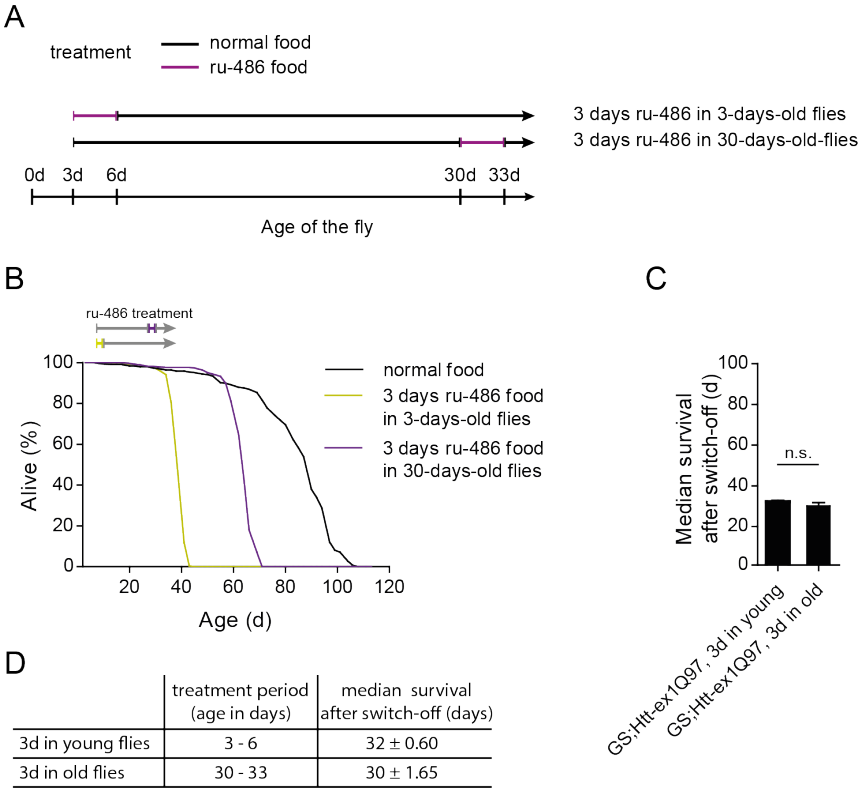

D

	treatment period (age in days)	median survival after switch-off (days)
3d in young flies	3 - 6	32 ± 0.60
3d in old flies	30 - 33	30 ± 1.65

Figure 2.33: Analysis of HTT aggregation in HD flies after short-time expression of the protein in brains.
(A) Representative confocal images of whole brains of different GS;HTTex1Q97 flies after hormone treatment. The RBP signal is shown in magenta and the MAB5492 signal in green. For each group a representative magnification of the right central brain region (scale bars: 20 μm) is displayed. **(B)** Quantification of HTT antibody staining intensity measured over the whole brain. Error bars represent mean ± SEM; one-way ANOVA Dunnett's post hoc test compared to 6-ON or 6d-ON/10d-OFF treated GS;HTTex1Q97 flies; n.s. means not statistically significant; *** p <0.01; *** p <0.001.

2.7 Modulation of mutant HTT aggregation and toxicity in HD transgenic flies

There are several possibilities to modulate HTT aggregation and toxicity [120] - [122]. In a currently ongoing study the application of an antisense oligonucleotide (ASO) drug is examined [123], which aims at the reduction of monomeric HTT protein level in patient brains. The results of the short-time treated GS;HTTex1Q97 flies suggest that a decrease of HTT expression with the Gene-Switch expression system when HTT aggregates have already formed in fly brains has a minor effect on disease progression and elongates the life span of flies only for a few days (Fig. 2.26). If the mechanism of the disease is similar in humans and in flies, the ASO approach might not work as a therapeutic approach because the toxic effects of HTT aggregates in patient brains cannot be efficiently reduced through inhibition of HTT expression. Another therapeutic approach for the treatment of HD is the identification of small chemical compounds that target HTT aggregates and their propagation. In previous studies it was demonstrated that chemical compounds can be successfully applied as an aggregation modifier, such as EGCG and methylene blue [120, 204]. Such molecules might be suitable as therapeutic drugs for the treatment of Huntington's disease because they might elongate the survival of HD patients for longer periods of time. To examine whether the mutant HTT aggregation and toxicity can be modulated by therapeutic molecules in *Drosophila* models of HD, I first investigated whether overproduction of the human molecular chaperone Hsp70 influences HTTex1Q97 aggregation and toxicity in HD transgenic flies.

2.7.1 Co-expression of the human molecular chaperone HSPA1L reduces HTTex1Q97-induced toxicity in HD transgenic flies

It has been shown previously that overproduction of the human protein Hsp70 (HSPA1L) suppresses polyQ-mediated toxicity and neurodegeneration in a *Drosophila* model of Machado-Joseph disease, also known as spinocerebellar ataxia type 3 [104]. To examine whether the co-expression of HSPA1L can suppress the HTT-induced toxicity, transgenic flies were generated containing the UAS-HSPA1L and UAS-HTTex1Q97 transgenes. The human HSPA1L gene encodes a 70 kDa heat shock protein Hsp70 and act as a molecular chaperone in cells by promoting the folding of translated proteins. It was integrated on the second chromosome in the *Drosophila* genome and therefore can be expressed in a similar manner as the HTT transgene. Flies bearing the HSPA1L and HTTex1Q97 (GS;HSPA1L;HTTex1Q97) transgenes were treated for six days with the hormone and were subsequently transferred to food that lacks the inducer ru-486 (Fig. 2.34 A). In control flies, the HSPA1L gene was expressed alone for six days (GS;HSPA1L$^{6d\text{-}ON/OFF}$). Finally, the survival of differently treated fly lines was assessed using the

established life span assay. I found that the median life span of GS;HSPA1L;HTTex1Q97$^{6d\text{-}ON/OFF}$ flies is 39 days, while the median life span of GS;HTTex1Q97$^{6d\text{-}ON/OFF}$ flies is 33 days (Fig. 2.34 B and C). This indicates that the co-expression of the molecular chaperone HSPA1L reduces the toxicity of the HTTex1Q97 protein and significantly extends the survival of flies. In comparison, the median life span of flies that express the HSPA1L gene but not the HTT gene is not significantly elongated (Fig. 2.34 C). Together these results indicate that the mutant HTT toxicity can be modulated by the overproduction of a molecular chaperone.

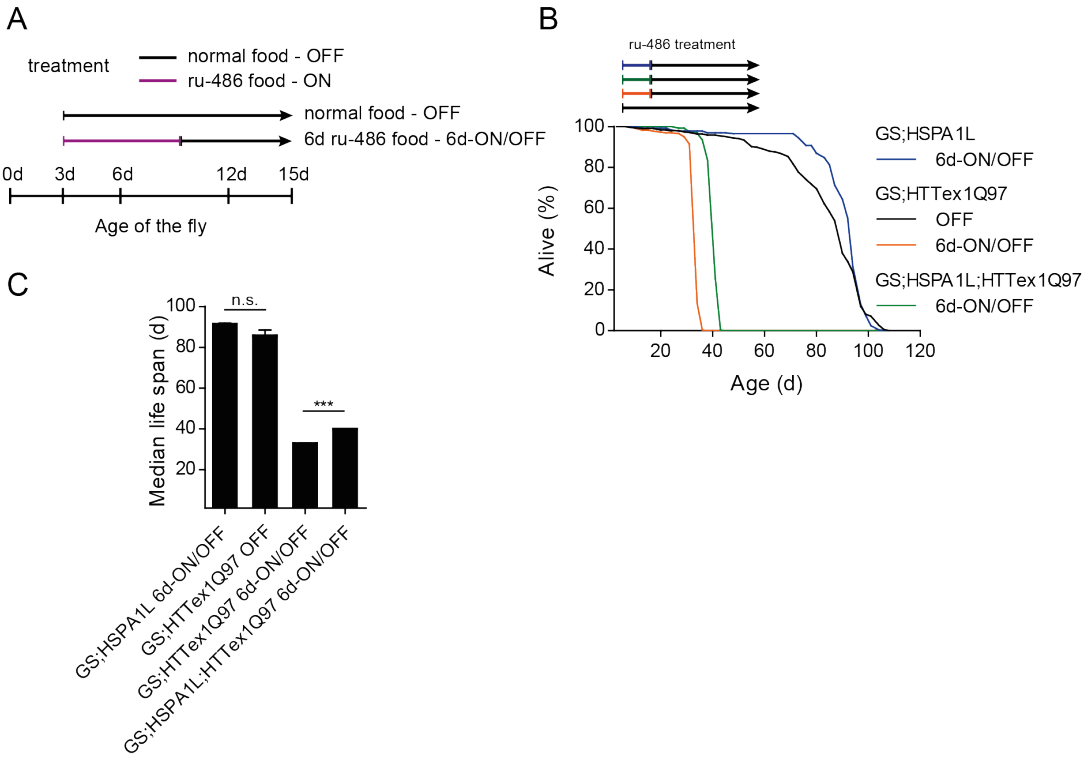

Figure 2.34: Co-expression of HSPA1L and HTTex1Q97 elongates the survival in HD transgenic flies.
(A) Scheme of the temporal hormone treatment strategy. The black lines indicate cultivation times without hormone treatment (normal food) and the purple lines indicate cultivation times with hormone treatment. The treatment started at day three post-eclosion. **(B)** Life span analysis of GS;HTTex1Q97^{OFF} (black), GS;HTTex1Q97$^{6dON/OFF}$ (orange), GS;HSPA1L;HTTex1Q97$^{6d\text{-}ON/OFF}$ (green) and GS;HSPA1L$^{6dON/OFF}$ (blue) flies. Life span is plotted as the percentage of surviving flies of two or three replicates (untreated GS;HTTex1Q97 n = 99, 96, 107; treated GS;HTTex1Q97 n = 108, 105, 94; GS;HSPA1L;HTTex1Q97 n = 103, 82, 83; GS;HSPA1L n = 91, 62). **(C)** Median life spans of treated and untreated fly lines. Error bars represent mean ± SEM from two / three independent replicates; unpaired t-test; *** p <0.001.

2.7.2 Co-expression of HSPA1L decreases the formation of seeding-competent HTTex1Q97 aggregates in HD transgenic flies

In order to analyze the effect of HSPA1L co-expression on the formation of HTTex1Q97 aggregates, head lysates from induced and non-induced flies (GS;HSPA1L;HTTex1Q97 and GS;HTTex1Q97) were systematically analyzed with DB assays and FRAs. Flies were treated for six days with hormone food and then transferred for four days to normal food lacking ru-486. Finally, brain lysates were prepared and analyzed with DB assays and FRAs. In comparison to control flies (GS;HTTex1Q97), I found a significant reduction of HTTex1Q97 aggregates in brains of GS;HSPA1L;HTTex1Q97 flies when samples were analyzed with DB assays (Fig. 2.35 A). This indicates that co-expression of HSPA1L significantly reduces the HTT aggregate load in fly heads. The amount of SDS- and heat-stable HTT aggregates in GS;HSPA1L;HTTex1Q97 flies was slightly reduced than in GS;HTTex1Q97 flies (Fig. 2.35 B).

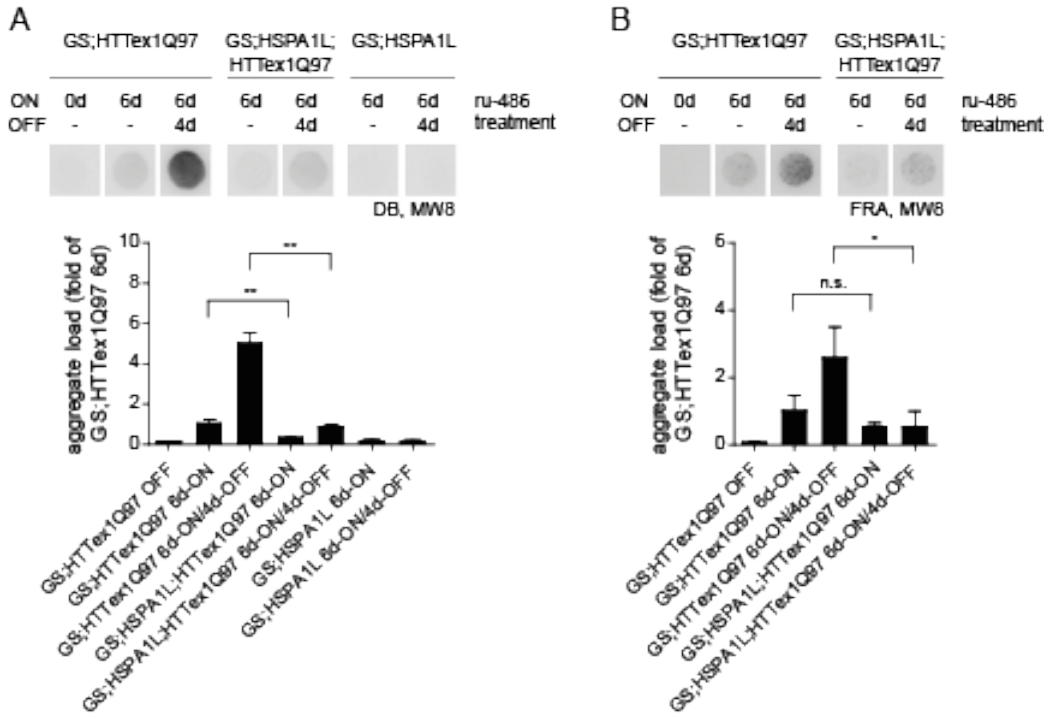

Figure 2.35: HSPA1L co-expression reduces the formation of HTT aggregates in transgenic fly heads.
(A) Analysis of HTTex1Q97 aggregation in treated and untreated HD transgenic fly lines with DB assays: GS;HTTex1Q97 flies, GS;HSPA1L;HTTex1Q97 flies and GS;HSPA1L flies. Equal amounts of protein were loaded onto membranes (30 μg) and analyzed using the MW8 antibody. Shown are representative dot blots (above) of independent biological triplicates and the quantification of immunoreactive dots (below). Error bars represent mean $\pm$ SEM; unpaired t-test; ** p <0.01. **(B)** Analysis of HTT aggregate formation using FRAs (150 μg protein). Aggregates were detected and quantified using the MW8 antibody (above) and quantification (below); unpaired t-test; n.s. means not statistically significant.

The GS;HSPA1L;HTTex1Q97 flies contain two UAS-transgenes, which might result in lower expression of both transgenes compared to flies that express a single transgene. In order to investigate whether the reduction of HTT aggregates in HSPA1L expressing flies is caused by a reduction of HTT gene expression, I quantified the HTT mRNA levels in both transgenic fly lines with a qPCR assay. I found that the HTT mRNA level in GS;HTTex1Q97 and GS;HSPA1L;HTTex1Q97 flies after six days of expression are not significantly different (Fig. 2.36 A), indicating same expression of HTTex1Q97 fragment in GS;HTTex1Q97 and GS;HSPA1L;HTTex1Q97 flies.
Next, I quantified the HSPA1L protein levels in head extracts of GS;HSPA1L and GS;HSPA1L;-HTTex1Q97 fly lines. Analysis of protein extracts by SDS-PAGE and immunoblotting revealed no significant difference in HSPA1L expression in GS;HSPA1L and GS;HSPA1L;HTTex1Q97 flies after six days of hormone treatment (Fig. 2.36 B and C), indicating that the reduction of HTT aggregates in GS;HSPA1L;HTTex1Q97 flies is caused by the overproduction of HSPA1L.

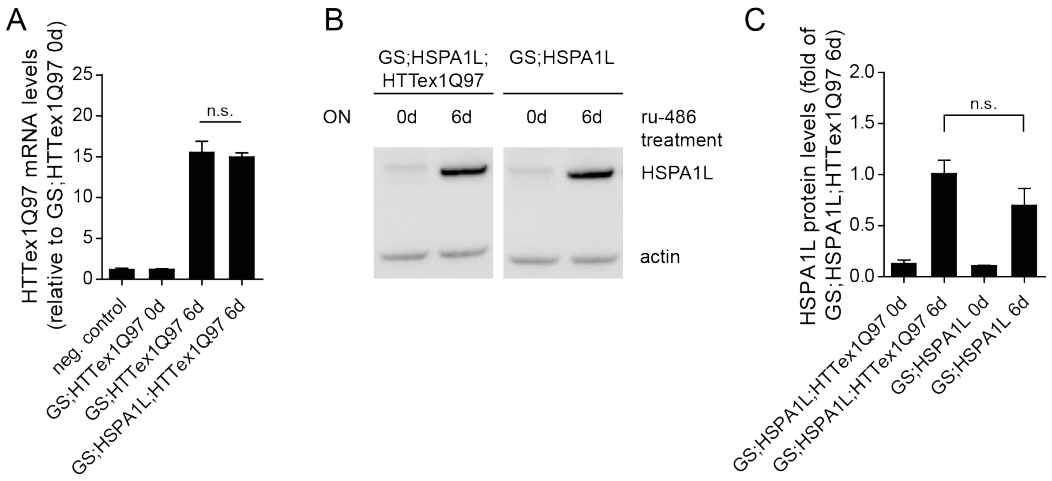

Figure 2.36: Analysis of HTTex1Q97 expression in GS;HTTex1Q97 and GS;HSPA1L;-HTTex1Q97 flies.
(A) Analysis of HTTex1Q97 mRNA levels in treated and untreated GS;HTTex1Q97 and GS;HSPA1L;HTTex1Q97 flies. Error bars represent mean ± SEM; unpaired t-test. **(B)** Comparison of HSPA1L protein levels in GS;HSPA1L;HTTex1Q97 and GS;HSPA1L flies before and after treatment with ru-486. Protein extracts prepared from fly heads were analyzed in SDS-PAGE and immunoblotting Equal amounts of protein were loaded (20 μg). **(C)** Quantification of HSPA1L protein levels form B. Error bars represent mean ± SEM; unpaired t-test.

Finally, I investigated whether the HTT aggregates in head lysates prepared from GS;HSPA1L;-HTTex1Q97 flies possess seeding activity using the established FRASE assay. Flies (GS;HTTex1-Q97 and GS;HSPA1L;HTTex1Q97) were treated for six days with hormone and then transferred for 18 days on normal food without hormone. In addition, flies (GS;HTTex1Q97) were investigated that were cultivated for 24 days on normal food lacking the hormone. I found that the HTT seeding activity in head lysates prepared from GS;HSPA1L;HTTex1Q97$^{6d\text{-}ON/18d\text{-}OFF}$ flies is significantly lower than the seeding activity in head lysates that were prepared from GS;HTTex1Q97$^{6d\text{-}ON/18d\text{-}OFF}$ flies (Fig. 2.37 A and B). These results indicate that HSPA1L co-expression decreases the abundance of seeding-competent HTTex1Q97 aggregates in *Drosophila* brains.

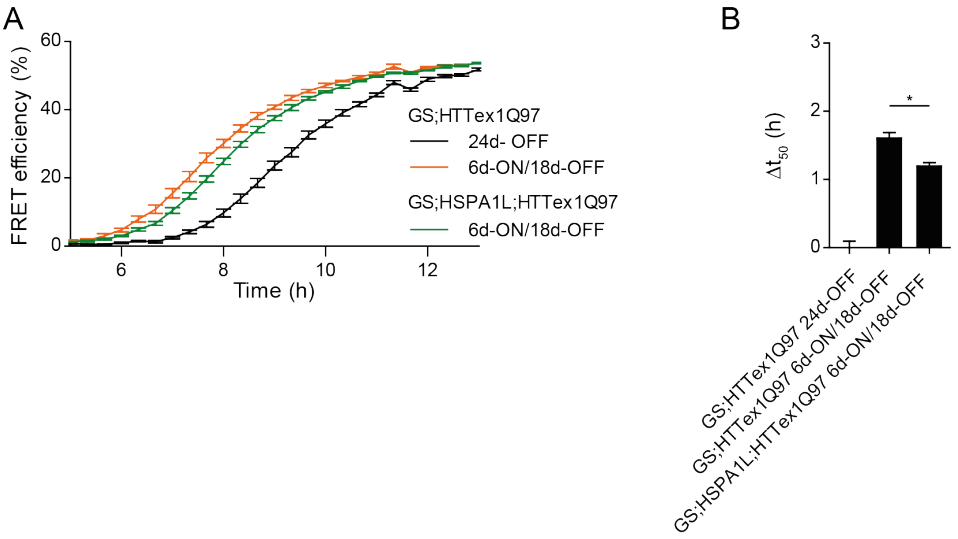

Figure 2.37: HSPA1L co-expression reduces the seeding activity of mutant HTT aggregates in *Drosophila* brains.

(A) Head lysates of GS;HTTex1Q97$^{24d\text{-}ON}$ (black), GS;HTTex1Q97$^{6d\text{-}ON/18d\text{-}OFF}$ (orange), GS;HSPA1L;HTTex1Q97$^{6d\text{-}ON/18d\text{-}OFF}$ (green) flies were analyzed using the FRASE HTT seeding assay. Values are means ± SEM of three biological replicates each performed in triplicates. **(B)** Quantification of the HTT seeding activity in fly brain extracts by subtracting the t_{50} value of the sample from the control (GS;HTTex1Q97$^{24d\text{-}OFF}$). Error bars represent mean ± SEM; unpaired t-test; * p <0.05.

2.7.3 The molecular chaperone HSPA1L co-localizes with HTT aggregates in HD transgenic fly brains

Previous studies have shown that the *Drosophila* Hsp70 protein co-localizes with nuclear inclusions that contain the ATXN3 protein in a *Drosophila* model of Machado-Joseph disease [104]. To examine whether the human HSPA1L protein co-localizes with the HTT aggregates in HD flies, a whole brain staining of GS;HSPA1L;HTTex1Q97 flies was performed. The antibodies anti-HSPA1L and MAB5492 were used for the detection of HTT aggregates and the protein HSPA1L. I found that a large fraction of the produced HSPA1L co-localizes with punctate HTT aggregates in fly brains (Fig. 2.38). These studies indicate that the punctate HTT aggregates are encased by the HSPA1L protein, which forms a halo around the aggregated proteins (Fig. 2.38, white arrows).

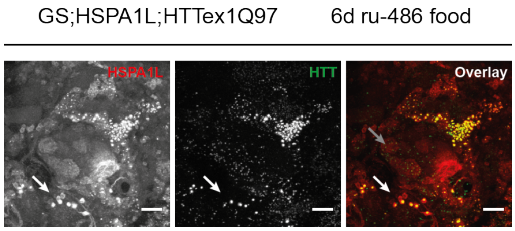

Figure 2.38: HSPA1L localizes with punctate HTT aggregates in brains of HD transgenic flies.
Representative confocal images of the right central brain regions GS;HSPA1L;HTTex1Q97$^{6d\text{-}ON}$ flies. The HSPA1L signal is shown in red and the HTT signal (MAB5492) in green (scale bars: 20 μm). The white arrow indicates co-localization of HSPA1L with HTT aggregates. The grey arrow indicates areas in the brain where the HSPA1L protein is not associated with HTT aggregates.

2.8 Investigating the effects of small molecules on mutant HTT aggregation in cell and fly models of HD

My studies indicate that the molecular chaperone HSPA1L is able to decrease mutant HTT-induced toxicity and to elongate the survival of HD transgenic flies that express the HTTex1Q97 protein in neurons (Fig. 2.34). Next, I assessed whether chemical compounds can be identified that directly target HTT aggregates and reduce their toxicity in HD transgenic flies.

2.8.1 High throughput screening of small molecule modulators of HTTex1Q48 aggregation in SH-EP cells

To find chemical compounds that modulate HTT aggregation and toxicity, a cell-based assay was established. The principle of this method is shown in Figure 2.39 A. The assay facilitates the detection of small molecules that promote the clearance of pre-aggregated Alexa633-labelled HTTex1Q48 aggregates in SH-EP cells (Fig. 2.39 A). After establishment of the assay, I screened 1200 chemical compounds (FDA approved drugs and natural compounds) for their ability to promote the clearance of HTT aggregates in SH-EP cells. All compounds were tested at a concentration of 10 μM for 48 hours in the cell-based assay (Fig. 2.39 A). The HTT aggregate load in cells as well as the cell number was quantified using a high content microscope. The systematic screening in cells revealed 13 primary hit compounds (Fig. 2.39 B), including known inhibitors of HTT aggregation such as EGCG [120], which were further investigated in other model systems.

To validate the effects of the initially identified small molecules, additional studies were performed with hit compounds in mammalian cells. In this case the effects of compounds on the degradation of preformed HTTex1Q48-YPet aggregates was assessed (Fig. 2.39 B). I confirmed that 13 compounds decrease the abundance of HTTex1Q48-YPet aggregates in SH-EP cells, suggesting that they might also be active in HD transgenic flies.

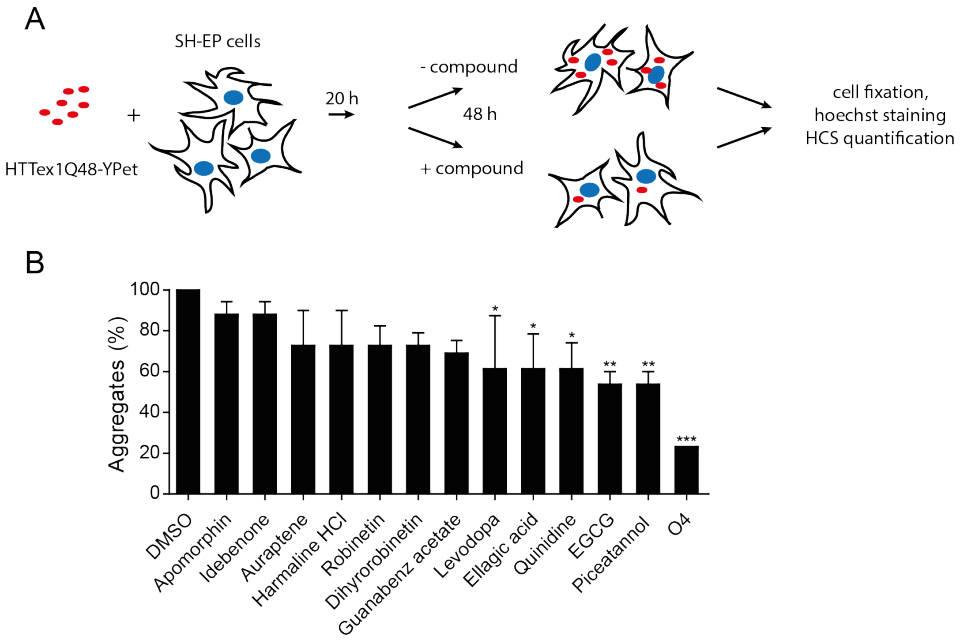

Figure 2.39: Identification of chemical compounds that decrease the abundance of preformed HTT aggregates in SH-EP cells.
(A) Scheme of the assay procedure. Labelled HTT aggregates were incubated with SH-EP cells and then treated with chemical compounds (~1200 FDA approved drugs and natural compounds). After 48 hours the cells were fixed and analyzed with a high content screening reader. **(B)** Effects of hit compounds on HTT aggregate load in SH-EP cells; compound effects were normalized to DMSO. Error bars represent mean ± SEM of three technical replicates; one-way ANOVA Dunnett's post hoc test compared to DMSO; * p <0.05; ** p <0.01; *** p <0.001.

2.8.2 Analysis of selected hit compounds in HD transgenic flies

To investigate whether the hit compounds that are active in cell-based assays (Fig. 2.39) can influence mutant HTT aggregation in HD transgenic flies, I first treated three days old GS;HTTex1Q97 flies that do not express the transgene for four days with the selected compounds (Fig. 2.40 A). Then, the flies were transferred for six days to food that contains both the hormone and the selected compounds to induce HTTex1Q97 expression to potentially inhibit aggregation. Finally, after six days on hormone / compound food, the flies were transferred for additional four days to food that only contains the compounds, which preferentially influence HTT aggregation (Fig. 2.40 A). Thus, in this experimental paradigm the effects of chemical compounds in the spontaneous formation of HTTex1Q97 aggregates and their clearance will be assessed in fly brains. Furthermore, through the initial pretreatment of flies with the chemical compounds for four days it should be ensured that the compounds are already presented in fly brains before the expression of the HTTex1Q97 protein is induced by hormone addition. Finally, the effects of chemical com-

pounds on HTT aggregation are quantified with DB assays using the MW8 antibody.
All compounds were dissolved in ethanol and mixed into the fly food with a final concentration of 1 % ethanol and 1 mM compound. Flies that were treated exclusively with the hormone were labeled as ”compound” and flies cultivated on normal food without compound were labelled as ”-ru486 / -compound”.

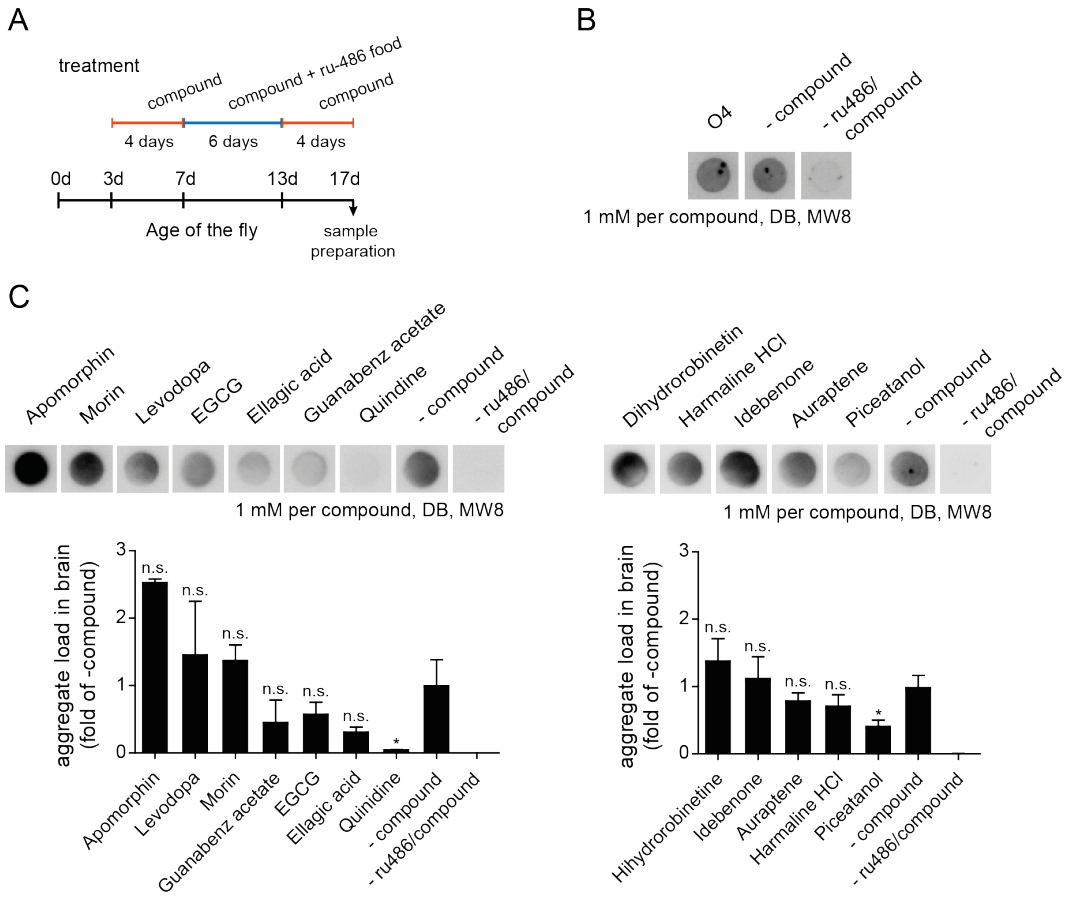

Figure 2.40: Analysis of hit compound in the inducible *Drosophila* model of HD.
(A) Scheme of the compound and hormone treatment procedure. The flies were treated for four days with the compound, followed by six days on food with the hormone and the compound. Subsequently the flies were transferred onto compound food for four days. **(B)** Effect of the compound O4 on the formation of HTTex1Q97 aggregates in GS;HTTex1Q97 flies. Aggregates were detected with DB assays (30 μg protein were spotted onto membranes). The treatment of flies with O4 did not influence HTTex1Q97 aggregation. **(C)** Analysis of the hit compounds on the aggregate load in GS;HTTex1Q97 flies. Compound effects were quantified with DB assays (30 μg protein) using the MW8 antibody. Shown is a representative dot blot (above) of independent biological triplicates and the quantification of the dots on the membrane (below). Error bars represent mean $\pm$ SEM; one-way ANOVA Dunnett's post hoc test compared to -compound; n.s. means not statistically significant; * p <0.05.

I found that the compound O4 that potently influences polyQ-mediated HTT aggregation in cell-free and cell-based assays does not reduce HTTex1Q97 aggregation in HD flies. The known modulators of HTT aggregation such as EGCG, Ellagic acid and Guanabenz acetate [120, 205] showed a weak effect on HTT aggregation in transgenic flies. However, compared to control flies this effect was not statistically significant (Fig. 2.40 B). Interestingly, the compounds Piceatanol and Quinidine most potently decreased the formation of HTTex1Q97 aggregates in brains of HD transgenic flies (Fig. 2.40 C). The compound Quinidine is an FDA approved drug that act as a class 1a antiarrhythmic agent [206]. It works by blocking the fast inward sodium current in cells.

2.8.3 Quinidine treatment reduces the abundance of HTTex1Q97 aggregates in brains of HD transgenic flies

The initial experiments showed that 1 mM Quinidine effectively reduces the formation of HTT aggregates in GS;HTTex1Q97 flies. In order to determine the effective dose, transgenic flies were next exposed to different concentrations of Quinidine and fly head lysates were then systematically analyzed with DB assays and FRAs (Fig. 2.41 A). The treatment of flies with 0.5 mM Quinidine had no effect on the formation of HTTex1Q97 aggregates (Fig. 2.41 B). However, with higher concentrations of Quinidine, the level of aggregates was decreased in a concentration-dependent manner. The administration of 1 or 2 mM Quinidine nearly complete prevented of formation of HTTex1Q97 aggregates when samples were analyzed with DB assays. The analysis of head lysates with FRAs revealed similar results (Fig. 2.41 C and D), indicating that concentrations of Quinidine between 0.2 mM and 2 mM are sufficient to decrease the abundance of large SDS-stable aggregates in fly brains.

To confirm the results obtained with DB assays and FRAs (Fig. 2.41), whole brains of treated and untreated GS;HTTex1Q97 flies were also analyzed with immunohistological methods. Analysis of brains with confocal microscopy revealed that treatment of HD flies with 1 mM Quinidine indeed significantly reduces the abundance of large HTTex1Q97 aggregates in the fly brains (Fig. 2.42 A and B).

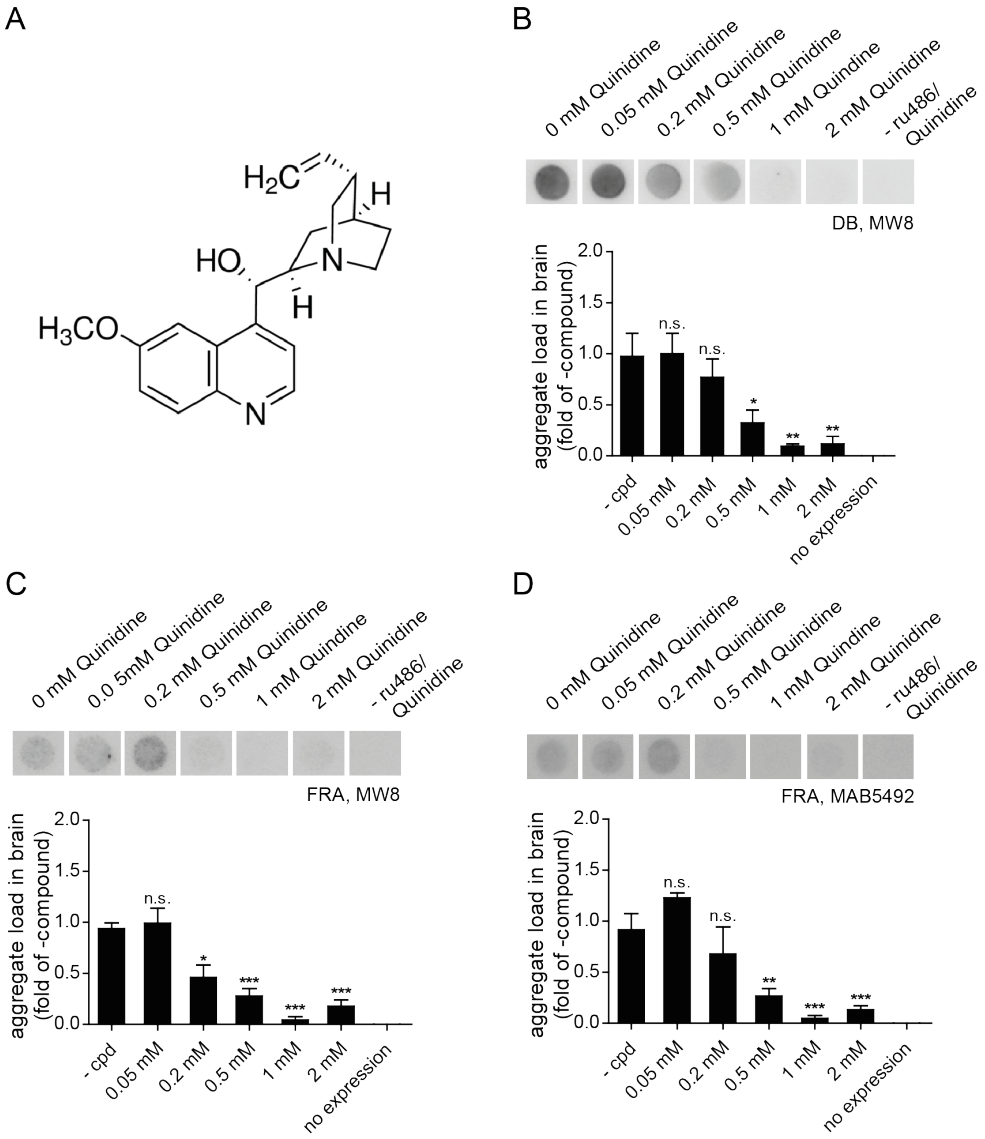

Figure 2.41: Treatment of flies with Quinidine reduces the abundance of large HTTex1Q97 aggregates in heads of HD transgenic flies.
(A) Quinidine structure. **(B)** Effects of Quinidine on the HTTex1Q97 aggregate load in GS;HTTex1Q97 flies; samples were analyzed by native DB assays. Flies were treated as shown in Figure 2.40. Equal amounts of protein were loaded (30 μg) analyzed using the MW8 antibody. Shown is a representative dot blot (above) of independent biological triplicates and the quantification of the dots on the membrane (below). Error bars represent mean $\pm$ SEM; one-way ANOVA Dunnett's post hoc test compared to 0 mM Quinidine; n.s. means not statistically significant; * p <0.05, ** p <0.01. **(C)** Effects of Quinidine on the aggregate load in HD flies; samples were analyzed with FRAs (150 μg protein) using the MW8 antibody. Error bars represent mean $\pm$ SEM; one-way ANOVA Dunnett's post hoc test compared to 0 mM Quinidine. **(D)** Effects of Quinidine on the HTT aggregate load in HD flies; samples were analyzed with FRAs using the MAB5492 antibody.

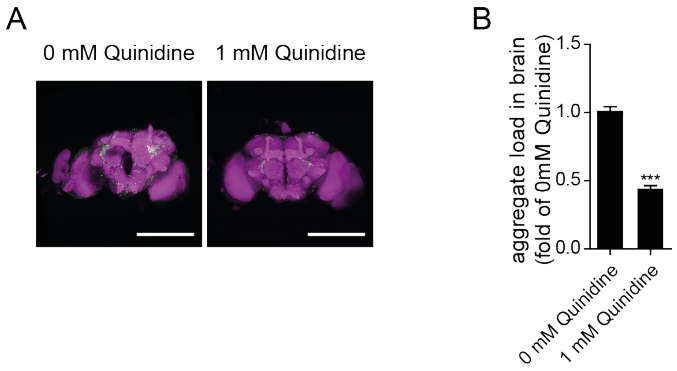

Figure 2.42: Quinidine treatment decreases the abundance of large HTTex1Q97 aggregates in fly brains.
(A) Representative confocal images of whole brains of Quinidine treated and untreated flies. Flies were treated as described in Figure 2.40. The RBP signal is shown in magenta and the MAB5492 in green (scale bars: 200 μm). **(B)** Quantification of HTT antibody staining intensity measured over the whole brain of GS;HTTex1Q97 flies (0 mM n = 8; 1 mM n = 4). Error bars represent mean $\pm$ SEM; unpaired t-test; *** p <0.001.

2.8.4 Investigating the effects of Quinidine treatment on the survival of HD transgenic flies

My investigations indicate that Quinidine effectively reduces the formation of insoluble HTT aggregates in heads of HD transgenic flies. To study whether long-time treatment with Quinidine influences the life span of HD flies, they were treated with the compound as shown in Figure 2.43 A. Surprisingly, my systematic studies revealed that the treatment of flies with increasing concentrations of Quinidine decreases survival of flies (Fig. 2.43 B and C). This indicates that either the compound per se is toxic for flies or through Quinidine treatment even more toxic HTT aggregates are formed in brains.
In order to analyze whether Quinidine per se is toxic for flies, I also treated chronically three days old GS;HTTex1Q97 flies with 1 mM Quinidine and investigated their survival in life span assays. These flies showed no reduction in survival after 60 days of treatment suggesting that the compound per se is non-toxic for flies. Thus, my studies indicate that Quinidine only indices toxicity in flies when mutant HTT protein is expressed at least for a short time.

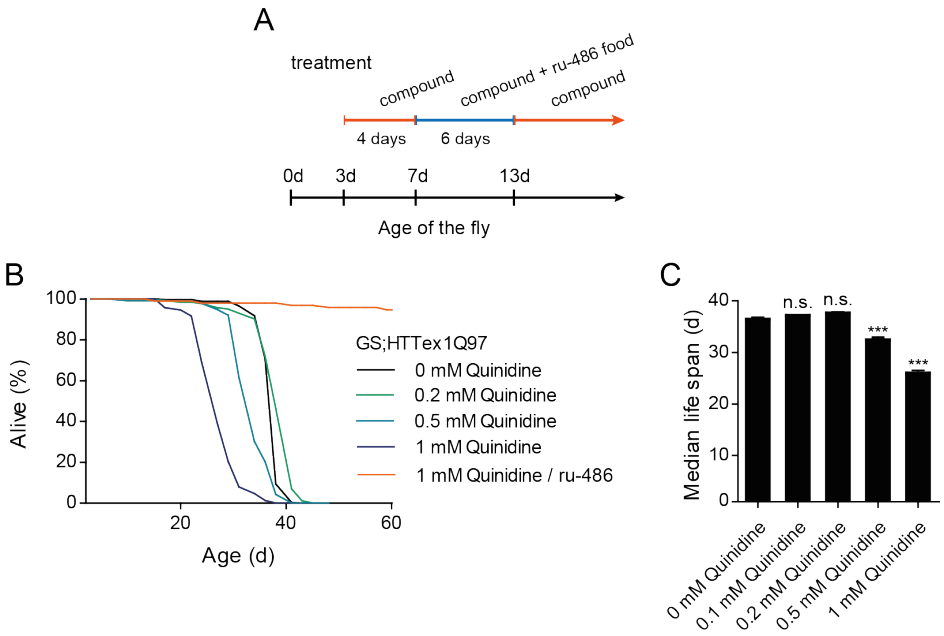

Figure 2.43: Quinidine treatment shortens the life span of HD transgenic flies.
(A) Scheme of the Quinidine treatment procedure. The GS;HTTex1Q97 flies were cultivated on food with Quinidine for four days and were then transferred on to food with hormone and Quinidine for six days. Then, they were cultivated on food with Quinidine alone until they die. **(B)** Life span analysis of flies treated with 0 mM (black), 0.2 mM (green), 0.5 mM (cyan) and 1 mM Quinidine (blue). As a control group, three days old flies were treated continuously with 1 mM Quinidine without hormone treatment (orange). Flies were analyzed for 60 days. The survival is plotted as the percentage of surviving flies of three replicate (0 mM Quinidine n = 86, 96, 82; 0.2 mM Quinidine n = 84, 90, 83; 0.5 mM Quinidine n = 81, 74, 67; 1 mM Quinidine n = 90, 102, 89; 1 mM Quinidine / -ru486 n = 95). **(C)** Median life span of HD flies treated with different concentrations of Quinidine. Error bars represent mean ± SEM; one-way ANOVA Dunnett's post hoc test compared to 0 mM Quinidine; n.s. means not statistically significant; *** p <0.001.

3 Discussion

In the present thesis, I have generated new *Drosophila melanogaster* models of Huntington's disease (HD) and characterized these models by a combination of biochemical and behavioral analyses. The systematic characterization of the exon-1 fly models revealed polyQ length-dependent behavioral phenotypes and time-dependent aggregation of mutant HTT fragments.
Subsequently, I have focused on the establishment of an inducible *Drosophila* model of HD that allows the production of mutant HTTex1Q97 in adult flies. The transgenic flies were subsequently analyzed with regard to long-term and short-term expression of the mutant HTT fragment. Chronic as well as short-time expression of the mutant HTT protein resulted in locomotion impairments and reduced survival. Moreover, lifespan analysis revealed that age does not influence the effect of mutant HTT expression. Finally, the effect of a molecular chaperone and chemical compounds on mutant HTT was investigated.

3.1 Modeling HD in *Drosophila melanogaster*

3.1.1 The generated fly models of HD allow comparative studies of different transgenic fly lines

The new *Drosophila melanogaster* models of Huntington's disease (HD) contain HTT fragments of different sizes, including the HTT exon-1 fragment, HTT fragments with the first 513 amino acids or full-length HTT. The different HTT fragments were combined with different CAG repeats containing wild-type and mutant-associated repeats. The transgenic flies containing the wild-type and mutant HTT fragments were generated using the site-specific ΦC31 integrase [165, 166]. This approach provides a benefit over the previously used HD fly models mentioned in Table 1.2 that were produced by p-element mutagenesis [58], [144] - [147]. The p-element mutagenesis leads to a random insertion of the transgene in the fly genome [159]. The location of the transgene, however, can influence the expression of the gene of interest, in particular in heterochromatin rich regions that are tightly coiled and genetically inactive [207]. Lower expression levels could lead to a weaker phenotype in the transgenic flies. This is especially important when the effects of fragments with the same amino acid sequence but different CAG repeats are compared. The extent to which the expression level of transgenes influences the phenotype has

been shown descriptively by Weiss *et al.* [208]. The pan-neuronal expression of a cDNA fragment that encodes a 588 amino acid long N-terminal human HTT fragment with 138 glutamine repeats, which was located in two different chromosomal regions in transgenic flies, revealed a difference in the median lifespan of these fly lines of approximately 30 days. This dramatic difference illustrates the influence of different expression levels on mutant HTT-induced toxicity. In comparison, the newly generated transgenic HD flies that were produced by inserting the HTT cDNAs in the same landing site should display equal expression levels. Indeed, this was confirmed by the analysis of HTT mRNA levels of induced GS;HTTex1Q17 and GS;HTTex1Q97 flies (Fig. 2.19). The GS;HTTex1Q17 and GS;HTTex1Q97 flies produced approximately equal HTT transcript levels. Therefore, this integration system is a powerful tool that enables the direct comparison of flies expressing different transgenes and HTT fragments in particular.

3.1.2 Exon-1 proteins are efficiently produced in HD transgenic flies

The production of short N-terminal HTT fragments has been observed in transgenic mouse models and brains of HD patients [9]. In mice expressing full-length HTT, N-terminal fragments with a size comparable to exon-1 are generated by proteolysis or alternative splicing [59, 191]. This fragment has been widely used to study mutant HTT induced toxicity and aggregation *in vitro* and in different animal and cellular models of HD [56, 58, 68, 103, 191, 209].
Hence, HD flies that produce HTT exon-1 proteins with different polyQ lengths including Q0, Q17, Q49 and Q97 were generated. These glutamine lengths (e.g. Q17, Q49 and Q97) represent a number of wild-type and mutant-associated lengths. The HTTex1Q0 fragment does not reflect a healthy individual, as a glutamine length of at least 6 was reported in humans [210]. Since the *Drosophila* homologue of human HTT does not contain a glutamine repeat within the exon-1 [211] and Lee *et al.* used an N-terminal HTT fragment with zero glutamines as a control fragment [146], this fragment was integrated in the analysis of this thesis. First, the expression of the HTTex1Q0, HTTex1Q17, HTTex1Q49 and HTTex1Q97 proteins was analyzed by Western blotting and immunohistochemistry (Fig. 2.7 and 2.13). Surprisingly, these studies revealed that soluble HTT exon-1 proteins cannot be detected in flies, while insoluble HTTex1Q97 aggregates were detectable. In contrast, the soluble HTT513 and HTTfl proteins were monitored using the anti-HTT antibody MAB2166 that has been used previously to detect full-length HTT in transgenic fly heads (Fig. 2.2 and 2.6) [147]. I suggest that the soluble HTT exon-1 proteins are rapidly degraded in flies. In previous studies, the production of HTT exon-1 fragments in transgenic flies was not sufficiently examined with HTT-specific antibodies. In a recent study, the expression of HTT exon-1 fragment with a fluorescent tag was shown by Western blotting using a GFP-specific antibody [208]. However, such a tag could increase the solubility of the HTT exon-1 proteins and thereby facilitate the detection. The group of Lawrence Marsh pub-

lished two studies in which HTT exon-1 proteins were shown by Western blotting. However, in both studies the applied antibodies were not disclosed [58, 212]. Since the transcription of the exon-1 fragments and the aggregation of HTTex1Q49 and HTTex1Q97 were shown (Fig. 2.7), it can be assumed that the HTTex1Q0, HTTex1Q17, HTTex1Q49 and HTTex1Q97 proteins are expressed in the transgenic flies.

3.1.3 PolyQ-length dependent aggregation and toxicity of HTT exon-1 fragments in HD transgenic flies

The new *Drosophila* fly models of HD that expresses the HTT exon-1 proteins constitutively exhibited an explicit polyQ length-dependent toxicity phenotype and aggregation behavior. This observation is in agreement with previous findings in other polyQ disease model systems such as the yeast *Saccharomyces cerevisiae*, the zebrafish *Dario rerio*, the worm *Caenorhabditis elegans*, an the fruit fly *Drosophila melanogaster* [92], [213] - [216].
In detail, the expression of the HTTex1Q0 and HTTex1Q17 fragment has no influence on the photoreceptor cell morphology, locomotor performance and the survival (Fig. 2.8, 2.9 and 2.11). These results are in agreement with the data of Lee *et al.*, who showed that the expression of a HTT exon-1 fragment without glutamines (Htt-Q0) have no discernible effect on behavior, lifespan or neuronal morphology [146]. Melkani *et al.* showed that Httex1-Q25-eGFP expressing flies have a similar life span than flies that contain exclusively the heart-specific gene driver [216]. In the same study of Melkani *et al.*, the cardiac-specific expression of Httex1-Q49-eGFP exhibited a significant reduction of the life span [216]. This result is very similar to my study where the expression of HTTex1Q49 in transgenic flies leads to a significant reduction of the survival (Fig. 2.9). The expression of HTTex1Q49 showed no eye degeneration, however, a very severe eye phenotype was observed when the HTTex1Q97 protein was produced in flies (Fig. 2.11). Several studies also described a dramatic degeneration of photoreceptor cells in flies that express the HTT.Q93.ex1p fragment or other mutant HTT fragments, including HTTQ120, HTT.128Q.1-336, HTT.Q128, HTT.128Q.FL, in the *Drosophila* eye [58], [144] - [147]. Furthermore, an impaired locomotion and dramatic shortened survival was observed in flies expressing the HTTex1Q97 fragment, which was also described in previous studies (Fig. 2.9). Menzies *et al.* reported that flies expressing a HTT exon-1 fragment with 93 polyQ repeats had a median life span in the range of 20 to 25 days [217] that is similar to observations in my study where a median life span of ~20 days was obtained for HTTex1Q97 expressing flies (Fig. 2.9). Another study showed an arrhythmic activity that decreased gradually over time after glia-specific expression of a HTT exon-1 fragment with 103 glutamines (hHtt103Q) [218]. With the pan-neuronal expression of HTTex1Q97 an arrhythmic activity was never observed, but a general reduction of the locomotion activity. This difference might be due to the glia-specific expression of (hHtt103Q),

which might have a more severe influence on the phenotype of the transgenic flies than the Elav-specific expression in neurons as reported by Miguel *et al.* [219].
A polyQ length-dependent effect is also evident for the aggregation behavior of HTT exon-1 proteins (HTTex1Q0, HTTex1Q17, HTTex1Q49 and HTTex1Q97) in the HD transgenic flies. I observed that the HTTex1Q97 protein forms SDS-insoluble, heat-stable and seeding competent aggregates in neurons as well as in non-neuronal tissues (Fig. 2.13 - 2.15 and 2.17). The results obtained with the HTTex1Q97 protein are in agreement with several studies that have shown previously that long pathogenic polyQ tracts in HTT fragments are critical for the formation of SDS-insoluble aggregates in flies [68, 209, 213]. Also, the observation that the HTTex1Q97 protein forms aggregates in neuronal and non-neuronal tissues in transgenic flies is in agreement with a previous study (Weiss *et al.* [208]). Interestingly, I found that insoluble HTTex1Q97 aggregates can be already detected in three days old flies and that their abundance increases over time (Fig. 2.14). Furthermore, I found that HTTex1Q49 aggregates cannot be detected in young flies, but in middle-age flies (Fig. 2.14), suggesting age-dependent formation of HTT aggregates in transgenic flies. Studies from Zhang *et al.* showed that Httex1-Q46-eGFP aggregates are detectable in 30 days old flies but not in two days old flies. This supports my results with the HTTex1Q49 protein [220].

3.1.4 The mutant HTT-induced toxicity increases with shorter HTT fragments

The examination of HTTflQ145 (full-length protein) and HTTex1Q97 (exon-1 fragment) in flies revealed that short HTT fragments with an elongated polyQ tract show a stronger disease phenotype than full-length HTT with an elongated polyQ tract. Life span as well as the locomotor activity of HTTex1Q97 expressing flies is stronger impaired compared to flies expressing the HTTflQ145 protein (Fig. 2.3 and 2.8). The HTTflQ145 flies live approximately 25 days longer than HTTex1Q97 flies, although they harbor a much longer glutamine tract [39, 40]. Interestingly, the analysis of the *Drosophila* eye of three days old HTTflQ145 flies revealed a normal retina structure. It has been shown that expression of pathogenic full-length HTT is only able to induce retina defects in old flies (20 days old $128QHTT^{FL}$ flies) [147]. In contrast, the photoreceptor cells in the eyes of HTTex1Q97 flies are disrupted already in very young animals. These results indicate that N-terminal HTT fragments with long pathogenic polyQ tracts are more toxic to flies than the full-length HTT protein with similar polyQ sequences.
A number of studies have demonstrated that full-length HTT can be cleaved by several proteases resulting in the release of short N-terminal fragments [53, 50]. Furthermore, it was demonstrated previously that N-terminal HTT fragments are more toxic and more aggregation prone than the full-length protein [50, 52, 55, 221]. Hackam and colleagues expressed successively smaller

HTT fragments with 128 glutamines, including exon-1 and full-length HTT, in human embryonic kidney cells [78]. The expression of shorter HTT fragments showed a stronger apoptotic stress than longer HTT fragments. Moreover, Barabro *et al.* analyzed transgenic flies that expressed naturally occurring N-terminal HTT peptides (e.g. HTT exon-1, HTT513 and HTT586) and observed that the HTT exon-1 fragment in flies is the most pathogenic huntingtin fragment compared to various longer transgenes [212].

3.1.5 Limitations of the constitutive expression system

A limitation of the constitutive expression system (GAL4 / UAS) is that the pathogenic HTTex1Q97 protein is already produced in very young flies (Fig. 2.14). This means the formation of HTT aggregates starts in an early stage of the development; the embryonic developmental stage 12 [182]. The toxic HTT protein could interfere during the development of the transgenic flies. Whether the phenotypic impairments trace back to the disturbances in the fly neurons or the interference during the development is not resolvable.
Furthermore, this expression system has a clear drawback for the analysis of therapeutic drugs in transgenic flies. During the development from the third instar larvae to the hatching fly the chemical compounds cannot be absorbed from the transgenic flies. The pupal stage lasts for about six days, in which the chemical compound is not provided to fly neurons. Nevertheless, the production of the mutant HTT protein in the fly neurons proceeds continuously. In a preliminary analysis, I investigated whether the chemical compound EGCG has an influence on mutant HTT-induced toxicity in Elav;HTTex1Q97 flies. Interestingly, EGCG which is a known modulator of HD toxicity and aggregation [120], showed no effect on the toxicity of the constitutive expressed HTTex1Q97 protein (data not shown). Thus, this constitutive expression system is not suitable for the analysis of therapeutic drugs. In contrast, the inducible Gene-Switch expression system allows the production in the adulthood of the flies so that the chemical compounds can be fed while the production of the mutant HTT protein takes place.

3.2 Establishment of an inducible HD fly model of HD

3.2.1 The dynamics of inducible HTT expression

In this study the hormone-inducible Gene-Switch expression system was used for the production of various polyQ-containing HTT proteins. The induction of transgene expression was achieved by dissolving the hormone ru-486 in the standard fly media (in-food method). It is interesting to mention that other delivery methods have been used, such as adding the hormone-supplemented yeast paste to the food [222] or dropping the hormone onto the food (on-food method) [223, 224]. To ensure that the flies do not have a choice between hormone and hormone-free food, the in-food

method was used.
To select the concentration of the hormone, different doses of the hormone were applied to GS;HTT513Q17 flies (Fig. 2.18 B). With a concentration of 400 μM of the ru-486 hormone similar HTT513Q17 protein levels were obtained in fly heads than with the constitutive GAL4 / UAS expression system. Furthermore, the concentration of 400 μM (~172 $\frac{\mu g}{ml}$) ru-486 has been used previously to induce transgene expression in transgenic flies [202]. I found that the HTTex1Q97 mRNA is detectable after one day of hormone treatment.
Osterwalder *et al.* treated Elav-GeneSwitch;UAS-EGFP flies for different time period with the ru-486 hormone. They detected the EGFP protein after five hours of hormone exposure [173]. I suggest that this difference is due to the fact that different protocols were utilized in my study compared to previously published experiments. Osterwalder *et al.* used larvae bathed in the hormone, whereas in my experiments the in-food method with adult flies was applied [223]. I found that the level of the HTTex1Q17 and HTTex1Q97 mRNA is stable during a time period of twelve days (Fig. 2.19). However, Wong *et al.* showed that the food intake decreases markedly with the age [225]. Thus, a reduction of the food intake and absorption of the ru-486 hormone due to the decreased feeding behavior in aged flies expressing the mutant HTT fragment cannot be excluded.

3.2.2 Transgene expression in the absence of ru-486

An inducible expression system should possess minimal or no expression of the transgene in the absence in the absence of the inducer. My studies showed no detectable HTT513Q17 protein in flies that were cultivated on food lacking the ru-486 hormone (Fig. 2.18). Also no HTTex1Q17 and HTTex1Q97 mRNA was detectable in the absence of the hormone (Fig. 2.19). Nevertheless, the brain staining of GS;HTTex1Q97$^{24d\text{-}OFF}$ flies (24 days on food lacking the hormone) revealed the presence of HTTex1Q97 aggregates (Fig. 2.29 E). This implies that transcription of the HTT transgene is not shut down completely and small amounts of HTT are produced in flies, when they are cultivated on food lacking the hormone. However, these very low transcript or protein levels cannot be detected by qRT-PCR or Western blotting (Fig. 2.19). A weak background ("leaky") expression in the absence of the hormone has been previously observed with the Gene-Switch system [179]. For example, in the study by Osterwalder *et al.* very low expression of the reporter gene EGFP was detected without hormone treatment [173]. Many other studies obtained similar results [223, 224, 226]. Although I observed a weak expression of the HTT gene in the uninduced transgenic flies, they did not show an impaired movement or survival phenotype (Fig. 2.20). Together, my studies indicate a leaky HTT expression beneath the detection limit. However, the marginally produced protein was not sufficient to cause a disease phenotype in flies.
Previously published studies that used the Gene-Switch expression system reported the kinetics of

transgene expression [200, 201] and have not investigated the kinetics of transgene suppression. I found that after turning-off the expression system through transfer flies onto normal food the HTT mRNA disappeared completely after 24 hours (Fig. 2.24). The previously discussed section indicates that a weak expression of the HTT transgene in treated flies that were transferred to food lacking the hormone cannot be excluded.

3.2.3 Suppression of mutant HTT expression does not complete rescue the HD phenotype in transgenic flies

Many therapeutic studies aim to reduce the abundance of mutant HTT mRNA levels in patient brains using antisense oligonucleotides (ASOs) or siRNAs [124, 227, 228]. In order to answer whether the disease can be delayed after onset of motor defects and the formation of insoluble HTT aggregates, Yamamoto and colleagues established a conditional mouse model of HD [229]. In this study they expressed a HTT exon-1 fragment with 93 glutamines that induced the formation of neuronal inclusions with HTT aggregates and progressive motor impairments. After the inhibition of HTT expression at an age of 18 weeks, the HD phenotype in transgenic mice was decreased [229]. In detail, nuclear and cytoplasmic aggregates disappeared, progressive striatal atrophy halted and the clasping phenotype has ameliorated compared to the chronically induced animals. The study postulated that HD neuropathology and motor dysfunction are reversal and constant expression of mutant HTT is necessary for disease progression.

The results from the Yamamoto lab are in strong contrast to the results of my study. In flies, the suppression of mutant HTT expression after six days of induction revealed no improvement of the survival. Exclusively, suppression of mutant HTT expression after three days showed an improvement of the life span. In contrast to the Yamamoto study, I found that the HTTex1Q97 aggregates do not disappear after the expression of the transgene was suppressed. In strong contrast to published results, my studies indicate that the abundance of HTT aggregates increases over time in flies until they reach a steady state (Fig. 2.31). The data of my study implicate that the HD phenotype may not be reversed if the expression of the mutant HTT protein is reduced. My results are supported by recent observations by Molero and colleagues who selectively expressed mutant HTT in transgenic mouse chronically or only during the development [230]. Production of mutant HTT during the development resulted in reductions of muscle strength and alterations in locomotor activity and motor coordination. These partial defects were not as serve as those in mice that produced the mutant HTT protein chronically [230].

The data of my study indicate that the suppression of mutant HTT expression is not sufficient to rescue the HD phenotype. Thus, a therapeutic intervention should start as early as possible to delay the age of onset and to reduce the overall lethality. This is in agreement with data from Molero *et al.*, who showed that suppression after the development is not sufficient to prevent the

HD phenotype [230].

3.2.4 Formation of aggregates prior phenotypic changes

The inducible Gene-Switch expression system, which I applied in this study, has the advantage that pathogenic HTT fragments can be expressed in adult flies. This is not possible with the conventional GAL4 / UAS system where the expression of mutant HTT starts during the development of the transgenic flies. The GAL4 / UAS system achieves a high level expression of the transgene during the development, including the larvae and pupal stage. The Gene-Switch expression system avoids transgene expression during these developmental stages, which have no equivalent in mammals.
I found that the constitutive expression of mutant HTT causes an enormous aggregate load in very young flies, due to the expression of the HTT gene throughout the developmental stages (Fig. 2.14). In comparison, the inducible expression system allows the investigation of the effects of pathogenic HTT aggregates in the adult flies. Interestingly, my studies indicate that HTTex1Q97 aggregates appear prior to the phenotypic changes that emerged after 24 days of chronic expression. These findings are in agreement with data that were obtained by Weiss *et al.* who showed the presence of HTT aggregates in primary striatal neurons several days before the onset of neurite degeneration [231]. Moreover, a significant amount of HTT exon-1 aggregates was detected in the brains of R6/2 mice at an age of two weeks, preceding the development of first motor impairments by weeks [231] - [233].

3.2.5 HTT aggregates as a potential driver of disease progression in transgenic flies

To investigate the effects of HTTex1Q97 aggregates on disease progression, the amount of aggregates was analyzed in flies that expressed the transgene for different periods of time. I observed that the earliest detectable aggregates are present in flies after three days of HTTex1Q97 expression, suggesting that this time period is sufficient to form MAB5492-reactive aggregates in the fly brain (Fig. 2.29). With longer HTT expression, the amount of aggregates increased significantly. In addition, the formation of HTT aggregates was systematically examined in short-time induced flies using the filter assay and immunohistochemistry. After turning-off the expression, the amount of aggregates slightly increased within the next ten days. An explanation could be the ongoing production of mutant HTT mRNA for twelve hours due to the remaining hormone food in the stomach of the flies after the transfer onto normal food. The very low levels of translated HTT protein in neurons might increase the aggregate quantity in fly brains. Further cultivation on food lacking the ru-486 hormone does not influence the aggregate quantity in flies, suggesting that there is no efficient degradation of HTT aggregates in fly brains. Data from the literature

show exclusively opposite results. After turning-off the expression for 72 hours, the amount of HTT aggregates in an inducible PC12 cell line was reduced dramatically [234]. Moreover, the inducible mouse model of Yamamoto *et al.* showed a clearance of HTT aggregates after several weeks without gene expression [229]. One could speculate that the fruit fly is not able to degrade HTT aggregates. However, the study of Latouche *et al.* showed the clearance of intranuclear aggregates in fly neurons in the absence of the transgene in an inducible fly model of SCA7 [200]. This suggests that the fruit flies should be able to clear polyQ-containing HTT aggregates. The work of Weiss *et al.* showed that after 72 hours of transgene repression, the amount of HTT aggregates in the salivary glands was decreased although a total recovery was not observed [208]. In this published study a mRFP tagged 588-aa N-terminal fragment of human HTT was investigated. The fluorescent tag allows a specific analysis without antibody staining, but could influence both the formation and degradation of aggregates.

Even though the quantity of HTT aggregates did not change after ten days on food lacking the ru-486 hormone, a change in their distribution was observed (Fig. 2.31 and 2.32). Recent studies highlighted the transcellular propagation of HTT aggregates [85]. However, the mechanism of aggregate spreading and the importance of this process for the disease are so far unclear [72, 85]. Babcock *et al.* demonstrated the spreading of aggregates derived from a 588-aa N-terminal fragment, whereas mutant exon-1 HTT aggregates failed to spread beyond the expression area [85]. For further analysis, the transgene has to be expressed specifically in certain neurons.

HD patients appear normal for decades before developing disease symptoms [235]. Two hypotheses concerning the late-onset of HD pathogenesis are discussed in the literature. The first claims that the adult-onset of HD is a result of progressive accumulation of toxic HTT fragments [236]. In this hypothesis, aging should not accelerate the pathogenesis in HD. Alternatively, there a speculations that aging leads to an increased vulnerability of striatal neurons due to impaired proteostasis [237]. It is has been shown that the ubiquitin / proteasome pathway is altered by aging [238] - [241]. An elevated vulnerability in older flies has also been observed in models of other neurodegenerative diseases such as Alzheimer's disease [242]. To analyze whether mutant HTT toxicity is age-dependent, the protein was expressed in young and middle-aged flies. In this study the short-time expression in young and middle-aged flies resulted in a similar time period between turning-off of HTT expression and the death of the flies. These results indicate that the effect of HTTex1Q97 on fly survival is age-independent.

A comparison of the aggregate quantity by DB assays, FRAs and immunohistological methods revealed that the amount of aggregates in the fly brain is reduced by half in short-time induced flies than in chronically induced flies although the survival is equal (Fig. 2.26 and 2.28). This difference in quantity suggests that the abundance of large HTT aggregates that are detectable by the mentioned methods is not directly related to the age of onset and disease progression in flies. One might speculate that small HTT aggregates play an impact on the HTT-induced toxicity.

Previous studies have shown that small, soluble oligomeric structures rather than large, insoluble aggregates cause dysfunction and toxicity in protein misfolding diseases [88, 90, 243, 244].
Other polyQ-rich proteins such as the transcription factor CREB are known to co-aggregate with mutant HTT [73]. Proteins in the fruit fly that contain long polyQs are predominantly transcription factors [245]. The co-aggregation of important cellular transcription factors could cause transcriptional dysregulation that might result in neuronal dysfunction and cell death. One might speculate that the small amount of HTT aggregates that are detected in fly brains after short-time expression (six days) is sufficient for polyQ-rich proteins to co-aggregate with pathogenic HTT and to cause transcriptional dysregulation over time. To proof this hypothesis, immunohistochemistry analysis could be performed to test whether polyQ-rich transcription factors incorporate into pathogenic HTT aggregates. In addition, mass-spectrometry analysis of purified aggregates could provide further insights into the disease mechanism.

3.2.6 The relevance of seeding-competent HTT aggregates for the appearance of symptoms in HD transgenic flies

There is experimental evidence that spreading of mutant HTT aggregates play a critical role in the pathogenesis of HD [84, 85, 246]. In order to analyze whether HTT seeding drives HD, the FRASE assay that allow a quantification of seeding-competent structures was used.
Unpublished data from our laboratory revealed that HTT seeding activity is detectable in soluble and insoluble protein fractions (data not shown). However, the abundance in soluble protein fractions was higher, which indicates that the seeding activity predominantly results from small rather than large HTT aggregates. It has been shown that the FRASE assay detects seeding competent HTT aggregates that are small and cannot be detected by FRAs (data not shown). This is in agreement with my data that show no correlation between large HTT aggregates and the seeding activity in GS;HTTex1Q97$^{24d\text{-}ON}$ and GS;HTTex1Q97$^{6d\text{-}ON/18d\text{-}OFF}$ flies. However, the GS;HTTex1Q97$^{24d\text{-}ON}$ and GS;HTTex1Q97$^{6d\text{-}ON/18d\text{-}OFF}$ flies showed a similar survival and seeding activity in the FRASE assay. One might speculate that small HTT aggregates that cannot be detected by DB assays, FRAs and immunohistological methods are responsible for the seeding events potentially drive the pathogenesis in HD transgenic flies. Thus, the seeding activity rather than the abundance of large HTT aggregates correlates with the HTT-induced toxicity.
The assumption, that seeding active HTT aggregates drive the HD pathogenesis in flies is supported by the HSPA1L experiments. Co-expression of HSPA1L causes a reduction of the seeding activity, which results in an elongated survival of HD transgenic flies.

3.3 Application of the inducible fly model for the analysis of modifiers of mutant HTT aggregation and toxicity

3.3.1 The HTT-induced toxicity can be modulated by a molecular chaperone

In order to investigate whether interference of HTT aggregates by a chaperone affects the HTT-induced toxicity, co-expression of HSPA1L was examined. The HSPA1L protein decreased the aggregate quantity and extended the life span (Fig. 2.34 and 2.35). The effect of HSPA1L might even be underestimated, as the chaperone can only be co-expressed in parallel to HTT. Using an additional GAL4-independent expression system would enable the prolonged expression of the chaperone and could further improve the phenotype. My observations are in agreement with other studies, which showed that molecular chaperones including HSPA1L are able to modulate and repress polyQ mediated toxicity [104, 105], [247] - [249]. Also the observation that HSPA1L forms a shell around the HTTex1Q97 aggregates is in agreement with earlier observations, indicating that Hsp70 protein encapsulate HTT aggregates in HeLa cells [250].

3.3.2 The small molecule Quinidine influences HTT aggregation in HD transgenic flies

Considerable efforts have been invested in HD drug discovery. Several studies focus on lowering mutant HTT levels in the brain by RNAi treatment to reduce all deleterious downstream effects of the protein and to slow down or prevent HD pathogenesis [251, 124, 125]. The data of this thesis indicate suppression of HTT expression might only delay the age of onset and disease progression in an insufficient way, since inhibition of expression to six days (Fig. 2.27) does not slow down HD pathogenesis. Therefore, an additional therapeutic drug approach that reduces mutant HTT aggregate level would be necessary. For the analysis of effects of chemical compounds on HTT aggregation and toxicity, the inducible fly model was used. In contrast, all previous compound studies in flies used the constitutive expression system, which allows no compound treatment during the development as well as prior and after the transgene expression [139, 120].
For the analysis of chemical compounds in HD transgenic flies, flies were treated with hit compounds that were active in the cell-based assay. I found a significant reduction of HTTex1Q97 aggregates in flies that were treated with the chemical compound Quinidine (Fig. 2.41). Quinidine has not been associated with HD, but was analyzed in combination with Dextromethorphan in AD patients in a phase 2 clinical trial to reduce Agitation and Aggression [252].
A systematically analysis by DA assays, FRAs and immunohistoligical methods showed a reduction of large HTT aggregates in the fly brains. Surprisingly, flies treated with increasing Quinidine concentrations are stronger affected in the survival. The decrease of HTT aggregates

with increasing concentrations of Quinidine could suggest that the compound leads to an inhibition of mutant HTT aggregation. However, analysis of Quinidine in an *in vitro* aggregation assay (data not shown) revealed no inhibition of mutant HTT aggregation. However, Quinidine could potentially prevent the deposition into large insoluble HTT aggregates with the result that smaller and more toxic soluble aggregates are formed. This explains the increased toxicity and the decreased aggregate load at the same time. Several studies illustrated a higher toxicity when the formation of inclusion bodies was inhibited [88, 90].
Although the usage of Quinidine as a therapeutic molecule is not suitable, it could be utilized for further mechanistic studies. A general and detailed morphological and biochemical characterization of biological samples from flies that were treated with Quinidine would be necessary to clarify the mechanism that leads to toxicity in mutant HTT expressing flies. Moreover, the analysis of the seeding competence of the HTT aggregates prepared from Quinidine treated flies would be of importance.

4 Material & Methods

4.1 Material

4.1.1 Fly strains

GAL4 drivers	
$Elav^{c115}$-GAL4	[253]
X^{+};GMR-GAL4	[254]
14-3-fkh-GAL4	[255]
Ok107-GAL4	[256]
GSelav-GAL4	Bloomington Stock 43642
Miscellaneous strains	
Canton-S	[257]
w^{1118}	[258]
Balancer strain (CyO/Sp;MKRS,Sb/TM6,Tb)	own production
UAS-GFP	Bloomington Stock 1521
$GAL80^{ts}$ second chromosome	[180]
UAS-HSPA1L	[104]

If no other source is stated, flies were either taken from our own stock collection or obtained from the Bloomington stock collection.

4.1.2 *E. coli* strains

Mach1™ T1	*E.coli* F^{-} Φ80(lacZ)ΔM15 ΔlacX74 hsdR(r_K^{-} m_K^{+}) ΔrecA1398 endA1 tonA (Invitrogen) recommended strain for the Gateway® Cloning System. Invitrogen
BL21- CodonPlus(DE3)-RP	*E. coli* B F^{-} ompT hsdS(r_B^{-} m_B^{-}) dcm^{+} Tet^{r} gal λ(DE3) endA Hte [argU proLCam^{r}] strain (Stratagene); for high level protein expression induced by IPTG, Agilent Technologies

4.1.3 Expression vectors and plasmids

pDONR™ 221	A Gateway® vector containing attP sites; contains ccdB gene and kanamycin resistance gene; to generate entry clones. Invitrogen
pGEX-6P1	Expression vector for IPTG inducible expression of glutathione S-transferase (GST)-fusion proteins in E.coli under control of a synthetic tac-promotor; contains lacIq repressor and Ampicillin resistance genes; encodes a PreScission™ protease cleavage site downstream of the GST sequence (GE Healthcare). Amersham
pUAST-attB-rfA	Expression vector for expression in transgenic flies under the GAL4 inducible UAS promoter; contains attB site for site-specific integration in the fly genome by ΦC31 integrase (provided by Prof. Sigrist, FU Berlin).

4.1.4 Antibodies

Antibody	Species	Supplier
MW1	mouse	DSHB
MW8	mouse	DSHB
MAB5492	mouse	EMD Millipore
MAB5374 (EM48)	mouse	Chemicon
MAB1574 (1C2)	mouse	EMD Millipore
3B5H10	mouse	Sigma-Aldrich
CAG53b	rabbit	own production [66]
HD1	rabbit	own production [57]
Anti-Agg53	rabbit	own production
anti-RBP	rabbit	provided by Prof. Sigrist, FU Berlin [197]
anti-HSPA1Lă(ADI-SPA-812)	rabbit	Enzo
anti-β-actin (A5441)	mouse	Sigma
anti-GFP (ab290)	rabbit	Abcam
Antibody	Conjugate	Supplier
anti-rabbit	Peroxidase	Cell Signaling
anti-mouse	Peroxidase	Cell Signaling
anti-rabbit	Alexa Fluor®488	Molecular Probes
anti-mouse	Alexa Fluor®647	Molecular Probes

4.1.5 PCR Primers

Name	5' – 3' sequence
pUAST-fwd	AACCAAGTAAATCAACTGC
pUAST-rev	ATCTCTGTAGGTAGTTTGTC
HTT-ex1-fwd	GACCCTGGAAAAGCTGATGA
HTT-ex1-rev	TCATGGTCGGTGCAGCGGCT
attB-HTT-ex1-fwd	GGGGACAAGTTTGTACAAAAAAGCAGGCTGG ATGGCGACCCTGGAAAAGCTG
attB-HTT-ex1-Stop1-rev (ex1Q0)	GGGGACCACTTTGTACAAGAAAGCTGGTCATG GTCTATGCAATGGTTCTTCAGC
attB-HTT-ex1-Stop2-rev (ex1Q97)	GGGGACCACTTTGTACAAGAAAGCTGGTCATG GTCGGTGCAGCGGCTCCTCAGC
rp49-fwd	TACAGGCCCAAGATCGTGAA
rp49-rev	ACGTTGTGCACCAGGAACTT

Primers had HPLC purification grade and were synthesized by BioTeZ Berlin-Buch GmbH in a quantity of 10 nM. Primers were dissolved in autoclaved water (concentration of 10 $\frac{pmol}{\mu l}$).

4.1.6 Enzymes, proteins and markers

1 kb DNA Ladder	Invitrogen
AntarcticPphosphatase	NEB
Benchmark Pre-stained Protein Ladder	Thermo Scientific
BP Clonase® II Enzyme Mix	Thermo Scientific
BSA 10 $\frac{mg}{ml}$	NEB
Complete™ Protease Inhibitor Cocktail	Roche
dNTP mix (10 mM each)	Invitrogen
GeneRuler™ 100 bp DNA ladder	Thermo Scientific
LR Clonase® II Enzyme Mix	Thermo Scientific
M-MLV Reverse Transcriptase	Thermo Scientific
Oligo(dT)12-18 Primer	Invitrogen
PageRuler™ Plus Prestained Protein Ladder	Thermo Scientific
PreScission Protease™	GE Healthcare
Proteinase K	Sigma Aldrich
Ready-Load 1 kb Plus DNA ladder	Thermo Scientific
Restriction Enzymes (BsrGI, BstXI, SacI, SalI, PvuI)	Thermo Scientific
T4 DNA Ligase	NEB

4.1.7 Kits

BCA Protein assay reagent	Thermo Scientific
ChemiGlow West	Alpha Innotech
SuperScript® first strand cDNA synthesis	Invitrogen
DNeasy blood and tissue kit	Qiagen
Expand™ long template PCR system	Roche
QIAprep spin miniprep kit	Qiagen
Qiagen plasmid midi kit	Qiagen
QIAquick PCR purification/gel extraction kit	Qiagen
Pwo SuperYield DNA polymerase kit	Roche
SYBR® Green PCR master mix	Applied Biosystems

4.1.8 Buffers, solutions and media

Aggregation buffer, 10x	0.5 M Tris-HCl pH 7.4, 1.5 M NaCl, 10 mM EDTA
Ampicillin, 1000x	100 $\frac{mg}{ml}$ dissolved in 50 % ethanol, stored at - 20 °C
Brain lysis buffer	10 mM Tris-HCl pH 7.4, 0.8 M NaCl, 1 mM EDTA, 10 % Sucrose (fresh), 1x protease inhibitor
Brain staining buffer	5 % NGS, 0.1 % NaN_3 in PBT (0.3 %)
Blocking buffer	3 % milk powder in PBS-T
Coomassie destaining solution	20 % ethanol, 10 % acetic acid
Coomassie staining solution	30 % ethanol, 10 % acetic acid, 0.05 % Coomassie brilliant blue R250
Dialysis buffer	50 mM Tris, 150 mM NaCl, 1 mM EDTA, 5 % Glycerol, pH 7.4
Denaturation buffer	4 % SDS, 400 mM DTT
DNA sample buffer, 4x	0.25 % bromophenol blue, 0.25 % xylene cyanole FF, 30 % glycerol
Elution buffer	Buffer 1, 20 mM red. glutathione, pH 8.6
HL3	70 mM NaCl, 5 mM KCl, 20 mM $MgCl_2$, 10 mM $NaHCO_3$, 5 mM Trehalose, 115 mM Sucrose, 5 mM Hepes, pH 7.2
LB-(Luria Bertani) agar	1 % Bacto Peptone, 0.5 % yeast-extract, 1 % NaCl, 2 % Agar
LB-(Luria Bertani) medium	1 % Bacto Peptone, 0.5 % yeast-extract, 1 % NaCl
Leachingbuffer	50 mM Tris, 150 mM NaCl
PBS, 10x	1.37 mM NaCl, 27 mM KCl, 100 mM Na_2HPO_4, 17.6 mM KH_2PO_4, pH 7.4

PBS-T	1x PBS, 0.05 % Tween-20
PBT (0.3 %)	1x PBS, 0.3 % Triton™ X-100
PBT (1 %)	1x PBS, 1 % Triton™ X-100
PBT/NGS	1x PBS, 0.1 % Triton™ X-100, 0.1 % BSA, 5 % NGS
Protein extraction buffer	2 % SDS, complete protease inhibitor
PEM	0.1 M PIPES, 2 mM EGTA, 1 mM $MgSO_4$, pH 7.0
4 % PFA	4 g PFA dissolved in 100 ml PBS and heated at 50 °C for 5 minutes to obtain a clear solution, pH 7.4, stored at - 20 °C
P1 buffer	5 mM Tris, 150 mM NaCl, 1 mM EDTA, 50 mM Na_2HPO_4, pH 8.0
RIPA-buffer	50 mM Tris-HCl pH 8.0, 150 mM NaCl, 2 mM EDTA, 1 % NP40, 1 % Na-deoxycholat
S.O.C. medium	2 % Tryptone, 0.5 % yeast-extract, 10 mM NaCl, 2.5 mM KCl, 10 mM $MgCl_2$, 10 mM $MgSO_4$, 20 mM Glucose
Tris-Lysisbuffer	100 mM Tris-HCl pH 7.4, 1 % Triton™ X-100
Western blotting buffer	25 mM Tris, 190 mM Glycin, 15 % ethanol
Standard fly medium (6 l)	25 g Agar-Agar, 45 g beer yeast, 50 g soy flour, 400 g corn flour, 75 ml sugar beet syrup, 300 ml Malzin, 8 g Nipagin, 25 ml EtOH, 32 ml propionic acid
Special fly medium (6 l)	48 g Agar-Agar, 480 g beer yeast, 120 g Bacto-peptone, 120 g Bacto-yeast, 420 ml sugar beet syrup, 3 g $MgSO_4$, 3 g $CaCl_3$, 6 g Nipagin, 60 ml EtOH, 36 ml propionic acid

4.1.9 Chemicals and Consumables

Acetic acid	Carl Roth
Agar-Agar	Gewürzmühle Brecht
Agarose, ultrapure	Life Technologies
Amershan™ Protran™ 0.1 μm NC	GE Healthcare
Ampicillin sodium salt	Sigma-Aldrich
Apomorphin	Sigma Aldrich
Auraptene	Sigma Aldrich
Bacto peptone	BD
Bacto tryptone	BD
Bacto yeast extract	Carl Roth
Bear yeast	Gewürzmühle Brecht
Bouin's Fixative	Sigma Aldrich

Bromphenol blue	Merck Eurolab GmbH
Chloramphenicol	Sigma Aldrich
Chloroform	Merck
Coomassie brilliant blue G-250	Merck
Corn flour	Bauck GmbH
Dialysis membrane (MWCO 10 kDa)	SpectraPor® Dialysis
Dihydrorobinetine	Carl Roth
Dimethylsulfoxide (DMSO)	Sigma Aldrich
Dithiothreitol (DTT)	AppliChem
EGCG	Sigma Aldrich
Ellagic acid	Sigma Aldrich
Entelan	Merck
Ethidium bromide solution	Sigma Aldrich
Ethylenediamine tetraacetic acid (EDTA)	Sigma Aldrich
Ethylene glycol tetraacetic acid (EGTA)	Sigma Aldrich
Filter paper	GE Healthcare
Glutathione sepharose 4B	GE Healthcare
Glycerol	Carl Roth
Glycin	MP Biomedicals
Guanabenz acetate	Tocris
Harmaline HCl	Sigma Aldrich
Idebenone	Sigma Aldrich
Immu-Mount™	Thermo Scientific
Isopropyl-β-D-1-thiogalactopyranoside (IPTG)	ApplieChem
Isopropyl alcohol	Carl Roth
Kanamycin sulfate	Sigma Aldrich
L-Glutathione reduced	Sigma Aldrich
Levodopa	Fluka
Limonene	Sigma Aldrich
Lysozyme	Merck
Malzin	Ulmer Spatz
Methanol	Carl Roth
Methyl 4-Hydroxybenzonate (Nipagin)	AppliChem
MicrofugeR Tube Polypropylene 1.5 ml	Beckham Coulter
Mifepristone (ru-486)	Biomol
Morin	Sigma Aldrich

Normal goat serum	Genpro Biotech
NP-40	Calbiochem
NuPage® LDS Sample Buffer, 4x	Novex
NuPage® MES SDS Running Buffer, 20x	Invitrogen
O4	Timtek
Paraformaldehyde	Sigma Aldrich
Parablast embeeding media	Sigma Aldrich
Piceatanol	Sigma Aldrich
p-t-Octylphenyl-polyoxyethylen (TritonX-100)	Sigma Aldrich
Polyoxyethylensorbitan-Monolaureat (Tween 20)	Sigma Aldrich
Polypropylene Colum (5ml)	Quiagen
Protein LoBind tubes 0.5, 1.5 ml	Eppendorf
PVDF Immobiolon Transfer Membran	Millipore
Quinidine	Sigma Aldrich
RNase-free water	Ambion
Rotiphorese® Gel30 (30 % acrylamide and bisacrylamid stock solution)	Carl Roth
SDS (ultra pure)	Carl Roth
Skim milk powder	Sigma Aldrich
Soy flour	Bauck GmbH
Sucrose	Fluka
Sugar beet sirup	Grafschafter Krautfabrik
TEMED	Amresco
Trehalose	Sigma Aldrich
TRIS Base, Tris(hydroxymethyl)aminomethane	Merck
Trizol	Ambion
VectaShield (H-1000)	Vector Laboratories
Fly vials (plastic) 26, 49 mm diameter	K-TK
Whatman™ cellulose acetate membrane (0.2 μm)	GE Healthcare
Xylol	Carl Roth
Yeast extract	Carl Roth
0.5, 1.5, 2 ml tubes	BD Falcon
15 ml, 50 ml tubes	Eppendorf
384 well-plates	BD

The remaining chemicals necessary for the preparation of buffers (salts, acids, etc.) were purchased from Carl Roth.

4.1.10 Laboratory Equipment

ArrayScan VTI (Cellomics)	Thermo Scientific
Biophotometer	Eppendorf
Centrifuge Evolution RC	Sorvall
Criterion cell for SDS-PAGE	BioRad
DAM) System	TriKinetics
DNA electrophoresis chamber	BioRad
Electroporator	BioRad
Gel electrophoresis equipment	BioRad
Gene Genius UV imager	Bio Imaging Systems
HybriDot Manifold vacuum fitration unit	Whatman
Infinite M200 microplate reader	TECAN
LAS-3000 photo imager	Fujifilm
Magnetic stirrer MR3001	Heidolph
Micro 22R centrifuge	Hettich
Multichannel pipettes	Eppendorf
NanoDrop 8000	peQlab
Optima TLX Ultracentrifuge	JPK
Power Pac 1000	BioRad
PTC200 Peltier Thermal Cycler	MJ Research
Shaking Incubator	Infrors Unitron
Stereomicroscope	Olympus
Thermomixer comfort	Eppendorf
Tissue Homogenizer (Pestle)	FischerScientific
Trans-blot semi-dry transfer cell	BioRad
Ultrasonic cell disruptor	BioRad
Vortex-Genie 2	Scientific Industries
Water bath TW8	Julabo
Real-time PCR system	ThermoFisher

4.1.11 Software

Image processing was performed using Adobe Photoshop. Data analysis and statistical tests were performed using GraphPad PRISM. The Figures were created using Adobe Illustrator.

4.2 Methods

4.2.1 Molecular biology methods

DNA constructs

Plasmids were generated using the classical cloning methods and Gateway technology (Invitrogen). Available plasmids containing HTTex1Q17, HTTex1Q49, HTTex1Q97(-stop), HTT336Q0, HTTflQ23, HTTflQ73, HTTflQ145 and HTT513Q17 were used.

Gateway cloning (BP and LR reaction)

In order to generate an entry clone containing a gene of interest, gateway cloning was performed. Target sequences were amplified by PCR from available plasmids. The used primer pairs contain four guanine residues at the 5' end followed by an attB site and template-specific sequences. The PCR products were purified from an agarose gel by gel extraction and cloned by BP clonase-mediated homologous recombination between an attB-PCR product and a donor vector carrying attP recognition sites (pDONR221). The resulting entry clone was used for the LR reaction. The LR clonase excises the insert and integrates it into a destination vector. The reactions were performed as recommended by the manufacturer. The successful shuttling of the sequence was verified by restriction digest and sequencing.

Preparation of plasmid DNA

For plasmid preparation of small cultures 5 ml LB medium with appropriate antibiotics was inoculated with a single *E.coli* colony containing the respective plasmid. After overnight incubation at 37 °C on a shaker, the cells were harvested by centrifugation at 4,000 rpm for 10 min. Plasmid DNA was isolated using the QIAprep spin miniprep kit as recommended. For plasmid preparation of 100 ml the Qiagen plasmid midi kit was used.

Measurement of DNA and RNA concentrations

The DNA and RNA concentrations were determined by measuring the absorbance at 260 nm using the UV-Vis Spectrophotometer NanoDrop8000. In addition to that, the measuring at 280 nm was performed to asses protein concentrations.

Restriction digest

Restriction digests were performed as recommended by the manufacturer. Reactions were incubated at 37 °C for two hours. The reaction was stopped by adding 4x DNA sample buffer and

separated by agarose gel electrophoresis. For cloning steps the enzyme was heat-inactivated at 65 °C for 20 min.

DNA electrophoresis

Separation of DNA was carried out in 1 % agarose gels containing 0.5 $\frac{g}{ml}$ ethidium bromide at 3 – 7 $\frac{V}{cm}$. The samples were mixed with 4x DNA sample buffer and equal amounts were loaded onto the gel. Additionally DNA mass standard was loaded to determine the band size. 1x TBE buffer running buffer was used. The separation of bands was analyzed using a UV transilluminator.

Extraction of DNA from agarose gels

The QIAquick PCR purification kit was used to extract DNA fragments from agarose gels. DNA samples were separated as described before. The bands were excised with a scalpel on a UV transilluminator. The gel pieces were weighted and then processed as described by the manufactuers instructions. Samples were stored at -20 °C.

Transformation

For transformation of plasmids 25 μl chemically competent *E.coli* cells were mixed with the DNA of choice, either 10 μl of the ligation reaction or 5 μl of the BP- or LR-reaction. The cells were incubated on ice for 30 min and then were heat-shocked at 42 °C in a water bath for 45 sec to induce cell permeability. Afterwards, the cells were put back on ice for 5 min to allow resealing of the cell walls and 200 μl pre-warmed S.O.C. medium was added to the sell suspension. The mix was incubated for one hour at 37 °C and 450 rpm in a thermomixer. In case of a ligation, 100 μl of the cells were streaked onto agar plates with appropriate antibiotics. In case of a purified plasmid, 50 μl of the cells were used. The agar plates were incubated overnight at 37 °C.

PCR

The Pwo Polymerase and the Expand Long Template Polymerase and HTTex1- and pUAST-primer pairs were used as recommended to amplify from genomic or plasmid DNA.

cDNA synthesis

For cDNA synthesis from mRNA, 5 μg total RNA was mixed with 1 μl dNTP mix and 1 μl oligo(dT)12-18 primers to a total volume of 12 μl. The mix was heated to 65 °C for 5 min and subsequently chilled on ice. Following, 0.2 μl DTT (1 M) and 4 μl 5x first-strand buffer was added and incubated at 37 °C for 2 min. Finally 200 U of the M-MLV RT was mixed by gently

pipetting and incubated for 50 min at 37 °C. The reaction was heat-inactivated at 70 °C for 10 min. The cDNA samples were stored at -20 °C.

Quantitative polymerase chain reaction (qPCR)

To SYBR® Green PCR master mix was used for qPCR using the HTT-ex1 primer pair and the rp49 primer pairs as a reference gene. The primer pairs were mixed with 6 μl of the SYBR mix and water to a total volume of 10 μl. To be examined cDNA was diluted 1:10 and 2 μl was added to the SYBR mixture. The sample was analyzed using the ViiA7 Real-time PCR system as recommended.

Sequencing

Sequencing of plasmids was done by Stratec, Berlin. The pUAST and HTT-ex1 primer pairs were used for sequencing of the HTTex1 fragments and the HTT513Q17 construct. When sequencing the full-length constructs, new primers were designed in accordance to the previous sequence (Stratec, Berlin) and further sequenced.

4.2.2 Biochemical methods

Expression of recombinant GST-tagged fusion proteins

The BL21-RP *E.coli* strains carrying the expression plasmid, GST-HTTex1Q48, GST-HTTex1-Q48CyPet and GST-HTTex1Q48YPet were inoculated overnight in 20 ml LB medium containing ampicillin and chloramphenicol at 37 °C and 230 rpm. On the next day 1 L of the LB medium was inoculated with the 20 ml culture for the CyPet-/YPet-tagged proteins at 30 °C and the untagged protein at 37 °C until the OD600 reached 0.6. The overexpression of the recombinant protein was induced by addition of 1 mM IPTG and incubation for the CyPet-/YPet-tagged proteins at 18 °C and the untagged protein at 30 °C for four hours. The cells were pelleted at 4,000 rpm and 4 °C (Sorvall Evolution RC, rotor SLC-6000) for 20 min and the pellets were frozen at -80 °C.

Purification of recombinant GST-tagged fusion proteins

The frozen cell pellets of the recombinant GST-fusion proteins were purified under native conditions. The cells were lysed by resuspending in 30 ml P1 buffer with lysozyme ($1\frac{mg}{ml}$) and protease inhibitor, incubated on ice for 30 min and ultrasonicated 8 times for 45 sec (Ultrasonic cell disruptor). The lysate was incubated with a final concentration of 1 % Triton™ X-100 on ice for 5 min and centrifuged at 15,000 rpm for 40 min (Sorvall Evolution RC, rotor SS34). Supernatants were mixed with 4 ml 50 % pre-equilibrated glutathione sepharose 4B and incubated in a rotator

for one hour at 4 °C. The beads were moved to a polypropylene column and the flow-through was discarded. The column was washed with 10 ml P1 buffer containing 0.1 % Triton X-100 and protease inhibitor and 10 ml P1 buffer. The proteins were eluted with 4 ml elution buffer, rotating for 30 min at room temperature. The fraction was dialysed overnight at 4 °C using a membrane with a molecular weight cut off of 10 kDa. The next day, the dialysis buffer was exchanged and dialysis was processed for four hours. After dialysis, the protein was removed from the membrane, the concentration was measured and aliquots were stored at -80 °C.

Measurement of protein concentration

The protein concentration GST-fusion proteins were determined in a spectrophotometer by measuring the absorption at 280 nm. The absorbance was analyzed according to Lambert-Beer's law ($E_{280\,nm} = \varepsilon * c * d$) with E being the absorption, ε the extinction coefficient, c the protein concentration and d the path length (1 mm for nanodrop). The protein concentration of cell lysates was determined using a staining assay (BCA assay, Pierce). The BCA assay was performed as recommended. The Absorption of the sample at λ = 562 mm was compared to a calibrated curve of defined BSA concentrations.

SDS-polyacrylamide gel electrophoresis (SDS-PAGE)

SDS-PAGE was used to separate proteins by their molecular weight. Samples were mixed with LDS sample buffer and 200 mM DTT and were boiled for 5 min at 95 °C. Electrophoresis was carried out at first at 80 V for 20 min and then continued at 120 V for 1 h with NuPAGE® MES SDS running buffer. The further readout was done with Coomassie staining or western blot analysis.

Component	Stacking gel	Separating gel
H_2O	2.975 ml	3.8 ml
Tris-HCl (0.5M), pH 6.8	1.25 ml	-
Tris-HCl (1.5M), pH 8.8	-	2.6 ml
10 % SDS	50 μl	100 μl
30 % Acrylamide/Bis-acrylamide	0.67 ml	3.4 ml
10 % Ammonium persulfate	50 μl	100 μl
TEMED	5 μl	10 μl

Coomassie staining

For protein staining after electrophoresis separation, the gel was incubated in Coomassie staining solution overnight. The gel was transferred into Coomassie destaining solution until the protein

bands are seen without background staining. Pictures were taken by a scanner.

Western blotting

Denatured head lysates were separated on a 4 – 12 % SDS-PAGE. Proteins were blotted to Immobilon PSQ-transfer membrane (PVDF) with western blot buffer using a Semi-dry Transblot Apparatus. The blotting was performed at 20 V for one hour. The membranes were incubated in blocking solution (5 % milk/PBS-Tween) for one hour at room temperature. After blocking the membranes were incubated with the primary antibodies (diluted 1:1000) overnight at 4 °C followed by a secondary antibody conjugated to Peroxidase. For detection, the membranes were immersed in ChemiGlow substrate and visualized by an LAS3000 image reader. The protein bands / dots were quantified using the AIDA software.

Fluorescence Resonance Energy Transfer (FRET)-based huntingtin aggregation assay

Purified GST-HTTex1Q48-CyPet and GST-HTTex1Q48-YPet proteins were thawed on ice and centrifuged at 55,000 rpm (Optima TLX) for 40 min at 4 °C to pellet the pre-existing oligomers. 80 % of the supernatant was transferred to a new low bind tube and the protein concentration was determined using the nanodrop. The aggregation was initiated as listed in table. The reaction was performed in a 384 well plate (30 μl / well in triplicate from a 100 μl reaction).

Ingredient	per 100 μl sample
GST-HTTex1Q48-CyPet	1 μM
GST-HTTex1Q48-YPet	1 μM
10x aggregation buffer	10 μl minus $\frac{1}{10}$ volume of protein
PreScission Protease®	1.4 μl
100 mM DTT	1 μl
fly lysate if stated	2.5 μg
H_2O	add to 100 μl

The samples were analyzed in a Tecan infinite M200 microplate reader and three fluorescence channels were measured: the acceptor channel (YPet (AA): $\lambda_{extinction}$ = 500 nm, $\lambda_{emission}$ = 530 nm), donor channel (CyPet (DD): $\lambda_{extinction}$ = 435 nm, $\lambda_{emission}$ = 477 nm) and the FRET channel (FRET (DA): $\lambda_{extinction}$ = 435 nm, $\lambda_{emission}$ = 530 nm) (Nguyen and Daugherty, 2005). The plate was measured for a 24 hours period every 20 min after 5 sec shaking at 25 °C in the Tecan reader. Acceptor only, donor only and unlabeled protein aggregation samples (2 μM protein respectively) were carried on every plate for correction factor definition. For data processing,

the fluorescence signal of the unlabeled protein signal was subtracted from all channels. The sensitized emission (SE) was corrected according to Jiang and Sorkin [259] for donor bleedthrough (cD) and acceptor cross excitation (cA) as shown below. At the end, the data was acceptor normalized (FRET efficiency in %).

$$cD = \frac{DA}{DD} \qquad cA = \frac{DA}{AA} \qquad SE = DA - cD \times DD \; - cA \times AA$$

$$FRET\; efficiency\,(\%) = \frac{SE}{AA} \times 100\%$$

Seeding effects indicated as $\Delta t_{50}\,(h)$ were quantified by subtracting the $t_{50}\,(h)$ values of the sample from the control. The $t_{50}\,(h)$ value is the time at half maximal FRET efficiency that was obtained by curve fitting using the Richard's five-parameter dose-response curve (GraphPad Prism).

$$Seeding\; activity\,(h) = FRET_{50}(control) - FRET_{50}(sample)$$

4.2.3 *Drosophila* work

Husbandry of *Drosophila melanogaster*

All flies were kept in a humidified 65 %, temperature-controlled incubator with a twelve hours on/off light cycle at 25 °C in vials containing standard medium [260].

Compound and Mifepristone Treatment of *Drosophila melanogaster*

The compounds and the ru-486 hormone (Mifepristone) were mixed into 40 °C warm standard fly food in the desired concentration. The ru-486 hormone was solved in ethanol and diluted to a concentration of 40,000 μM. The hormone was mixed into the food 1:100 with a final concentration of 1 % ethanol. For compounds which were solved in ethanol and DMSO, a final concentration of 2 % ethanol and 0.125 % DMSO was used in the fly food.

Transgenic strains

Expression constructs encoding several Huntingtin sequences combined with different polyglutamine lengths were generated by PCR and the constructs were cloned by gateway cloning into the GAL4-responsive pUAST expression vector (pUAST-attB-rfA, provided by Prof. Dr. Sigrist, Freie Universität, Berlin) for the generation of transgenic fly strains. Estimated cytology docking site for integration was 68E (third chromosome) and transgenesis was mediated by ΦC31-Integration System at Rainbow Transgenic Flies Inc. (Camarillo, CA, USA). The obtained

transgenic lines were crossed with the balancer strain (CyO/Sp;TM6,Tb/MKRS,Sb) to produce a stable fly line.

DNA Extraction from *Drosophila* tissue

For purification of total DNA from transgenic flies the DNeasy blood & tissue kit were used as recommended.

RNA Extraction from *Drosophila* tissue

Fly heads were homogenized in 1 ml Trizol with a micropestle and subsequently centrifuged at 12,000 x g for 10 minutes at 4 °C. After the supernatant was transferred to a new tube, 0.2 ml of chloroform was added. The tubes were shaken vigorously by hand for 15 seconds. The sample were incubated for 2 – 3 minutes at room temperature and centrifuged at 12,000 x g for 15 minutes at 4 °C. The aqueous phase was removed and precipitated with 0.5 ml 100 % isopropanol for 10 minutes at room temperature. After centrifugation at 12,000 x g for 10 minutes and 4 °C, the pellet was washed with 1 ml 70 % ethanol. The sample was vortexed briefly and then centrifuged at 7,500 x g for 5 minutes at 4 °C. The RNA pellet was dried for 10 minutes, resuspended in RNase-free water and incubated at 55 °C for 10 minutes. The samples were stored at -80 °C until use.

Head lysate for western blot

For denatured head lysates, fly heads that had been frozen were collected using sieves. The tissues were homogenised with a tissue homogeniser in PE-Buffer. After centrifugation at 8,000 rpm for 10 minutes the lysate was collected and the concentration analyzed by BCA assay. Then 200 mM DTT and protein loading buffer was added and the lysate was boiled for 10 min at 95 °C. Equal amounts were loaded on a SDS-gel.

Denatured and native head lysates for FRA and dot blot

To analyse the aggregate load in the *Drosophila* head, native lysates were produced by homogenisation of fly heads a micropestle with Tris-Lysisbuffer or RIPA buffer and protease inhibitor. The lysate was centrifuged at 8,000 rpm for 10 min. The concentration was analyzed by BCA assay and equal amounts of the lysate was loaded on a nitrocellulose membrane or a cellulose acetate membrane. For the denatured lysates, fly heads were homogenised in 2 % SDS buffer and protease inhibitor and centrifuged at 8,000 rpm for 10 min. The concentration was analyzed by BCA assay, the lysate was mixed 1:1 with the denaturation buffer and heated for 5 min at 95 °C. Equal amounts of the lysate were loaded on a cellulose acetate membrane.

Head lysates for FRET assay

For analysis of head lysates in the FRET assay, fly heads were collected and were homogenised in brain lysis buffer and protease inhibitor. The lysate was centrifuges at 8,000 rpm for 10 min at 4 °C. The protein concentration was determined by BCA assay and 2.5 μg of the head lysate was analyzed in the FRET assay.

Retina degeneration assay

To analyse the *Drosophila* retina, dissected fly heads were fixed with Bouin's Fixative for at least 48 hours. Heads were washed with Leachingbuffer overnight. Subsequently, the head were washed several times with 70 % ethanol. The in ethanol inlaid heads can be stored up to one week in the fridge. Afterwards, the heads were dehydrated in increasing concentrations of ethanol (70 %, 80 %, 90 %, 100 %, for one hour at each). Heads were washed for 10 minutes in a mixture of ethanol and Xylol (1:1) and twice in Xylol for 10 minutes. The heads were transferred in paraffin at 60 °C for one hour and following embedded in fresh paraffin. Using a microtome, 10 μm serial sections were obtained and were mounted on polylysine-coated glass slides. The sections were washed twice with Xylol to remove the paraffin and covered with glass coverslip using Entelan. Samples of the control were additionally counterstained with Eosin before covering. The sections were analyzed using the Stereomicroscope. The following crosses were used in retina degeneration analysis: GMR-GAL4 (in a wildtype w+ background) and w^{1118} female virgins were crossed with males bearing a HTT transgene. As a gene driver control GMR-GAL4 female virgins were crossed with w^{1118} males.

Olfactory and shock Avoidance

To assess avoidance to electric shock, native flies were placed at a choice point between two arms of a T-maze. One arm of the T-maze is a normal tube and the other a tube lined with electrifiable grids. The native flies were shocked at 200 V every 5 seconds for 1 min and given 2 min to choose between the normal and the shock tube. Avoidance is measured by a performance index calculated as the fraction of flies that avoid the shock tube minus the fraction of flies that do not. To assess olfactory avoidance, native flies were given the choice between the odor limonene and air. The air flow in both arms of the maze was kept constant at 7 liter per minute. The undiluted limonene (82.5 μl) was applied in the odor container (7 mm diameter.) Avoidance is represented by a performance index, which is calculated as the fraction of flies that avoid the odorant minus the fraction of flies that do not. Flies expressing HTTex1Q97 pan-neuronally (Elav;HTTex1Q97) were analyzed for shock and limonene avoidance. For genetic background controls, flies containing Elav or HTTex1Q97 were reciprocally crossed with their genetic background, w^{1118} flies.

The CantonS flies were used as an internal control.

Climbing Assay

Motor performance test were done using ten age-matched adult females. Under CO_2 anaesthesia, two days old females were collected into vials, at a density of ten flies per vial and eleven vials per experimental group. For the measurement, the flies were placed in an empty vial and tapped down. The percentage of flies that climbed past a 9 cm high line after 15 s was recorded. The measurement was started with three days old flies. Flies were measured two times per week. The following crosses were used in the climbing assay, activity monitoring assay and adult life span assay: Elav-GAL4 and w^{1118} female virgins were crossed with males bearing a HTT transgene. As a gene driver control Elav-GAL4 female virgins were crossed with w^{1118} males.

Adult life span

For the life span assay, three days old female flies were anaesthetised and placed in groups of ten animals in small vials with eleven vials per experimental group. The flies were transferred to fresh medium two times per week. After each transfer, the deaths were recorded.

Activity Monitoring Assay

Locomotor activity was monitored using the *Drosophila* Activity Monitoring (DAM) System as previously described [183]. Flies were lightly anesthetized with CO_2 and placed individually in 65 mm x 5 mm glass locomotor-monitoring tubes containing standard medium. The glass tubes were closed using cotton buds. The tubes were kept into the monitors placed in a temperature-controlled incubator with LD 12:12. To avoid confounding effects of egg-laying females, male flies were used. At least 16 individual flies of each genotype were analyzed and randomly distributed in the monitors to avoid position effects. Activity data were collected in 5 min bins. To display the morning activity, the mean of the beam breaks between 7:00 am and 7:30 am was calculated for each day.

Dissection and immunostaining of *Drosophila* salivary glands

Salivary glands were dissected in PBS from third-instar wandering larvae and were fixed immediately in 4 % formaldehyde in PEM for 30 min. After three washes for 5 min and a following was step for 30 min in PBT (0.1 %), the samples were blocked for at least one hour in 5 % normal goat serum (NGS) in PBT (0.1 %) in a humidified chamber at 4 °C. Samples were incubated with the primary antibody with a concentration of 1:100 in 5 % NGS in PBT (0.1 %) overnight at 4 °C. Afterwards, the samples were washed five times for 5 min and four times for 30 min in PBT

(0.1 %). After final wash the samples were blocked again for at least one hour, were incubated with the secondary antibody with a concentration of 1:100 in 5 % NGS in PBT (0.1 %) overnight at 4 °C and were washed five times for 5 min and four times for 30 min in PBT (0.1 %) and two times for 5 min in PBS. Samples were incubated for 15 min with Hoechst (1:10000 in PBS), washed in two times for 5 min in PBS and covered with Immu-Mount and a coverslip. Images were captured using the SP2 confocal microscope.

Dissection and immunostaining of *Drosophila* adult brain

The whole brain from adult flies were dissected in ice-cold haemolymph-like saline (HL3) solution [261], fixed for 20 min in 4 % paraformaldehyde (PFA) in PBS and then permeabilized PBT (1 %) for 20 min at room temperature. The samples were blocked in 10 % NGS in PBT (0.3 %) for at least two hours. For antibody binding, brains were incubated with the primary antibody in a concentration of 1:500 in brain staining buffer for 48h at 4 °C. The brains were washed two times for 30 min with PBT (0.3 %) at room temperature, followed by incubation in PBT (0.3 %) overnight at 4 °C. The brains were then washed two times for 30 min with PBT (0.3 %) at room temperature, were incubated with the secondary antibody in brain staining buffer for 24 hours at 4 °C and were washed six times for 30 min in PBT (0.3 %) at room temperature. Afterwards, the brains were stored in VectaShield at least for one day at -20 °C. The brains were mounted on slides between two coverslips, were covered with an additional coverslip and sealed with nail polish. Images were captured using the SP8 confocal microscope. Images were analyzed using Fiji.

5 Summary

Huntington's disease (HD) is caused by an elongated CAG repeat located in the exon-1 *huntigtin (HTT)* gene. The disease is characterized by progressive motor, cognitive, and psychiatric impairments.

In order to analyze the molecular pathomechanism of HD in vivo, new *Drosophila melanogaster* models of HD that express different N-terminal huntingtin (HTT) fragments as well as full-length HTT were established. The different HTT fragments contain polyglutamine (polyQ) sequences of different lengths, including wild-type and mutant-associated lengths. The transgenic flies were generated using ΦC31-mediated insertion of different HTT transgenes at the same genomic landing site. A systematic biochemical and behavioral characterization of transgenic flies that express the HTT exon-1 fragments or full-length proteins using the constitutive GAL4 / UAS expression system revealed locomotor impairments and shortened survival in a polyQ-length dependent manner.

Next, an inducible pan-neuronal *Drosophila* model of HD was established and systematically characterized. The inducible expression allows the production of the wild-type and mutant HTT exon-1 proteins exclusively in the adulthood of flies. Furthermore, the inducible Gene-Switch expression system enables researchers to turn off the production of the HTT proteins after a selected period of time. The chronically adult-onset production of a mutant HTT exon-1 protein with 97 glutamines (HTTex1Q97) led to a rapid accumulation of mutant HTT aggregates in fly brains and caused shortening of the life span and late-onset motor impairments. Interestingly, short-time expression of the HTTex1Q97 fragment in adult flies revealed very similar locomotor impairments and reduced survival. However, age does not influence the effect of the mutant HTT protein on the survival of flies. Finally, after the short-time expression of the HTTex1Q97 protein in fly brains the amount of insoluble HTT aggregates increased over time until a steady state level was reached. Further analysis showed that co-expression of HSPA1L reduces the amount of HTT aggregates and suppresses the mutant HTT-induced toxicity in transgenic flies. Finally, the effects of chemical compounds on mutant HTT protein aggregation were investigated.

Taken together, in this study an inducible fly model of HD was established and systematically characterized for long-time and short-time protein expression. The findings of this thesis show that the decrease of mutant HTT expression when HTT aggregates have already formed has a minor effect on the disease progression. Moreover, the quantifiable survival phenotype of the in-

ducible HD fly model presented in this study facilitates the investigation of chemical compounds that might influence the pathogenesis of HD.

6 Zusammenfassung

Chorea Huntington (HD) wird durch eine CAG-Repeat-Verlängerung im Exon-1 des *Huntigtin*-Gens verursacht. Die Krankheit ist durch fortschreitende motorische, kognitive und psychiatrische Beeinträchtigungen charakterisiert.
Um den molekularen Pathomechanismus von HD in vivo zu analysieren, wurden neue *Drosophila melanogaster* Modelle etabliert, die verschiedene N-terminale HTT Fragmente sowie Volllängen-HTT exprimieren. Die HTT Fragments enthalten Polyglutamin (PolyQ)-Sequenzen mit verschiedenen Längen. Für die Herstellung der transgenen Fliegen wurde das ΦC31 Integrationssystem verwendet, dass eine ortsspezifische Integration des Transgenes in das Genom der Fliege vermittelt. Eine systematische biochemische und verhaltensspezifische Charakterisierung der transgenen Fliegen, die das HTT Exon-1 Fragment sowie Volllängen-HTT konstitutiv mittels des GAL4 / UAS Expressionssystems exprimieren, zeigte einen Polyglutaminlängen abhängigen Phänotyp.
Im Anschluss wurde eine induzierbares Fliegen-Modell etabliert und systematisch charakterisiert. Das induzierbare System erlaubt die Expression von normalen und mutierten HTT Exon-1 Fragmenten in Fliegen, die bereits das Erwachsenenalter erreicht haben. Darüber hinaus ermöglicht das Expressionssystem die Unterdrückung der Expression zu einem gewünschten Zeitpunkt. Die chronische Expression eines mutierten HTT Exon-1 Proteins mit 97 Glutaminen im Erwachsenenalter führte zu einer Akkumulation von HTT Aggregaten im Fliegengehirn, sowie zu einer verkürzten Lebensspanne und einer spätmanifesten Beeinträchtigung der Bewegungsfähigkeiten. Die Verkürzung der Expressionszeit führte nur zu ähnlichen Bewegungsbeeinträchtigungen sowie verkürzten Lebensspanne. Dabei zeigte sich, dass das Alter der Fliegen keinen Einflußauf den Phänotyp hat. Zudem blieb die Aggregatmenge nach abschalten der Expression gleich. In weiteren Analysen wurde gezeigt, dass die Co-Expression von HSPA1L die Menge an HTT Aggregaten reduziert und die durch das mutierte HTT vermittelte Toxizität signifikant verringert wird. Schließlich konnte der Effekt von kleinen Molekülen auf die Aggregation des HTTex1Q97 Proteins demonstriert werden.
Im Zuge dieser Arbeit wurde ein induzierbares Fliegen-Modell für HD etabliert und in Bezug auf Langzeit- und Kurzzeit-Expression systematisch charakterisiert. Die Ergebnisse dieser Arbeit zeigen, dass die Reduzierung des krankheitsverursachenden Proteins, als alleiniger Therapieansatz, vermutlich keine vielversprechende Verbesserung bringen kann. Darüber hinaus bietet

der quantifizierbare Phänotyp des induzierbaren Fliegen-Modells die Möglichkeit, die Wirkung von Proteinen sowie kleinen Molekülen auf die Aggregation und die Toxizität von mutierten HTT zu untersuchen.

7 Appendix

```
HTTex1Q0     ATGGCGACCCTGGAAAAGCTGATGAAGGCTTTCGAATCTTTGAAATCTTTTCCACCACCT   60
             CCTCCACCTCCACCACCACCACCTCAATTGCCACAACCACCACCACAAGCTCAACCATTA   120
             TTACCACAACCTCAGCCTCCACCCCCTCCCCCACCTCCACCTCCAGGTCCAGCTGTTGCT   180
             GAAGAACCATTGCATAGACCATGA                                       204

HTTex1Q17    ATGGCGACCCTGGAAAAGCTGATGAAGGCCTTCGAGTCCCTCAAGTCCTTCCAGCAGCAG   60
             CAGCAGCAGCAGCAGCAGCAGCAGCAGCAGCAGCAACAGCCGCCACCGCCGCCGCCG     120
             CCGCCGCCGCCTCCTCAGCTTCCTCAGCCGCCGCCGCAGGCACAGCCGCTGCTGCCTCAG   180
             CCGCAGCCGCCCCCGCCGCCGCCCCCGCCGCCACCCGGCCCGGCCGCGGCTGAGGAGCCG   240
             CTGCACCGACCATGA                                                255

HTTex1Q49    ATGGCGACCCTGGAAAAGCTGATGAAGGCCTTCGAGTCCCTCAAGTCCTTCCAGCAGCAG   60
             CAGCAGCAGCAGCAGCAGCAGCAGCAGCAGCAGCAGCAGCAGCAGCAGCAGCAGCAG     120
             CAGCAGCAGCAGCAGCAGCAGCAGCAGCAGCAGCAGCAGCAGCAGCAGCAGCAGCAG     180
             CAGCAGCAGCAACAGCCGCCACCGCCGCCGCCGCCGCCGCCGCCTCCTCAGCTTCCTCAG   240
             CCGCCGCCGCAGGCACAGCCGCTGCTGCCTCAGCCGCAGCCGCCCCCGCCGCCGCCCCCG   300
             CCGCCACCCGGCCCGGCCGCGGCTGAGGAGCCGCTGCACCGACCATGA               348

HTTex1Q97    ATGGCGACCCTGGAAAAGCTGATGAAGGCCTTCGAGTCCCTCAAGTCCTTCCAACAGCAG   60
             CAACAGCAACAACAGCAGCAACAGCAACAACAGCAGCAACAGCAACAACAGCAGCAACAG   120
             CAACAACAGCAGCAACAGCAACAACAGCAGCAACAGCAACAACAGCAGCAACAGCAACAA   180
             CAGCAGCAACAGCAACAACAGCAGCAACAGCAACAACAGCAGCAACAGCAACAACAGCAG   240
             CAACAGCAACAACAGCAGCAACAGCAACAACAGCAGCAACAGCAACAACAGCAGCAACAG   300
             CAACAACAGCAGCAACAGCAACAACAGCAGCAACAGCAACAACCGCCACCGCCGCCGCCG   360
             CCGCCGCCGCCTCCTCAGCTTCCTCAGCCGCCGCCGCAGGCACAGCCGCTGCTGCCTCAG   420
             CCGCAGCCGCCCCCGCCGCCGCCCCCGCCGCCACCCGGCCCGGCCGCGGCTGAGGAGCCG   480
             CTGCACCGACCATGA                                                495
```

Figure 7.1: Sequence of the HTT exon-1 cDNAs.

```
HTT513Q17       ATGGCGACCCTGGAAAAGCTGATGAAGGCCTTCGAGTCCCTCAAGTCCTTCCAGCAGCAG      60
                CAGCAGCAGCAGCAGCAGCAGCAGCAGCAGCAGCAACAGCCGCCACCGCCGCCGCCG      120
                CCGCCGCCGCCTCCTCAGCTTCCTCAGCCGCCGCCGCAGGCACAGCCGCTGCTGCCTCAG      180
                CCGCAGCCGCCCCCGCCGCCGCCCCCGCCGCCACCCGGCCCGGCCGCGGCTGAGGAGCCG      240
                CTGCACCGACCAAAGAAAGAACTTTCAGCTACCAAGAAAGACCGTGTGAATCATTGTCTG      300
                ACAATATGTGAAAACATAGTGGCACAGTCTGTCAGAAATTCTCCAGAATTTCAGAAACTT      360
                CTGGGCATCGCTATGGAACTTTTTCTGCTGTGCAGTGATGACGCAGAGTCAGATGTCAGG      420
                ATGGTGGCTGACGAATGCCTCAACAAAGTTATCAAAGCTTTGATGGATTCTAATCTTCCA      480
                AGGTTACAGCTCGAGCTCTATAAGGAAATTAAAAAGAATGGTGCCCCTCGGAGTTTGCGT      540
                GCTGCCCTGTGGAGGTTTGCTGAGCTGGCTCACCTGGTTCGGCCTCAGAAATGCAGGCCT      600
                TACCTGGTGAACCTTCTGCCGTGCCTGACTCGAACAAGCAAGAGACCCGAAGAATCAGTC      660
                CAGGAGACCTTGGCTGCAGCTGTTCCCAAAATTATGGCTTCTTTTGGCAATTTTGCAAAT      720
                GACAATGAAATTAAGGTTTTGTTAAAGGCCTTCATAGCGAACCTGAAGTCAAGCTCCCCC      780
                ACCATTCGGCGGACAGCGGCTGGATCAGCAGTGAGCATCTGCCAGCACTCAAGAAGGACA      840
                CAATATTTCTATAGTTGGCTACTAAATGTGCTCCTCGTTCCTGTCGAGGATGAACACTCC      900
                ACTCTGCTGATTCTTGGCGTGCTGCTCACCCTGAGGTATTTGGTGCCCTTGCTGCAGCAG      960
                CAGGTCAAGGACACAAGCCTGAAAGGCAGCTTCGGAGTGACAAGGAAAGAAATGGAAGTC     1020
                TCTCCTTCTGCAGAGCAGCTTGTCCAGGTTTATGAACTGACGTTACATCATACACGGCAC     1080
                CAAGACCACAATGTTGTGACCGGAGCCCTGGAGCTGTTGCAGCAGCTCTTCAGAACGCCT     1140
                CCACCCGAGCTTCTGCAAACCCTGACCGCAGTCGGGGGCATTGGGCAGCTCACCGCTGCT     1200
                AAGGAGGAGTCTGGTGGCCGAAGCCGTAGTGGGAGTATTGTGGAACTTATAGCTGGAGGG     1260
                GGTTCCTCATGCAGCCCTGTCCTTTCAAGAAAACAAAAAGGCAAAGTGCTCTTAGGAGAA     1320
                GAAGAAGCCTTGGAGGATGACTCTGAATCGAGATCGGATGTCAGCAGCTCTGCCTTAACA     1380
                GCCTCAGTGAAGGATGAGATCAGTGGAGAGCTGGCTGCTTCTTCAGGGGTTTCCACTCCA     1440
                GGGTCAGCAGGTCATGACATCATCACAGAACAGCCACGGTCACAGCACACACTGCAGGCG     1500
                GACTCAGTGGATTGA                                                  1515
```

Figure 7.2: Sequence of the HTT513Q17 cDNA.

```
HTTflQ145       ATGGCGACCCTGGAAAAGCTGATGAAGGCCTTCGAGTCCCTCAAGTCCTTCCAACAGCAG       60
                CAACAGCAACAACAGCAGCAACAGCAACAACAGCAGCAACAGCAACAACAGCAGCAACAG       120
                CAACAACAGCAGCAACAGCAACAACAGCAGCAACAGCAACAACAGCAGCAACAGCAACAA       180
                CAGCAGCAACAGCAACAACAGCAGCAACAGCAACAACAGCAGCAACAGCAACAACAGCAG       240
                CAACAGCAACAACAGCAGCAACAGCAACAACAACAGCAGCAACAGCAACAACAGCAGCAA       300
                CAGCAACAACAGCAGCAACAGCAACAACAGCAGCAACAGCAACAACAGCAACAGCAACAA       360
                CAGCAGCAACAGCAACAACAGCAGCAACAGCAACAACAGCAGCAACAGCAGCAACAACAG       420
                CAGCAACAGCAACAACAGCAGCAACAGCAACAACAGCAGCAACAGCAACAACAGCAGCAA       480
                CAGCAACCGCCACCGCCGCCGCCGCCGCCGCCGCCTCCTCAGCTTCCTCAGCCGCCGCCG       540
                CAGGCACAGCCGCTGCTGCCTCAGCCGCAGCCGCCCCCGCCGCCGCCCCCGCCGCCACCC       600
                GGCCCGGCTGTGGCTGAGGAGCCGCTGCACCGACCAAAGAAAGAACTTTCAGCTACCAAG       660
                AAAGACCGTGTGAATCATTGTCTGACAATATGTGAAAACATAGTGGCACAGTCTGTCAGA       720
                AATTCTCCAGAATTTCAGAAACTTCTGGGCATCGCTATGGAACTTTTTCTGCTGTGCAGT       780
                GATGACGCAGAGTCAGATGTCAGGATGGTGGCTGACGAATGCCTCAACAAAGTTATCAAA       840
                GCTTTGATGGATTCTAATCTTCCAAGGTTACAGCTCGAGCTCTATAAGGAAATTAAAAAG       900
                AATGGTGCCCCTCGGAGTTTGCGTGCTGCCCTGTGGAGGTTTGCTGAGCTGGCTCACCTG       960
                GTTCGGCCTCAGAAATGCAGGCCTTACCTGGTGAACCTTCTGCCGTGCCTGACTCGAACA       1020
                AGCAAGAGACCCGAAGAATCAGTCCAGGAGACCTTGGCTGCAGCTGTTCCCAAAATTATG       1080
                GCTTCTTTTGGCAATTTTGCAAATGACAATGAAATTAAGGTTTTGTTAAAGGCCTTCATA       1140
                GCGAACCTGAAGTCAAGCTCCCCCACCATTCGGCGGACAGCGGCTGGATCAGCAGTGAGC       1200
                ATCTGCCAGCACTCAAGAAGGACACAATATTTCTATAGTTGGCTACTAAATGTGCTCTTA       1260
                GGCTTACTCGTTCCTGTCGAGGATGAACACTCCACTCTGCTGATTCTTGGCGTGCTGCTC       1320
                ACCCTGAGGTATTTGGTGCCCTTGCTGCAGCAGCAGGTCAAGGACACAAGCCTGAAAGGC       1380
                AGCTTCGGAGTGACAAGGAAAGAAATGGAAGTCTCTCCTTCTGCAGAGCAGCTTGTCCAG       1440
                GTTTATGAACTGACGTTACATCATACACAGCACCAAGACCACAATGTTGTGACCGGAGCC       1500
                CTGGAGCTGTTGCAGCAGCTCTTCAGAACGCCTCCACCCGAGCTTCTGCAAACCCTGACC       1560
                GCAGTCGGGGGCATTGGGCAGCTCACCGCTGCTAAGGAGGAGTCTGGTGGCCGAAGCCGT       1620
                AGTGGGAGTATTGTGGAACTTATAGCTGGAGGGGGTTCCTCATGCAGCCCTGTCCTTTCA       1680
                AGAAAACAAAAAGGCAAAGTGCTCTTAGGAGAAGAAGAAGCCTTGGAGGATGACTCTGAA       1740
                TCGAGATCGGATGTCAGCAGCTCTGCCTTAACAGCCTCAGTGAAGGATGAGATCAGTGGA       1800
                GAGCTGGCTGCTTCTTCAGGGGTTTCCACTCCAGGGTCAGCAGGTCATGACATCATCACA       1860
                GAACAGCCACGGTCACAGCACACACTGCAGGCGGACTCAGTGGATCTGGCCAGCTGTGAC       1920
                TTGACAAGCTCTGCCACTGATGGGGATGAGGAGGATATCTTGAGCCACAGCTCCAGCCAG       1980
                GTCAGCGCCGTCCCATCTGACCCTGCCATGGACCTGAATGATGGGACCCAGGCCTCGTCG       2040
                CCCATCAGCGACAGCTCCCAGACCACCACCGAAGGGCCTGATTCAGCTGTTACCCCTTCA       2100
                GACAGTTCTGAAATTGTGTTAGACGGTACCGACAACCAGTATTTGGGCCTGCAGATTGGA       2160
                CAGCCCCAGGATGAAGATGAGGAAGCCACAGGTATTCTTCCTGATGAAGCCTCGGAGGCC       2220
                TTCAGGAACTCTTCCATGGCCCTTCAACAGGCACATTTATTGAAAAACATGAGTCACTGC       2280
                AGGCAGCCTTCTGACAGCAGTGTTGATAAATTTGTGTTGAGAGATGAAGCTACTGAACCG       2340
                GGTGATCAAGAAAACAAGCCTTGCCGCATCAAAGGTGACATTGGACAGTCCACTGATGAT       2400
                GACTCTGCACCTCTTGTCCATTGTGTCCGCCTTTTATCTGCTTCGTTTTTGCTAACAGGG       2460
                GGAAAAAATGTGCTGGTTCCGGACAGGGATGTGAGGGTCAGCGTGAAGGCCCTGGCCCTC       2520
                AGGTGGGAGCAGCTGTGGCCCTCCACCCGGAATCTTTCTTCAGCAAACTCTATAAAGTTC       2580
                CTCTGTCTTGACACCACGGAATACCCTGAGGAACAGTATGTCTCAGACATCTTGAACTAC       2640
                ATCGATCATGGAGACCCACAGGTTCGAGGAGCCACTGCCATTCTCTGTGGGACCCTCATC       2700
                TGCTCCATCCTCAGCAGGTCCCGCTTCCACGTGGGAGATTGGATGGGCACCATTAGAACC       2760
                CTCACAGGAAATACATTTTCTTTGGCGGATTGCATTCCTTTGCTGCGGAAAACACTGAAG       2820
                GATGAGTCTTCTGTTACTTGCAAGTTAGCTTGTACAGCTGTGAGGAACTGTGTCATGAGT       2880
                CTCTGCAGCAGCAGCTACAGTGAGTTAGGACTGCAGCTGATCATCGATGTGCTGACTCTG       2940
                AGGAACAGTTCCTATTGGCTGGTGAGGACAGAGCTTCTGGAAACCCTTGCAGAGATTGAC       3000
                TTCAGGCTGGTGAGCTTTTTGGAGGCAAAAGCAGAAAACTTACACAGAGGGGCTCATCAT       3060
                TATACAGGGCTTTTAAAACTGCAAGAACGAGTGCTCAATAATGTTGTCATCCATTTGCTT       3120
                GGAGATGAAGACCCCAGGGTGCGACATGTTGCCGCAGCATCACTAATTAGGCTTGTCCCA       3180
                AAGCTGTTTTATAAATGTGACCAAGGACAAGCTGATCCAGTAGTGGCCGTGGCAAGAGAT       3240
                CAAAGCAGTGTTTACCTGAAACTTCTCATGCATGAAACGCAGCCTCCATCTCATTTCTCC       3300
                GTCAGCACAATAACCAGAATATATAGAGGCTATAACCTACTACCAAGCATAACAGACGTC       3360
                ACTATGGAAAATAACCTTTCAAGAGTTATTGCAGCAGTTTCTCATGAACTAATCACATCA       3420
                ACCACCAGAGCACTCACATTTGGATGCTGTGAAGCTTTGTGTCTTCTTTCCACTGCCTTC       3480
                CCAGTTTGCATTTGGAGTTTAGGTTGGCACTGTGGAGTGCCTCCACTGAGTGCCTCAGAT       3540
```

Figure 7.3: Sequence of the HTTflQ145 cDNA, part 1.

```
HTTflQ145      GAGTCTAGGAAGAGCTGTACCGTTGGGATGGCCACAATGATTCTGACCCTGCTCTCGTCA      3600
               GCTTGGTTCCCATTGGATCTCTCAGCCCATCAAGATGCTTTGATTTTGGCCGGAAACTTG      3660
               CTTGCAGCCAGTGCTCCCAAATCTCTGAGAAGTTCATGGGCCTCTGAAGAAGAAGCCAAC      3720
               CCAGCAGCCACCAAGCAAGAGGAGGTCTGGCCAGCCCTGGGGGACCGGGCCCTGGTGCCC      3780
               ATGGTGGAGCAGCTCTTCTCTCACCTGCTGAAGGTGATTAACATTTGTGCCCACGTCCTG      3840
               GATGACGTGGCTCCTGGACCCGCAATAAAGGCAGCCTTGCCTTCTCTAACAAACCCCCCT      3900
               TCTCTAAGTCCCATCCGACGAAAGGGGAAGGAGAAAGAACCAGGAGAACAAGCATCTGTA      3960
               CCGTTGAGTCCCAAGAAAGGCAGTGAGGCCAGTGCAGCTTCTAGACAATCTGATACCTCA      4020
               GGTCCTGTTACAACAAGTAAATCCTCATCACTGGGGAGTTTCTATCATCTTCCTTCATAC      4080
               CTCAAACTGCATGATGTCCTGAAAGCTACACACGCTAACTACAAGGTCACGCTGGATCTT      4140
               CAGAACAGCACGGAAAAGTTTGGAGGGTTTCTCCGCTCAGCCTTGGATGTTCTTTCTCAG      4200
               ATACTAGAGCTGGCCACACTGCAGGACATTGGGAAGTGTGTTGAAGAGATCCTAGGATAC      4260
               CTGAAATCCTGCTTTAGTCGAGAACCAATGATGGCAACTGTTTGTGTTCAACAATTGTTG      4320
               AAGACTCTCTTTGGCACAAACTTGGCCTCCCAGTTTGATGGCTTATCTTCCAACCCCAGC      4380
               AAGTCACAAGGCCGAGCACAGCGCCTTGGCTCCTCCAGTGTGAGGCCAGGCTTGTACCAC      4440
               TACTGCTTCATGGCCCCGTACACCCACTTCACCCAGGCCCTCGCTGACGCCAGCCTGAGG      4500
               AACATGGTGCAGGCGGAGCAGGAGAACGACACCTCGGGATGGTTTGATGTCCTCCAGAAA      4560
               GTGTCTACCCAGTTGAAGACAAACCTCACGAGTGTCACAAAGAACCGTGCAGATAAGAAT      4620
               GCTATTCATAATCACATTCGTTTGTTTGAACCTCTTGTTATAAAAGCTTTAAAACAGTAC      4680
               ACGACTACAACATGTGTGCAGTTACAGAAGCAGGTTTTAGATTTGCTGGCGCAGCTGGTT      4740
               CAGTTACGGGTTAATTACTGTCTTCTGGATTCAGATCAGGTGTTTATTGGCTTTGTATTG      4800
               AAACAGTTTGAATACATTGAAGTGGGCCAGTTCAGGGAATCAGAGGCAATCATTCCAAAC      4860
               ATCTTTTTCTTCTTGGTATTACTATCTTATGAACGCTATCATTCAAAACAGATCATTGGA      4920
               ATTCCTAAAATCATTCAGCTCTGTGATGGCATCATGGCCAGTGGAAGGAAGGCTGTGACA      4980
               CATGCCATACCGGCTCTGCAGCCCATAGTCCACGACCTCTTTGTATTAAGAGGAACAAAT      5040
               AAAGCTGATGCAGGAAAAGAGCTTGAAACCCAAAAAGAGGTGGTGGTGTCAATGTTACTG      5100
               AGACTCATCCAGTACCATCAGGTGTTGGAGATGTTCATTCTTGTCCTGCAGCAGTGCCAC      5160
               AAGGAGAATGAAGACAAGTGGAAGCGACTGTCTCGACAGATAGCTGACATCATCCTCCCA      5220
               ATGTTAGCCAAACAGCAGATGCACATTGACTCTCATGAAGCCCTTGGAGTGTTAAATACA      5280
               TTATTTGAGATTTTGGCCCCTTCCTCCCTCCGTCCGGTAGACATGCTTTTACGGAGTATG      5340
               TTCGTCACTCCAAACACAATGGCGTCCGTGAGCACTGTTCAACTGTGGATATCGGGAATT      5400
               CTGGCCATTTTGAGGGTTCTGATTTCCCAGTCAACTGAAGATATTGTTCTTTCTCGTATT      5460
               CAGGAGCTCTCCTTCTCTCCCGTATTTAATCTCCTGTACAGTAATTAATAGGTTAAGAGAT      5520
               GGGGACAGTACTTCAACGCTAGAAGAACACAGTGAAGGGAAACAAATAAAGAATTTGCCA      5580
               GAAGAAACATTTTCAAGGTTTCTATTACAACTGGTTGGTATTCTTTTAGAAGACATTGTT      5640
               ACAAAACAGCTGAAGGTGGAAATGAGTGAGCAGCAACATACTTTCTATTGCCAGGAACTA      5700
               GGCACACTGCTAATGTGTCTGATCCACATCTTCAAGTCTGGAATGTTCCGGAGAATCACA      5760
               GCAGCTGCCACTAGGCTGTTCCGCAGTGATGGCTGTGGCGGCAGTTTCTACACCCTGGAC      5820
               AGCTTGAACTTGCGGGCTCGTTCCATGATCACCACCCACCCGGCCCTGGTGCTGCTCTGG      5880
               TGTCAGATACTGCTGCTTGTCAACCACACCGACTACCGCTGGTGGGCAGAAGTGCAGCAG      5940
               ACCCCGAAAAGACACAGTCTGTCCAGCACAAAGTTACTTAGTCCCCAGATGTCTGGAGAA      6000
               GAGGAGGATTCTGACTTGGCAGCCAAACTTGGAATGTGCAATAGAGAAATAGTACGAAGA      6060
               GGGGCTCTCATTCTCTTCTGTGATTATGTCTGTCAGAACCTCCATGACTCCGAGCACTTA      6120
               ACGTGGCTCATTGTAAATCACATTCAAGATCTGATCAGCCTTTCCCACGAGCCTCCAGTA      6180
               CAGGACTTCATCAGTGCCGTTCATCGGAACTCTGCTGCCAGCGGCCTGTTCATCCAGGCA      6240
               ATTCAGTCTCGTTGTGAAAACCTTTCAACTCCAACCATGCTGAAGAAAACTCTTCAGTGC      6300
               TTGGAGGGGATCCATCTCAGCCAGTCGGGAGCTGTGCTCACGCTGTATGTGGACAGGCTT      6360
               CTGTGCACCCCTTTCCGTGTGCTGGCTCGCATGGTCGACATCCTTGCTTGTCGCCGGGTA      6420
               GAAATGCTTCTGGCTGCAAATTTACAGAGCAGCATGGCCCAGTTGCCAATGGAAGAACTC      6480
               AACAGAATCCAGGAATACCTTCAGAGCAGCGGGCTCGCTCAGAGACACCAAAGGCTCTAT      6540
               TCCCTGCTGGACAGGTTTCGTCTGTCCACCATGCAAGACTCACTTAGTCCCTCTCCTCCA      6600
               GTCTCTTCCCACCCGCTGGACGGGGATGGGCACGTGTCACTGGAAACAGTGAGTCCGGAC      6660
               AAAGACTGGTACGTTCATCTTGTCAAATCCCAGTGTTGGACCAGGTCAGATTCTGCACTG      6720
               CTGGAAGGTGCAGAGCTGGTGAATCGGATTCCTGCTGAAGATATGAATGCCTTCATGATG      6780
               AACTCGGAGTTCAACCTAAGCCTGCTAGCTCCATGCTTAAGCCTAGGGATGAGTGAAATT      6840
               TCTGGTGGCCAGAAGAGTGCCCTTTTTGAAGCAGCCCGTGAGGTGACTCTGGCCCGTGTG      6900
               AGCGGCACCGTGCAGCAGCTCCCTGCTGTCCATCATGTCTTCCAGCCCGAGCTGCCTGCA      6960
               GAGCCGGCGGCCTACTGGAGCAAGTTGAATGATCTGTTTGGGGATGCTGCACTGTATCAG      7020
               TCCCTGCCCACTCTGGCCCGGGCCCTGGCACAGTACCTGGTGGTGGTCTCCAAACTGCCC      7080
               AGTCATTTGCACCTTCCTCCTGAGAAAGAGAAGGACATTGTGAAATTCGTGGTGGCAACC      7140
               CTTGAGGCCCTGTCCTGGCATTTGATCCATGAGCAGATCCCGCTGAGTCTGGATCTCCAG      7200
               GCAGGGCTGGACTGCTGCTGCCTGGCCCTGCAGCTGCCTGGCCTCTGGAGCGTGGTCTCC      7260
               TCCACAGAGTTTGTGACCCACGCCTGCTCCCTCATCTACTGTGTGCACTTCATCCTGGAG      7320
               GCCGTTGCAGTGCAGCCTGGAGAGCAGCTTCTTAGTCCAGAAAGAAGGACAAATACCCCA      7380
               AAAGCCATCAGCGAGGAGGAGGAGGAAGTAGATCCAAACACACAGAATCCTAAGTATATC      7440
               ACTGCAGCCTGTGAGATGGTGGCAGAAATGGTGGAGTCTCTGCAGTCGGTGTTGGCCTTG      7500
               GGTCATAAAAGGAATAGCGGCGTGCCGGCGTTTCTCACGCCATTGCTCAGGAACATCATC      7560
```

Figure 7.4: Sequence of the HTTflQ145 cDNA, part 2.

```
HTTflQ145     ATCAGCCTGGCCCGCCTGCCCCTTGTCAACAGCTACACACGTGTGCCCCCACTGGTGTGG     7620
              AAGCTTGGATGGTCACCCAAACCGGGAGGGGATTTTGGCACAGCATTCCCTGAGATCCCC     7680
              GTGGAGTTCCTCCAGGAAAAGGAAGTCTTTAAGGAGTTCATCTACCGCATCAACACACTA     7740
              GGCTGGACCAGTCGTACTCAGTTTGAAGAAACTTGGGCCACCCTCCTTGGTGTCCTGGTG     7800
              ACGCAGCCCCTCGTGATGGAGCAGGAGGAGAGCCCACCAGAAGAAGACACAGAGAGGACC     7860
              CAGATCAACGTCCTGGCCGTGCAGGCCATCACCTCACTGGTGCTCAGTGCAATGACTGTG     7920
              CCTGTGGCCGGCAACCCAGCTGTAAGCTGCTTGGAGCAGCAGCCCCGGAACAAGCCTCTG     7980
              AAAGCTCTCGACACCAGGTTTGGGAGGAAGCTGAGCATTATCAGAGGGATTGTGGAGCAA     8040
              GAGATTCAAGCAATGGTTTCAAAGAGAGAGAATATTGCCACCCATCATTTATATCAGGCA     8100
              TGGGATCCTGTCCCTTCTCTGTCTCCGGCTACTACAGGTGCCCTCATCAGCCACGAGAAG     8160
              CTGCTGCTACAGATCAACCCCGAGCGGGAGCTGGGGAGCATGAGCTACAAACTCGGCCAG     8220
              GTGTCCATACACTCCGTGTGGCTGGGGAACAGCATCACACCCCTGAGGGAGGAGGAATGG     8280
              GACGAGGAAGAGGAGGAGGAGGCCGACGCCCCTGCACCTTCGTCACCACCCACTTCTCCA     8340
              GTCAACTCCAGGAAACACCGGGCTGGAGTTGACATCCACTCCTGTTCGCAGTTTTTGCTT     8400
              GAGTTGTACAGCCGCTGGATCCTGCCGTCCAGCTCAGCCAGGAGGACCCCGGCCATCCTG     8460
              ATCAGTGAGGTGGTCAGATCCCTTCTAGTGGTCTCAGACTTGTTCACCGAGCGCAACCAG     8520
              TTTGAGCTGATGTATGTGACGCTGACAGAACTGCGAAGGGTGCACCCTTCAGAAGACGAG     8580
              ATCCTCGCTCAGTACCTGGTGCCTGCCACCTGCAAGGCAGCTGCCGTCCTTGGGATGGAC     8640
              AAGGCCGTGGCGGAGCCTGTCAGCCGCCTGCTGGAGAGCACGCTCAGGAGCAGCCACCTG     8700
              CCCAGCAGGGTTGGAGCCCTGCACGGCGTCCTCTATGTGCTGGAGTGCGACCTGCTGGAC     8760
              GACACTGCCAAGCAGCTCATCCCGGTCATCAGCGACTATCTCCTCTCCAACCTGAAAGGG     8820
              ATCGCCCACTGCGTGAACATTCACAGCCAGCAGCACGTACTGGTCATGTGTGCCACTGCG     8880
              TTTTACCTCATTGAGAACTATCCTCTGGACGTAGGGCCGGAATTTTCAGCATCAATAATA     8940
              CAGATGTGTGGGGTGATGCTGTCTGGAAGTGAGGAGTCCACCCCCTCCATCATTTACCAC     9000
              TGTGCCCTCAGAGGCCTGGAGCGCCTCCTGCTCTCTGAGCAGCTCTCCCGCCTGGATGCA     9060
              GAATCGCTGGTCAAGCTGAGTGTGGACAGAGTGAACGTGCACAGCCCGCACCGGGCCATG     9120
              GCGGCTCTGGGCCTGATGCTCACCTGCATGTACACAGGAAAGGAGAAAGTCAGTCCGGGT     9180
              AGAACTTCAGACCCTAATCCTGCAGCCCCCGACAGCGAGTCAGTGATTGTTGCTATGGAG     9240
              CGGGTATCTGTTCTTTTTGATAGGATCAGGAAAGGCTTTCCTTGTGAAGCCAGAGTGGTG     9300
              GCCAGGATCCTGCCCCAGTTTCTAGACGACTTCTTCCCACCCCAGGACATCATGAACAAA     9360
              GTCATCGGAGAGTTTCTGTCCAACCAGCAGCCATACCCCCAGTTCATGGCCACCGTGGTG     9420
              TATAAGGTGTTTCAGACTCTGCACAGCACCGGGCAGTCGTCCATGGTCCGGGACTGGGTC     9480
              ATGCTGTCCCTCTCCAACTTCACGGCAGAGGGCCCCGGTCGCCATGGCCACGTGGAGCCTC     9540
              TCCTGCTTCTTTGTCAGCGCGTCCACCAGCCCGTGGGTCGCGGCGATCCTCCCACATGTC     9600
              ATCAGCAGGATGGGCAAGCTGGAGCAGGTGGACGTGAACCTTTTCTGCCTGGTCGCCACA     9660
              GACTTCTACAGACACCAGATAGAGGAGGAGCTCGACCGCAGGGCCTTCCAGTCTGTGCTT     9720
              GAGGTGGTTGCAGCCCCAGGAAGCCCATATCACCGGCTGCTGACTTGTTTACGAAATGTC     9780
              CACAAGGTCACCACCTGC                                               9798
```

Figure 7.5: Sequence of the HTTflQ145 cDNA, part 3.

List of Figures

List of Tables

Bibliography

[1] L. Bertram and R. E. Tanzi. "The genetic epidemiology of neurodegenerative disease". In: *The Journal of clinical investigation* 115.6 (2005), pp. 1449–1457.

[2] A. M. Gorman. "Neuronal cell death in neurodegenerative diseases: recurring themes around protein handling." In: *J Cell Mol Med* 12.6A (Dec. 2008), pp. 2263–80. ISSN: 1582-1838. DOI: 10.1111/j.1582-4934.2008.00402.x.

[3] C. A. Ross and M. A. Poirier. "Protein aggregation and neurodegenerative disease." In: *Nat Med* 10 Suppl (July 2004), S10–7. ISSN: 1078-8956. DOI: 10.1038/nm1066.

[4] D. Scheuner et al. "Secreted amyloid beta-protein similar to that in the senile plaques of Alzheimer's disease is increased in vivo by the presenilin 1 and 2 and APP mutations linked to familial Alzheimer's disease." In: *Nat Med* 2.8 (Aug. 1996), pp. 864–70. ISSN: 1078-8956.

[5] M. H. Polymeropoulos et al. "Mutation in the α-synuclein gene identified in families with Parkinson's disease". In: *science* 276.5321 (1997), pp. 2045–2047. ISSN: 0036-8075.

[6] T. Kitada et al. "Mutations in the parkin gene cause autosomal recessive juvenile parkinsonism." In: *Nature* 392.6676 (Apr. 1998), pp. 605–8. ISSN: 0028-0836. DOI: 10.1038/33416.

[7] W. Guo et al. "An ALS-associated mutation affecting TDP-43 enhances protein aggregation, fibril formation and neurotoxicity." In: *Nat Struct Mol Biol* 18.7 (July 2011), pp. 822–30. ISSN: 1545-9985. DOI: 10.1038/nsmb.2053.

[8] R. Rademakers, M. Neumann, and I. R. Mackenzie. "Advances in understanding the molecular basis of frontotemporal dementia." In: *Nat Rev Neurol* 8.8 (Aug. 2012), pp. 423–34. ISSN: 1759-4766. DOI: 10.1038/nrneurol.2012.117.

[9] M. DiFiglia et al. "Aggregation of huntingtin in neuronal intranuclear inclusions and dystrophic neurites in brain." In: *Science* 277.5334 (Sept. 1997), pp. 1990–3. ISSN: 0036-8075.

[10] J. P. Taylor, J. Hardy, and K. H. Fischbeck. "Toxic proteins in neurodegenerative disease." In: *Science* 296.5575 (June 2002), pp. 1991–5. ISSN: 1095-9203. DOI: 10.1126/science.1067122.

[11] E. Bossy-Wetzel, R. Schwarzenbacher, and S. A. Lipton. "Molecular pathways to neurodegeneration." In: *Nat Med* 10 Suppl (July 2004), S2–9. ISSN: 1078-8956. DOI: 10.1038/nm1067.

[12] J. Schulte and J. T. Littleton. "The biological function of the Huntingtin protein and its relevance to Huntington's Disease pathology." In: *Curr Trends Neurol* 5 (Jan. 2011), pp. 65–78. ISSN: 0972-8252.

[13] A. R. La Spada et al. "Androgen receptor gene mutations in X-linked spinal and bulbar muscular atrophy." In: *Nature* 352.6330 (July 1991), pp. 77–9. ISSN: 0028-0836. DOI: 10.1038/352077a0.

[14] A. R. La Spada and J. P. Taylor. "Polyglutamines placed into context." In: *Neuron* 38.5 (June 2003), pp. 681–4. ISSN: 0896-6273.

[15] H. Y. Zoghbi and H. T. Orr. "Glutamine repeats and neurodegeneration." In: *Annu Rev Neurosci* 23 (2000), pp. 217–47. ISSN: 0147-006X. DOI: 10.1146/annurev.neuro.23.1.217.

[16] P. O. Bauer and N. Nukina. "The pathogenic mechanisms of polyglutamine diseases and current therapeutic strategies." In: *J Neurochem* 110.6 (Sept. 2009), pp. 1737–65. ISSN: 1471-4159. DOI: 10.1111/j.1471-4159.2009.06302.x.

[17] B. A. Margulis et al. "Pharmacological protein targets in polyglutamine diseases: mutant polypeptides and their interactors." In: *FEBS Lett* 587.13 (June 2013), pp. 1997–2007. ISSN: 1873-3468. DOI: 10.1016/j.febslet.2013.05.022.

[18] L. Schöls et al. "Autosomal dominant cerebellar ataxias: clinical features, genetics, and pathogenesis". In: *The Lancet Neurology* 3.5 (2004), pp. 291–304. DOI: 10.1016/S1474-4422(04)00737-9.

[19] G. Orozco Diaz et al. "Autosomal dominant cerebellar ataxia: clinical analysis of 263 patients from a homogeneous population in Holguín, Cuba." In: *Neurology* 40.9 (Sept. 1990), pp. 1369–75. ISSN: 0028-3878.

[20] I. Silveira et al. "Analysis of SCA1, DRPLA, MJD, SCA2, and SCA6 CAG repeats in 48 Portuguese ataxia families." In: *Am J Med Genet* 81.2 (Mar. 1998), pp. 134–8. ISSN: 0148-7299.

[21] H. Takano et al. "Close associations between prevalences of dominantly inherited spinocerebellar ataxias with CAG-repeat expansions and frequencies of large normal CAG alleles in Japanese and Caucasian populations." In: *Am J Hum Genet* 63.4 (Oct. 1998), pp. 1060–6. ISSN: 0002-9297. DOI: 10.1086/302067.

[22] J. D. Cleary and L. P. W. Ranum. "Repeat-associated non-ATG (RAN) translation in neurological disease." In: *Hum Mol Genet* 22.R1 (Oct. 2013), R45–51. ISSN: 1460-2083. DOI: 10.1093/hmg/ddt371.

[23] M. Bañez-Coronel et al. "RAN Translation in Huntington Disease." In: *Neuron* 88.4 (Nov. 2015), pp. 667–77. ISSN: 1097-4199. DOI: 10.1016/j.neuron.2015.10.038.

[24] T. Zu et al. "Non-ATG-initiated translation directed by microsatellite expansions." In: *Proc Natl Acad Sci U S A* 108.1 (Jan. 2011), pp. 260–5. ISSN: 1091-6490. DOI: 10.1073/pnas.1013343108.

[25] G. Huntington. "On chorea. George Huntington, M.D." In: *J Neuropsychiatry Clin Neurosci* 15.1 (2003), pp. 109–12. ISSN: 0895-0172. DOI: 10.1176/jnp.15.1.109.

[26] F. O. Walker. "Huntington's disease". In: *The Lancet* 369.9557 (2007), pp. 218–228. DOI: 10.1016/S0140-6736(07)60111-1.

[27] J. S. Paulsen et al. "Clinical markers of early disease in persons near onset of Huntington's disease." In: *Neurology* 57.4 (Aug. 2001), pp. 658–62. ISSN: 0028-3878.

[28] P. D. Thompson et al. "The coexistence of bradykinesia and chorea in Huntington's disease and its implications for theories of basal ganglia control of movement." In: *Brain* 111 (Pt 2) (Apr. 1988), pp. 223–44. ISSN: 0006-8950.

[29] J. S. Paulsen. "Cognitive impairment in Huntington disease: diagnosis and treatment." In: *Curr Neurol Neurosci Rep* 11.5 (Oct. 2011), pp. 474–83. ISSN: 1534-6293. DOI: 10.1007/s11910-011-0215-x.

[30] R. H. Myers. "Huntington's disease genetics." In: *NeuroRx* 1.2 (Apr. 2004), pp. 255–62. ISSN: 1545-5343. DOI: 10.1602/neurorx.1.2.255.

[31] G. A. Graveland, R. S. Williams, and M. DiFiglia. "Evidence for degenerative and regenerative changes in neostriatal spiny neurons in Huntington's disease." In: *Science* 227.4688 (Feb. 1985), pp. 770–3. ISSN: 0036-8075.

[32] S. Ena, A. de Kerchove d'Exaerde, and S. N. Schiffmann. "Unraveling the differential functions and regulation of striatal neuron sub-populations in motor control, reward, and motivational processes." In: *Front Behav Neurosci* 5 (2011), p. 47. ISSN: 1662-5153. DOI: 10.3389/fnbeh.2011.00047.

[33] I. Han et al. "Differential vulnerability of neurons in Huntington's disease: the role of cell type-specific features." In: *J Neurochem* 113.5 (June 2010), pp. 1073–91. ISSN: 1471-4159. DOI: 10.1111/j.1471-4159.2010.06672.x.

[34] H. B. Fernandes and L. A. Raymond. "NMDA Receptors and Huntingtons Disease". In: *Biology of the NMDA Receptor*. Ed. by A. M. Van Dongen. Frontiers in Neuroscience. Boca Raton (FL): CRC Press/Taylor & Francis, 2009. DOI: NBK5279.

[35] J.-P. .-.-. P. Vonsattel et al. "Neuropathological classification of Huntington's disease." In: *Journal of Neuropathology & Experimental Neurology* 44.6 (1985), pp. 559–577.

[36] J. Sassone et al. "Huntington's disease: the current state of research with peripheral tissues." In: *Exp Neurol* 219.2 (Oct. 2009), pp. 385–97. ISSN: 1090-2430. DOI: 10.1016/j.expneurol.2009.05.012.

[37] G. P. Bates et al. "Huntington disease." In: *Nat Rev Dis Primers* 1 (2015), p. 15005. ISSN: 2056-676X. DOI: 10.1038/nrdp.2015.5.

[38] "A novel gene containing a trinucleotide repeat that is expanded and unstable on Huntington's disease chromosomes. The Huntington's Disease Collaborative Research Group." In: *Cell* 72.6 (Mar. 1993), pp. 971–83. ISSN: 0092-8674.

[39] D. C. Rubinsztein et al. "Phenotypic characterization of individuals with 30-40 CAG repeats in the Huntington disease (HD) gene reveals HD cases with 36 repeats and apparently normal elderly individuals with 36-39 repeats." In: *Am J Hum Genet* 59.1 (July 1996), pp. 16–22. ISSN: 0002-9297.

[40] S. E. Andrew et al. "The relationship between trinucleotide (CAG) repeat length and clinical features of Huntington's disease." In: *Nat Genet* 4.4 (Aug. 1993), pp. 398–403. ISSN: 1061-4036. DOI: 10.1038/ng0893-398.

[41] N. G. Ranen et al. "Anticipation and instability of IT-15 (CAG)n repeats in parent-offspring pairs with Huntington disease." In: *Am J Hum Genet* 57.3 (Sept. 1995), pp. 593–602. ISSN: 0002-9297.

[42] C. Zuccato and E. Cattaneo. "Brain-derived neurotrophic factor in neurodegenerative diseases." In: *Nat Rev Neurol* 5.6 (June 2009), pp. 311–22. ISSN: 1759-4766. DOI: 10.1038/nrneurol.2009.54.

[43] P. Harjes and E. E. Wanker. "The hunt for huntingtin function: interaction partners tell many different stories." In: *Trends Biochem Sci* 28.8 (Aug. 2003), pp. 425–33. ISSN: 0968-0004. DOI: 10.1016/S0968-0004(03)00168-3.

[44] R. Vijayvargia et al. "Huntingtin's spherical solenoid structure enables polyglutamine tract-dependent modulation of its structure and function." In: *Elife* 5 (2016), e11184. ISSN: 2050-084X. DOI: 10.7554/eLife.11184.

[45] M. W. Kim et al. "Secondary structure of Huntingtin amino-terminal region." In: *Structure* 17.9 (Sept. 2009), pp. 1205–12. ISSN: 1878-4186. DOI: 10.1016/j.str.2009.08.002.

[46] C. Zuccato, M. Valenza, and E. Cattaneo. "Molecular mechanisms and potential therapeutical targets in Huntington's disease." In: *Physiol Rev* 90.3 (July 2010), pp. 905–81. ISSN: 1522-1210. DOI: 10.1152/physrev.00041.2009.

[47] M. H. Schaefer, E. E. Wanker, and M. A. Andrade-Navarro. "Evolution and function of CAG/polyglutamine repeats in protein-protein interaction networks." In: *Nucleic Acids Res* 40.10 (May 2012), pp. 4273–87. ISSN: 1362-4962. DOI: 10.1093/nar/gks011.

[48] M. A. Andrade and P. Bork. "HEAT repeats in the Huntington's disease protein". In: *Nature genetics* 11.2 (1995), pp. 115–116. ISSN: 1061-4036. DOI: 10.1038/ng1095-115.

[49] J. Xia et al. "Huntingtin contains a highly conserved nuclear export signal." In: *Hum Mol Genet* 12.12 (June 2003), pp. 1393–403. ISSN: 0964-6906.

[50] C. L. Wellington et al. "Inhibiting caspase cleavage of huntingtin reduces toxicity and aggregate formation in neuronal and nonneuronal cells." In: *J Biol Chem* 275.26 (June 2000), pp. 19831–8. ISSN: 0021-9258. DOI: 10.1074/jbc.M001475200.

[51] R. K. Graham et al. "Cleavage at the caspase-6 site is required for neuronal dysfunction and degeneration due to mutant huntingtin." In: *Cell* 125.6 (June 2006), pp. 1179–91. ISSN: 0092-8674. DOI: 10.1016/j.cell.2006.04.026.

[52] J. Gafni et al. "Inhibition of calpain cleavage of huntingtin reduces toxicity: accumulation of calpain/caspase fragments in the nucleus." In: *J Biol Chem* 279.19 (May 2004), pp. 20211–20. ISSN: 0021-9258. DOI: 10.1074/jbc.M401267200.

[53] C. L. Wellington et al. "Caspase cleavage of gene products associated with triplet expansion disorders generates truncated fragments containing the polyglutamine tract." In: *J Biol Chem* 273.15 (Apr. 1998), pp. 9158–67. ISSN: 0021-9258.

[54] C. Landles et al. "Caspase-6 does not contribute to the proteolysis of mutant huntingtin in the HdhQ150 knock-in mouse model of Huntington?'s disease". In: *PLOS Currents Huntington Disease* (2012).

[55] A. Lunkes et al. "Proteases acting on mutant huntingtin generate cleaved products that differentially build up cytoplasmic and nuclear inclusions." In: *Mol Cell* 10.2 (Aug. 2002), pp. 259–69. ISSN: 1097-2765.

[56] L. Mangiarini et al. “Exon 1 of the HD gene with an expanded CAG repeat is sufficient to cause a progressive neurological phenotype in transgenic mice”. In: *Cell* 87.3 (1996), pp. 493–506. ISSN: 0092-8674.

[57] E. Scherzinger et al. “Huntingtin-encoded polyglutamine expansions form amyloid-like protein aggregates in vitro and in vivo.” In: *Cell* 90.3 (Aug. 1997), pp. 549–58. ISSN: 0092-8674.

[58] J. S. Steffan et al. “Histone deacetylase inhibitors arrest polyglutamine-dependent neurodegeneration in Drosophila.” In: *Nature* 413.6857 (Oct. 2001), pp. 739–43. ISSN: 0028-0836. DOI: 10.1038/35099568.

[59] K. Sathasivam et al. “Aberrant splicing of HTT generates the pathogenic exon 1 protein in Huntington disease.” In: *Proc Natl Acad Sci U S A* 110.6 (Feb. 2013), pp. 2366–70. ISSN: 1091-6490. DOI: 10.1073/pnas.1221891110.

[60] J. S. Steffan et al. “SUMO modification of Huntingtin and Huntington’s disease pathology.” In: *Science* 304.5667 (Apr. 2004), pp. 100–4. ISSN: 1095-9203. DOI: 10.1126/science.1092194.

[61] X. Gu et al. “Serines 13 and 16 are critical determinants of full-length human mutant huntingtin induced disease pathogenesis in HD mice.” In: *Neuron* 64.6 (Dec. 2009), pp. 828–40. ISSN: 1097-4199. DOI: 10.1016/j.neuron.2009.11.020.

[62] L. M. Thompson et al. “IKK phosphorylates Huntingtin and targets it for degradation by the proteasome and lysosome.” In: *J Cell Biol* 187.7 (Dec. 2009), pp. 1083–99. ISSN: 1540-8140. DOI: 10.1083/jcb.200909067.

[63] E. Cattaneo, C. Zuccato, and M. Tartari. “Normal huntingtin function: an alternative approach to Huntington’s disease.” In: *Nat Rev Neurosci* 6.12 (Dec. 2005), pp. 919–30. ISSN: 1471-003X. DOI: 10.1038/nrn1806.

[64] C. Landles and G. P. Bates. “Huntingtin and the molecular pathogenesis of Huntington’s disease. Fourth in molecular medicine review series.” In: *EMBO Rep* 5.10 (Oct. 2004), pp. 958–63. ISSN: 1469-221X. DOI: 10.1038/sj.embor.7400250.

[65] S. Zeitlin et al. “Increased apoptosis and early embryonic lethality in mice nullizygous for the Huntington’s disease gene homologue.” In: *Nat Genet* 11.2 (Oct. 1995), pp. 155–63. ISSN: 1061-4036. DOI: 10.1038/ng1095-155.

[66] S. W. Davies et al. “Formation of neuronal intranuclear inclusions underlies the neurological dysfunction in mice transgenic for the HD mutation”. In: *Cell* 90.3 (1997), pp. 537–548. ISSN: 0092-8674.

[67] M. F. Perutz et al. “Glutamine repeats as polar zippers: their possible role in inherited neurodegenerative diseases.” In: *Proc Natl Acad Sci U S A* 91.12 (June 1994), pp. 5355–8. ISSN: 0027-8424.

[68] E. Scherzinger et al. “Self-assembly of polyglutamine-containing huntingtin fragments into amyloid-like fibrils: implications for Huntington’s disease pathology.” In: *Proc Natl Acad Sci U S A* 96.8 (Apr. 1999), pp. 4604–9. ISSN: 0027-8424.

[69] E. E. Wanker. “Protein aggregation and pathogenesis of Huntington’s disease: mechanisms and correlations.” In: *Biol Chem* 381.9-10 (2000), pp. 937–42. ISSN: 1431-6730. DOI: 10.1515/BC.2000.114.

[70] A. K. Thakur et al. “Polyglutamine disruption of the huntingtin exon 1 N terminus triggers a complex aggregation mechanism.” In: *Nat Struct Mol Biol* 16.4 (Apr. 2009), pp. 380–9. ISSN: 1545-9985. DOI: 10.1038/nsmb.1570.

[71] B. Sahoo et al. “Aggregation behavior of chemically synthesized, full-length huntingtin exon1.” In: *Biochemistry* 53.24 (June 2014), pp. 3897–907. ISSN: 1520-4995. DOI: 10.1021/bi500300c.

[72] M. M. P. Pearce et al. “Prion-like transmission of neuronal huntingtin aggregates to phagocytic glia in the Drosophila brain.” In: *Nat Commun* 6 (2015), p. 6768. ISSN: 2041-1723. DOI: 10.1038/ncomms7768.

[73] J. S. Steffan et al. “The Huntington’s disease protein interacts with p53 and CREB-binding protein and represses transcription.” In: *Proc Natl Acad Sci U S A* 97.12 (June 2000), pp. 6763–8. ISSN: 0027-8424. DOI: 10.1073/pnas.100110097.

[74] G. Schilling et al. “Characterization of huntingtin pathologic fragments in human Huntington disease, transgenic mice, and cell models.” In: *J Neuropathol Exp Neurol* 66.4 (Apr. 2007), pp. 313–20. ISSN: 0022-3069. DOI: 10.1097/nen.0b013e318040b2c8.

[75] J. K. Cooper et al. “Truncated N-terminal fragments of huntingtin with expanded glutamine repeats form nuclear and cytoplasmic aggregates in cell culture.” In: *Hum Mol Genet* 7.5 (May 1998), pp. 783–90. ISSN: 0964-6906.

[76] S. H. Li and X. J. Li. “Aggregation of N-terminal huntingtin is dependent on the length of its glutamine repeats.” In: *Hum Mol Genet* 7.5 (May 1998), pp. 777–82. ISSN: 0964-6906.

[77] D. Martindale et al. “Length of huntingtin and its polyglutamine tract influences localization and frequency of intracellular aggregates.” In: *Nat Genet* 18.2 (Feb. 1998), pp. 150–4. ISSN: 1061-4036. DOI: 10.1038/ng0298-150.

[78] A. S. Hackam et al. “The influence of huntingtin protein size on nuclear localization and cellular toxicity.” In: *J Cell Biol* 141.5 (June 1998), pp. 1097–105. ISSN: 0021-9525.

[79] W. Yang et al. "Aggregated polyglutamine peptides delivered to nuclei are toxic to mammalian cells." In: *Hum Mol Genet* 11.23 (Nov. 2002), pp. 2905–17. ISSN: 0964-6906.

[80] M. Kurosawa et al. "Depletion of p62 reduces nuclear inclusions and paradoxically ameliorates disease phenotypes in Huntington's model mice." In: *Hum Mol Genet* 24.4 (Feb. 2015), pp. 1092–105. ISSN: 1460-2083. DOI: 10.1093/hmg/ddu522.

[81] A. C. Woerner et al. "Cytoplasmic protein aggregates interfere with nucleocytoplasmic transport of protein and RNA." In: *Science* 351.6269 (Jan. 2016), pp. 173–6. ISSN: 1095-9203. DOI: 10.1126/science.aad2033.

[82] P.-H. H. Ren et al. "Cytoplasmic penetration and persistent infection of mammalian cells by polyglutamine aggregates." In: *Nat Cell Biol* 11.2 (Feb. 2009), pp. 219–25. ISSN: 1476-4679. DOI: 10.1038/ncb1830.

[83] I. Jeon et al. "Human-to-mouse prion-like propagation of mutant huntingtin protein." In: *Acta Neuropathol* 132.4 (Oct. 2016), pp. 577–92. ISSN: 1432-0533. DOI: 10.1007/s00401-016-1582-9.

[84] E. Pecho-Vrieseling et al. "Transneuronal propagation of mutant huntingtin contributes to non-cell autonomous pathology in neurons." In: *Nat Neurosci* 17.8 (Aug. 2014), pp. 1064–72. ISSN: 1546-1726. DOI: 10.1038/nn.3761.

[85] D. T. Babcock and B. Ganetzky. "Transcellular spreading of huntingtin aggregates in the Drosophila brain." In: *Proc Natl Acad Sci U S A* 112.39 (Sept. 2015), E5427–33. ISSN: 1091-6490. DOI: 10.1073/pnas.1516217112.

[86] S. Kuemmerle et al. "Huntingtin aggregates may not predict neuronal death in Huntington's disease". In: *Annals of neurology* 46.6 (1999), pp. 842–849.

[87] K. Sathasivam et al. "Formation of polyglutamine inclusions in non-CNS tissue." In: *Hum Mol Genet* 8.5 (May 1999), pp. 813–22. ISSN: 0964-6906.

[88] M. Arrasate et al. "Inclusion body formation reduces levels of mutant huntingtin and the risk of neuronal death." In: *Nature* 431.7010 (Oct. 2004), pp. 805–10. ISSN: 1476-4687. DOI: 10.1038/nature02998.

[89] F. Saudou et al. "Huntingtin acts in the nucleus to induce apoptosis but death does not correlate with the formation of intranuclear inclusions". In: *Cell* 95.1 (1998), pp. 55–66. ISSN: 0092-8674.

[90] J. P. Taylor et al. "Aggresomes protect cells by enhancing the degradation of toxic polyglutamine-containing protein." In: *Hum Mol Genet* 12.7 (Apr. 2003), pp. 749–57. ISSN: 0964-6906.

[91] Y. Wang et al. "Abnormal proteins can form aggresome in yeast: aggresome-targeting signals and components of the machinery." In: *FASEB J* 23.2 (Feb. 2009), pp. 451–63. ISSN: 1530-6860. DOI: 10.1096/fj.08-117614.

[92] P. J. Muchowski et al. "Requirement of an intact microtubule cytoskeleton for aggregation and inclusion body formation by a mutant huntingtin fragment." In: *Proc Natl Acad Sci U S A* 99.2 (Jan. 2002), pp. 727–32. ISSN: 0027-8424. DOI: 10.1073/pnas.022628699.

[93] Z. Ortega and J. J. Lucas. "Ubiquitin-proteasome system involvement in Huntington's disease." In: *Front Mol Neurosci* 7 (2014), p. 77. ISSN: 1662-5099. DOI: 10.3389/fnmol.2014.00077.

[94] S. Waelter et al. "Accumulation of mutant huntingtin fragments in aggresome-like inclusion bodies as a result of insufficient protein degradation." In: *Mol Biol Cell* 12.5 (May 2001), pp. 1393–407. ISSN: 1059-1524. DOI: PMC34592.

[95] S. Tydlacka et al. "Differential activities of the ubiquitin-proteasome system in neurons versus glia may account for the preferential accumulation of misfolded proteins in neurons." In: *J Neurosci* 28.49 (Dec. 2008), pp. 13285–95. ISSN: 1529-2401. DOI: 10.1523/JNEUROSCI.4393-08.2008.

[96] L. S. Havel et al. "Preferential accumulation of N-terminal mutant huntingtin in the nuclei of striatal neurons is regulated by phosphorylation." In: *Hum Mol Genet* 20.7 (Apr. 2011), pp. 1424–37. ISSN: 1460-2083. DOI: 10.1093/hmg/ddr023.

[97] S. A. Houck, S. Singh, and D. M. Cyr. "Cellular responses to misfolded proteins and protein aggregates." In: *Methods Mol Biol* 832 (2012), pp. 455–61. ISSN: 1940-6029. DOI: 10.1007/978-1-61779-474-2_32.

[98] P. J. Muchowski and J. L. Wacker. "Modulation of neurodegeneration by molecular chaperones." In: *Nat Rev Neurosci* 6.1 (Jan. 2005), pp. 11–22. ISSN: 1471-003X. DOI: 10.1038/nrn1587.

[99] D. G. Hay et al. "Progressive decrease in chaperone protein levels in a mouse model of Huntington's disease and induction of stress proteins as a therapeutic approach." In: *Hum Mol Genet* 13.13 (July 2004), pp. 1389–405. ISSN: 0964-6906. DOI: 10.1093/hmg/ddh144.

[100] N. Y. M. Huen and H. Y. E. Chan. "Dynamic regulation of molecular chaperone gene expression in polyglutamine disease." In: *Biochem Biophys Res Commun* 334.4 (Sept. 2005), pp. 1074–84. ISSN: 0006-291X. DOI: 10.1016/j.bbrc.2005.07.008.

[101] M. A. Rujano, H. H. Kampinga, and F. A. Salomons. "Modulation of polyglutamine inclusion formation by the Hsp70 chaperone machine." In: *Exp Cell Res* 313.16 (Oct. 2007), pp. 3568–78. ISSN: 0014-4827. DOI: 10.1016/j.yexcr.2007.07.034.

[102] V. Kakkar et al. "The S/T-Rich Motif in the DNAJB6 Chaperone Delays Polyglutamine Aggregation and the Onset of Disease in a Mouse Model." In: *Mol Cell* (Apr. 2016). ISSN: 1097-4164. DOI: 10.1016/j.molcel.2016.03.017.

[103] P. J. Muchowski et al. "Hsp70 and hsp40 chaperones can inhibit self-assembly of polyglutamine proteins into amyloid-like fibrils." In: *Proc Natl Acad Sci U S A* 97.14 (July 2000), pp. 7841–6. ISSN: 0027-8424. DOI: 10.1073/pnas.140202897.

[104] J. M. Warrick et al. "Suppression of polyglutamine-mediated neurodegeneration in Drosophila by the molecular chaperone HSP70." In: *Nat Genet* 23.4 (Dec. 1999), pp. 425–8. ISSN: 1061-4036. DOI: 10.1038/70532.

[105] H. Y. Chan et al. "Mechanisms of chaperone suppression of polyglutamine disease: selectivity, synergy and modulation of protein solubility in Drosophila." In: *Hum Mol Genet* 9.19 (Nov. 2000), pp. 2811–20. ISSN: 0964-6906.

[106] S. H. Shahmoradian et al. "TRiC's tricks inhibit huntingtin aggregation." In: *Elife* 2 (2013), e00710. ISSN: 2050-084X. DOI: 10.7554/eLife.00710.

[107] M. Stroedicke et al. "Systematic interaction network filtering identifies CRMP1 as a novel suppressor of huntingtin misfolding and neurotoxicity." In: *Genome Res* 25.5 (May 2015), pp. 701–13. ISSN: 1549-5469. DOI: 10.1101/gr.182444.114.

[108] E. A. Thomas et al. "The HDAC inhibitor 4b ameliorates the disease phenotype and transcriptional abnormalities in Huntington's disease transgenic mice." In: *Proc Natl Acad Sci U S A* 105.40 (Oct. 2008), pp. 15564–9. ISSN: 1091-6490. DOI: 10.1073/pnas.0804249105.

[109] T. J. van Ham et al. "Identification of MOAG-4/SERF as a regulator of age-related proteotoxicity." In: *Cell* 142.4 (Aug. 2010), pp. 601–12. ISSN: 1097-4172. DOI: 10.1016/j.cell.2010.07.020.

[110] X.-J. J. Li, H. Li, and S. Li. "Clearance of mutant huntingtin." In: *Autophagy* 6.5 (July 2010), pp. 663–4. ISSN: 1554-8635. DOI: 10.1093/hmg/ddq127.

[111] K. Lu, I. Psakhye, and S. Jentsch. "Autophagic clearance of polyQ proteins mediated by ubiquitin-Atg8 adaptors of the conserved CUET protein family." In: *Cell* 158.3 (July 2014), pp. 549–63. ISSN: 1097-4172. DOI: 10.1016/j.cell.2014.05.048.

[112] P.-F. F. Wei et al. "Accelerating the clearance of mutant huntingtin protein aggregates through autophagy induction by europium hydroxide nanorods." In: *Biomaterials* 35.3 (Jan. 2014), pp. 899–907. ISSN: 1878-5905. DOI: 10.1016/j.biomaterials.2013.10.024.

[113] A. Yamamoto, M. L. Cremona, and J. E. Rothman. "Autophagy-mediated clearance of huntingtin aggregates triggered by the insulin-signaling pathway." In: *J Cell Biol* 172.5 (Feb. 2006), pp. 719–31. ISSN: 0021-9525. DOI: 10.1083/jcb.200510065.

[114] B. Ravikumar et al. "Rab5 modulates aggregation and toxicity of mutant huntingtin through macroautophagy in cell and fly models of Huntington disease." In: *J Cell Sci* 121.Pt 10 (May 2008), pp. 1649–60. ISSN: 0021-9533. DOI: 10.1242/jcs.025726.

[115] A. Kumar et al. "Huntington's disease: an update of therapeutic strategies." In: *Gene* 556.2 (Feb. 2015), pp. 91–7. ISSN: 1879-0038. DOI: 10.1016/j.gene.2014.11.022.

[116] J. M. Ferrara et al. "Effect of tetrabenazine on motor function in patients with huntington disease." In: *Neurol Ther* 1.1 (Dec. 2012), p. 5. ISSN: 2193-8253. DOI: 10.1007/s40120-012-0005-7.

[117] I. Aharony et al. "A Huntingtin-based peptide inhibitor of caspase-6 provides protection from mutant Huntingtin-induced motor and behavioral deficits." In: *Hum Mol Genet* 24.9 (May 2015), pp. 2604–14. ISSN: 1460-2083. DOI: 10.1093/hmg/ddv023.

[118] R. J. Ferrante et al. "Histone deacetylase inhibition by sodium butyrate chemotherapy ameliorates the neurodegenerative phenotype in Huntington's disease mice." In: *J Neurosci* 23.28 (Oct. 2003), pp. 9418–27. ISSN: 1529-2401.

[119] G. Gardian et al. "Neuroprotective effects of phenylbutyrate in the N171-82Q transgenic mouse model of Huntington's disease." In: *J Biol Chem* 280.1 (Jan. 2005), pp. 556–63. ISSN: 0021-9258. DOI: 10.1074/jbc.M410210200.

[120] D. E. Ehrnhoefer et al. "Green tea (-)-epigallocatechin-gallate modulates early events in huntingtin misfolding and reduces toxicity in Huntington's disease models." In: *Hum Mol Genet* 15.18 (Sept. 2006), pp. 2743–51. ISSN: 0964-6906. DOI: 10.1093/hmg/ddl210.

[121] Y. Liu et al. "Sulforaphane enhances proteasomal and autophagic activities in mice and is a potential therapeutic reagent for Huntington's disease." In: *J Neurochem* 129.3 (May 2014), pp. 539–47. ISSN: 1471-4159. DOI: 10.1111/jnc.12647.

[122] S. Sarkar et al. "Small molecules enhance autophagy and reduce toxicity in Huntington's disease models." In: *Nat Chem Biol* 3.6 (June 2007), pp. 331–8. ISSN: 1552-4450. DOI: 10.1038/nchembio883.

[123] C. Henriques.

[124] H. B. Kordasiewicz et al. "Sustained therapeutic reversal of Huntington's disease by transient repression of huntingtin synthesis." In: *Neuron* 74.6 (June 2012), pp. 1031–44. ISSN: 1097-4199. DOI: 10.1016/j.neuron.2012.05.009.

[125] L. M. Stanek et al. "Silencing mutant huntingtin by adeno-associated virus-mediated RNA interference ameliorates disease manifestations in the YAC128 mouse model of Huntington's disease." In: *Hum Gene Ther* 25.5 (May 2014), pp. 461–74. ISSN: 1557-7422. DOI: 10.1089/hum.2013.200.

[126] S.-H. H. Yang and A. W. S. Chan. "Transgenic Animal Models of Huntington's Disease." In: *Curr Top Behav Neurosci* 7 (2011), pp. 61–85. ISSN: 1866-3370. DOI: 10.1007/7854_2010_105.

[127] S. Ramaswamy, J. L. McBride, and J. H. Kordower. "Animal models of Huntington's disease". In: *Ilar Journal* 48.4 (2007), pp. 356–373.

[128] G. Schilling et al. "Intranuclear inclusions and neuritic aggregates in transgenic mice expressing a mutant N-terminal fragment of huntingtin." In: *Hum Mol Genet* 8.3 (Mar. 1999), pp. 397–407. ISSN: 0964-6906.

[129] E. J. Slow et al. "Absence of behavioral abnormalities and neurodegeneration in vivo despite widespread neuronal huntingtin inclusions." In: *Proc Natl Acad Sci U S A* 102.32 (Aug. 2005), pp. 11402–7. ISSN: 0027-8424. DOI: 10.1073/pnas.0503634102.

[130] M. Gray et al. "Full-length human mutant huntingtin with a stable polyglutamine repeat can elicit progressive and selective neuropathogenesis in BACHD mice." In: *J Neurosci* 28.24 (June 2008), pp. 6182–95. ISSN: 1529-2401. DOI: 10.1523/JNEUROSCI.0857-08.2008.

[131] M. A. Pouladi, A. J. Morton, and M. R. Hayden. "Choosing an animal model for the study of Huntington's disease." In: *Nat Rev Neurosci* 14.10 (Oct. 2013), pp. 708–21. ISSN: 1471-0048. DOI: 10.1038/nrn3570.

[132] S.-H. H. Yang et al. "Towards a transgenic model of Huntington's disease in a non-human primate." In: *Nature* 453.7197 (June 2008), pp. 921–4. ISSN: 1476-4687. DOI: 10.1038/nature06975.

[133] J. C. Jacobsen et al. "An ovine transgenic Huntington's disease model." In: *Hum Mol Genet* 19.10 (May 2010), pp. 1873–82. ISSN: 1460-2083. DOI: 10.1093/hmg/ddq063.

[134] P. M. Dexter, K. A. Caldwell, and G. A. Caldwell. "A predictable worm: application of Caenorhabditis elegans for mechanistic investigation of movement disorders." In: *Neurotherapeutics* 9.2 (Apr. 2012), pp. 393–404. ISSN: 1878-7479. DOI: 10.1007/s13311-012-0109-x.

[135] F.-X. X. Lejeune et al. “Large-scale functional RNAi screen in C. elegans identifies genes that regulate the dysfunction of mutant polyglutamine neurons.” In: *BMC Genomics* 13 (2012), p. 91. ISSN: 1471-2164. DOI: 10.1186/1471-2164-13-91.

[136] J. Doumanis et al. “RNAi screening in Drosophila cells identifies new modifiers of mutant huntingtin aggregation.” In: *PLoS One* 4.9 (2009), e7275. ISSN: 1932-6203. DOI: 10.1371/journal.pone.0007275.

[137] S. Lenz et al. “Drosophila as a screening tool to study human neurodegenerative diseases.” In: *J Neurochem* 127.4 (Nov. 2013), pp. 453–60. ISSN: 1471-4159. DOI: 10.1111/jnc.12446.

[138] C. Voisine et al. “Identification of potential therapeutic drugs for huntington’s disease using Caenorhabditis elegans.” In: *PLoS One* 2.6 (2007), e504. ISSN: 1932-6203. DOI: 10.1371/journal.pone.0000504.

[139] N. Agrawal et al. “Identification of combinatorial drug regimens for treatment of Huntington’s disease using Drosophila.” In: *Proc Natl Acad Sci U S A* 102.10 (Mar. 2005), pp. 3777–81. ISSN: 0027-8424. DOI: 10.1073/pnas.0500055102.

[140] U. B. Pandey and C. D. Nichols. “Human disease models in Drosophila melanogaster and the role of the fly in therapeutic drug discovery.” In: *Pharmacol Rev* 63.2 (June 2011), pp. 411–36. ISSN: 1521-0081. DOI: 10.1124/pr.110.003293.

[141] K. M. Beckingham et al. “Drosophila melanogaster–the model organism of choice for the complex biology of multi-cellular organisms.” In: *Gravit Space Biol Bull* 18.2 (June 2005), pp. 17–29. ISSN: 1089-988X.

[142] A. Bachmann and E. Knust. “The use of P-element transposons to generate transgenic flies.” In: *Methods Mol Biol* 420 (2008), pp. 61–77. ISSN: 1064-3745. DOI: 10.1007/978-1-59745-583-1_4.

[143] E. W. Green and F. Giorgini. “Choosing and using Drosophila models to characterize modifiers of Huntington’s disease.” In: *Biochem Soc Trans* 40.4 (Aug. 2012), pp. 739–45. ISSN: 1470-8752. DOI: 10.1042/BST20120072.

[144] G. R. Jackson et al. “Polyglutamine-expanded human huntingtin transgenes induce degeneration of Drosophila photoreceptor neurons.” In: *Neuron* 21.3 (Sept. 1998), pp. 633–42. ISSN: 0896-6273.

[145] L. S. Kaltenbach et al. “Huntingtin interacting proteins are genetic modifiers of neurodegeneration.” In: *PLoS Genet* 3.5 (May 2007), e82. ISSN: 1553-7404. DOI: 10.1371/journal.pgen.0030082.

[146] W.-C. M. C. Lee, M. Yoshihara, and J. T. Littleton. "Cytoplasmic aggregates trap polyglutamine-containing proteins and block axonal transport in a Drosophila model of Huntington's disease." In: *Proc Natl Acad Sci U S A* 101.9 (Mar. 2004), pp. 3224–9. ISSN: 0027-8424. DOI: 10.1073/pnas.0400243101.

[147] E. Romero et al. "Suppression of neurodegeneration and increased neurotransmission caused by expanded full-length huntingtin accumulating in the cytoplasm." In: *Neuron* 57.1 (Jan. 2008), pp. 27–40. ISSN: 0896-6273. DOI: 10.1016/j.neuron.2007.11.025.

[148] A. Chongtham and N. Agrawal. "Curcumin modulates cell death and is protective in Huntington's disease model." In: *Sci Rep* 6 (2016), p. 18736. ISSN: 2045-2322. DOI: 10.1038/srep18736.

[149] B. L. Apostol et al. "A cell-based assay for aggregation inhibitors as therapeutics of polyglutamine-repeat disease and validation in Drosophila." In: *Proc Natl Acad Sci U S A* 100.10 (May 2003), pp. 5950–5. ISSN: 0027-8424. DOI: 10.1073/pnas.2628045100.

[150] B. H. Jennings. "Drosophila a versatile model in biology & medicine". In: *Materials Today* 14.5 (May 2011), pp. 190–195. ISSN: 1369-7021. DOI: /10.1016/S1369-7021(11)70113-4. URL: http://www.sciencedirect.com/science/article/pii/S1369702111701134.

[151] L. T. Reiter et al. "A systematic analysis of human disease-associated gene sequences in Drosophila melanogaster." In: *Genome Res* 11.6 (June 2001), pp. 1114–25. ISSN: 1088-9051. DOI: 10.1101/gr.169101.

[152] L. I. Mortin and J. W. Sedat. "Structure of Drosophila polytene chromosomes. Evidence for a toroidal organization of the bands." In: *J Cell Sci* 57 (Oct. 1982), pp. 73–113. ISSN: 0021-9533.

[153] N. J. Linford et al. "Measurement of lifespan in Drosophila melanogaster." In: *J Vis Exp* 71 (2013). ISSN: 1940-087X. DOI: 10.3791/50068.

[154] K. Weigmann et al. URL: http://flymove.uni-muenster.de/Genetics/Flies/LifeCycle/LifeCycleGes.html.

[155] A. S. Verma and A. Singh, eds. *Animal biotechnology : models in discovery and translation*. ISBN: 9780124160026.

[156] J. M. Karpilow et al. "Neuronal development in the Drosophila compound eye: photoreceptor cells R1, R6, and R7 fail to differentiate in the retina aberrant in pattern (rap) mutant." In: *J Neurobiol* 31.2 (Oct. 1996), pp. 149–65. ISSN: 0022-3034. DOI: 10.1002/(SICI)1097-4695(199610)31:2<149::AID-NEU2>3.0.CO;2-B.

[157] A. C. Keene and S. Waddell. "Drosophila olfactory memory: single genes to complex neural circuits." In: *Nat Rev Neurosci* 8.5 (May 2007), pp. 341–54. ISSN: 1471-003X. DOI: 10.1038/nrn2098.

[158] S. Waddell. "Dopamine reveals neural circuit mechanisms of fly memory." In: *Trends Neurosci* 33.10 (Oct. 2010), pp. 457–64. ISSN: 1878-108X. DOI: 10.1016/j.tins.2010.07.001.

[159] J. W. Sentry and K. Kaiser. "P element transposition and targeted manipulation of the Drosophila genome." In: *Trends Genet* 8.10 (Oct. 1992), pp. 329–31. ISSN: 0168-9525.

[160] H. L. Ou. "Gene knockout by inducing P-element transposition in Drosophila." In: *Genet Mol Res* 12.3 (2013), pp. 2852–7. ISSN: 1676-5680. DOI: 10.4238/2013.January.4.20.

[161] A. C. Spradling and G. M. Rubin. "Transposition of cloned P elements into Drosophila germ line chromosomes." In: *Science* 218.4570 (Oct. 1982), pp. 341–7. ISSN: 0036-8075.

[162] G. M. Rubin and A. C. Spradling. "Genetic transformation of Drosophila with transposable element vectors." In: *Science* 218.4570 (Oct. 1982), pp. 348–53. ISSN: 0036-8075. DOI: 6289436.

[163] G. M. Rubin and A. C. Spradling. "Vectors for P element-mediated gene transfer in Drosophila." In: *Nucleic Acids Res* 11.18 (Sept. 1983), pp. 6341–51. ISSN: 0305-1048.

[164] R. Klemenz, U. Weber, and W. J. Gehring. "The white gene as a marker in a new P-element vector for gene transfer in Drosophila." In: *Nucleic Acids Res* 15.10 (May 1987), pp. 3947–59. ISSN: 0305-1048. DOI: PMC340823.

[165] J. R. Bateman, A. M. Lee, and C.-t. T. Wu. "Site-specific transformation of Drosophila via phiC31 integrase-mediated cassette exchange." In: *Genetics* 173.2 (June 2006), pp. 769–77. ISSN: 0016-6731. DOI: 10.1534/genetics.106.056945.

[166] A. Keravala and M. P. Calos. "Site-specific chromosomal integration mediated by phiC31 integrase." In: *Methods Mol Biol* 435 (2008), pp. 165–73. ISSN: 1064-3745. DOI: 10.1007/978-1-59745-232-8_12.

[167] A. C. Groth et al. "Construction of transgenic Drosophila by using the site-specific integrase from phage phiC31." In: *Genetics* 166.4 (Apr. 2004), pp. 1775–82. ISSN: 0016-6731.

[168] J.-M. M. Knapp, P. Chung, and J. H. Simpson. "Generating customized transgene landing sites and multi-transgene arrays in Drosophila using phiC31 integrase." In: *Genetics* 199.4 (Apr. 2015), pp. 919–34. ISSN: 1943-2631. DOI: 10.1534/genetics.114.173187.

[169] J. Bischof et al. "An optimized transgenesis system for Drosophila using germ-line-specific phiC31 integrases." In: *Proc Natl Acad Sci U S A* 104.9 (Feb. 2007), pp. 3312–7. ISSN: 0027-8424. DOI: 10.1073/pnas.0611511104.

[170] M. P. Fish et al. "Creating transgenic Drosophila by microinjecting the site-specific phiC31 integrase mRNA and a transgene-containing donor plasmid." In: *Nat Protoc* 2.10 (2007), pp. 2325–31. ISSN: 1750-2799. DOI: 10.1038/nprot.2007.328.

[171] R. Lattao et al. "Tubby-tagged balancers for the Drosophila X and second chromosomes." In: *Fly (Austin)* 5.4 (2011), pp. 369–70. ISSN: 1933-6942. DOI: 10.4161/fly.5.4.17283.

[172] M. Ashburner, K. G. Golic, and R. S. Hawley. *Drosophila : a laboratory handbook*. Cold Spring Harbor, N.Y.: Cold Spring Harbor Laboratory Press, 2005. ISBN: 9780879697068.

[173] T. Osterwalder et al. "A conditional tissue-specific transgene expression system using inducible GAL4." In: *Proc Natl Acad Sci U S A* 98.22 (Oct. 2001), pp. 12596–601. ISSN: 0027-8424. DOI: 10.1073/pnas.221303298.

[174] A. del Valle Rodríguez, D. Didiano, and C. Desplan. "Power tools for gene expression and clonal analysis in Drosophila." In: *Nat Methods* 9.1 (Jan. 2012), pp. 47–55. ISSN: 1548-7105. DOI: 10.1038/nmeth.1800.

[175] J. B. Duffy. "GAL4 system in Drosophila: a fly geneticist's Swiss army knife." In: *Genesis* 34.1-2 (2002), pp. 1–15. ISSN: 1526-954X. DOI: 10.1002/gene.10150.

[176] A. H. Brand and N. Perrimon. "Targeted gene expression as a means of altering cell fates and generating dominant phenotypes." In: *Development* 118.2 (June 1993), pp. 401–15. ISSN: 0950-1991.

[177] S. E. McGuire, Z. Mao, and R. L. Davis. "Spatiotemporal gene expression targeting with the TARGET and gene-switch systems in Drosophila." In: *Sci STKE* 2004.220 (Feb. 2004), pl6. ISSN: 1525-8882. DOI: 10.1126/stke.2202004pl6.

[178] L. Nicholson et al. "Spatial and temporal control of gene expression in Drosophila using the inducible GeneSwitch GAL4 system. I. Screen for larval nervous system drivers." In: *Genetics* 178.1 (Jan. 2008), pp. 215–34. ISSN: 0016-6731. DOI: 10.1534/genetics.107.081968.

[179] G. Roman et al. "P[Switch], a system for spatial and temporal control of gene expression in Drosophila melanogaster." In: *Proc Natl Acad Sci U S A* 98.22 (Oct. 2001), pp. 12602–7. ISSN: 0027-8424. DOI: 10.1073/pnas.221303998.

[180] S. E. McGuire et al. "Spatiotemporal rescue of memory dysfunction in Drosophila." In: *Science* 302.5651 (Dec. 2003), pp. 1765–8. ISSN: 1095-9203. DOI: 10.1126/science.1089035.

[181] R. K. Slotkin and R. Martienssen. "Transposable elements and the epigenetic regulation of the genome". In: *Nature Reviews Genetics* 8.4 (2007), pp. 272–285.

[182] S. Robinow and K. White. "The locus elav of Drosophila melanogaster is expressed in neurons at all developmental stages." In: *Dev Biol* 126.2 (Apr. 1988), pp. 294–303. ISSN: 0012-1606.

[183] C. Pfeiffenberger et al. "Locomotor activity level monitoring using the Drosophila Activity Monitoring (DAM) System." In: *Cold Spring Harb Protoc* 2010.11 (Nov. 2010), pdb.prot5518. ISSN: 1559-6095.

[184] W.-Z. Z. Li et al. "A broad expression profile of the GMR-GAL4 driver in Drosophila melanogaster." In: *Genet Mol Res* 11.3 (2012), pp. 1997–2002. ISSN: 1676-5680. DOI: 10.4238/2012.August.6.4.

[185] Y. O. Ali et al. "Assaying locomotor, learning, and memory deficits in Drosophila models of neurodegeneration." In: *J Vis Exp* 49 (Mar. 2011). ISSN: 1940-087X. DOI: 10.3791/2504.

[186] E. Cook-Wiens and M. S. Grotewiel. "Dissociation between functional senescence and oxidative stress resistance in Drosophila." In: *Exp Gerontol* 37.12 (Dec. 2002), pp. 1347–57. ISSN: 0531-5565.

[187] J. Pallos et al. "Inhibition of specific HDACs and sirtuins suppresses pathogenesis in a Drosophila model of Huntington's disease." In: *Hum Mol Genet* 17.23 (Dec. 2008), pp. 3767–75. ISSN: 1460-2083. DOI: 10.1093/hmg/ddn273.

[188] T. Tully and W. G. Quinn. "Classical conditioning and retention in normal and mutant Drosophila melanogaster." In: *J Comp Physiol A* 157.2 (Sept. 1985), pp. 263–77.

[189] B. R. Malik and J. J. L. Hodge. "Drosophila adult olfactory shock learning." In: *J Vis Exp* 90 (Aug. 2014), e50107. ISSN: 1940-087X. DOI: 10.3791/50107.

[190] E. E. Watkin et al. "Phosphorylation of mutant huntingtin at serine 116 modulates neuronal toxicity." In: *PLoS One* 9.2 (2014), e88284. ISSN: 1932-6203. DOI: 10.1371/journal.pone.0088284.

[191] C. Landles et al. "Proteolysis of mutant huntingtin produces an exon 1 fragment that accumulates as an aggregated protein in neuronal nuclei in Huntington disease." In: *J Biol Chem* 285.12 (Mar. 2010), pp. 8808–23. ISSN: 1083-351X. DOI: 10.1074/jbc.M109.075028.

[192] N. Carty et al. "Characterization of HTT inclusion size, location, and timing in the zQ175 mouse model of Huntington's disease: an in vivo high-content imaging study." In: *PLoS One* 10.4 (2015), e0123527. ISSN: 1932-6203. DOI: 10.1371/journal.pone.0123527.

[193] J. Legleiter et al. "Monoclonal antibodies recognize distinct conformational epitopes formed by polyglutamine in a mutant huntingtin fragment." In: *J Biol Chem* 284.32 (Aug. 2009), pp. 21647–58. ISSN: 0021-9258. DOI: 10.1074/jbc.M109.016923.

[194] V. Maybeck and K. Röper. "A targeted gain-of-function screen identifies genes affecting salivary gland morphogenesis/tubulogenesis in Drosophila." In: *Genetics* 181.2 (Feb. 2009), pp. 543–65. ISSN: 0016-6731. DOI: 10.1534/genetics.108.094052.

[195] M. Jayaraman et al. "Assays for studying nucleated aggregation of polyglutamine proteins." In: *Methods* 53.3 (Mar. 2011), pp. 246–54. ISSN: 1095-9130. DOI: 10.1016/j.ymeth.2011.01.001.

[196] E. E. Wanker et al. "Membrane filter assay for detection of amyloid-like polyglutamine-containing protein aggregates." In: *Methods Enzymol* 309 (1999), pp. 375–86. ISSN: 0076-6879. DOI: 10507036.

[197] K. S. Y. Liu et al. "RIM-binding protein, a central part of the active zone, is essential for neurotransmitter release." In: *Science* 334.6062 (Dec. 2011), pp. 1565–9. ISSN: 1095-9203. DOI: 10.1126/science.1212991.

[198] M. Jucker and L. C. Walker. "Self-propagation of pathogenic protein aggregates in neurodegenerative diseases." In: *Nature* 501.7465 (Sept. 2013), pp. 45–51. ISSN: 1476-4687. DOI: 10.1038/nature12481.

[199] E. Preisinger et al. "Evidence for a recruitment and sequestration mechanism in Huntington's disease." In: *Philos Trans R Soc Lond B Biol Sci* 354.1386 (June 1999), pp. 1029–34. ISSN: 0962-8436. DOI: 10.1098/rstb.1999.0455.

[200] M. Latouche et al. "A conditional pan-neuronal Drosophila model of spinocerebellar ataxia 7 with a reversible adult phenotype suitable for identifying modifier genes." In: *J Neurosci* 27.10 (Mar. 2007), pp. 2483–92. ISSN: 1529-2401. DOI: 10.1523/JNEUROSCI.5453-06.2007.

[201] O. Sofola et al. "Inhibition of GSK-3 ameliorates Abeta pathology in an adult-onset Drosophila model of Alzheimer's disease." In: *PLoS Genet* 6.9 (Sept. 2010), e1001087. ISSN: 1553-7404. DOI: 10.1371/journal.pgen.1001087.

[202] J. Hoffmann et al. "Overexpression of Sir2 in the adult fat body is sufficient to extend lifespan of male and female Drosophila." In: *Aging (Albany NY)* 5.4 (Apr. 2013), pp. 315–27. ISSN: 1945-4589. DOI: 10.18632/aging.100553.

[203] A. Das et al. "Drosophila olfactory local interneurons and projection neurons derive from a common neuroblast lineage specified by the empty spiracles gene." In: *Neural Dev* 3 (2008), p. 33. ISSN: 1749-8104. DOI: 10.1186/1749-8104-3-33.

[204] E. M. Sontag et al. "Methylene blue modulates huntingtin aggregation intermediates and is protective in Huntington's disease models." In: *J Neurosci* 32.32 (Aug. 2012), pp. 11109–19. ISSN: 1529-2401. DOI: 10.1523/JNEUROSCI.0895-12.2012.

[205] Y. Feng et al. "Ellagic acid promotes Abeta42 fibrillization and inhibits Abeta42-induced neurotoxicity." In: *Biochem Biophys Res Commun* 390.4 (Dec. 2009), pp. 1250–4. ISSN: 1090-2104. DOI: 10.1016/j.bbrc.2009.10.130.

[206] R. A. Lehne and L. Rosenthal. *Pharmacology for nursing care*. Elsevier Health Sciences, 2014.

[207] N. L. Mahy et al. "Spatial organization of active and inactive genes and noncoding DNA within chromosome territories." In: *J Cell Biol* 157.4 (May 2002), pp. 579–89. ISSN: 0021-9525. DOI: 10.1083/jcb.200111071.

[208] K. R. Weiss et al. "Huntingtin aggregation kinetics and their pathological role in a Drosophila Huntington's disease model." In: *Genetics* 190.2 (Feb. 2012), pp. 581–600. ISSN: 1943-2631. DOI: 10.1534/genetics.111.133710.

[209] J. Legleiter et al. "Mutant huntingtin fragments form oligomers in a polyglutamine length-dependent manner in vitro and in vivo." In: *J Biol Chem* 285.19 (May 2010), pp. 14777–90. ISSN: 1083-351X. DOI: 10.1074/jbc.M109.093708.

[210] V. C. Wheeler et al. "Length-dependent gametic CAG repeat instability in the Huntington's disease knock-in mouse." In: *Hum Mol Genet* 8.1 (Jan. 1999), pp. 115–22. ISSN: 0964-6906.

[211] Z. Li et al. "A putative Drosophila homolog of the Huntington's disease gene." In: *Hum Mol Genet* 8.9 (Sept. 1999), pp. 1807–15. ISSN: 0964-6906.

[212] B. A. Barbaro et al. "Comparative study of naturally occurring huntingtin fragments in Drosophila points to exon 1 as the most pathogenic species in Huntington's disease." In: *Hum Mol Genet* 24.4 (Feb. 2015), pp. 913–25. ISSN: 1460-2083. DOI: 10.1093/hmg/ddu504.

[213] S. Krobitsch and S. Lindquist. "Aggregation of huntingtin in yeast varies with the length of the polyglutamine expansion and the expression of chaperone proteins." In: *Proc Natl Acad Sci U S A* 97.4 (Feb. 2000), pp. 1589–94. ISSN: 0027-8424.

[214] V. M. Miller et al. "CHIP suppresses polyglutamine aggregation and toxicity in vitro and in vivo." In: *J Neurosci* 25.40 (Oct. 2005), pp. 9152–61. ISSN: 1529-2401. DOI: 10.1523/JNEUROSCI.3001-05.2005.

[215] J. F. Morley et al. "The threshold for polyglutamine-expansion protein aggregation and cellular toxicity is dynamic and influenced by aging in Caenorhabditis elegans." In: *Proc Natl Acad Sci U S A* 99.16 (Aug. 2002), pp. 10417–22. ISSN: 0027-8424. DOI: 10.1073/pnas.152161099.

[216] G. C. Melkani et al. "Huntington's disease induced cardiac amyloidosis is reversed by modulating protein folding and oxidative stress pathways in the Drosophila heart." In: *PLoS Genet* 9.12 (2013), e1004024. ISSN: 1553-7404. DOI: 10.1371/journal.pgen.1004024.

[217] F. M. Menzies et al. "Puromycin-sensitive aminopeptidase protects against aggregation-prone proteins via autophagy." In: *Hum Mol Genet* 19.23 (Dec. 2010), pp. 4573–86. ISSN: 1460-2083. DOI: 10.1093/hmg/ddq385.

[218] T. Tamura et al. "Glial cell lineage expression of mutant ataxin-1 and huntingtin induces developmental and late-onset neuronal pathologies in Drosophila models." In: *PLoS One* 4.1 (2009), e4262. ISSN: 1932-6203. DOI: 10.1371/journal.pone.0004262.

[219] L. Miguel et al. "Both cytoplasmic and nuclear accumulations of the protein are neurotoxic in Drosophila models of TDP-43 proteinopathies." In: *Neurobiol Dis* 41.2 (Feb. 2011), pp. 398–406. ISSN: 1095-953X. DOI: 10.1016/j.nbd.2010.10.007.

[220] S. Zhang et al. "A genomewide RNA interference screen for modifiers of aggregates formation by mutant Huntingtin in Drosophila." In: *Genetics* 184.4 (Apr. 2010), pp. 1165–79. ISSN: 1943-2631. DOI: 10.1534/genetics.109.112516.

[221] T. Ratovitski et al. "N-terminal proteolysis of full-length mutant huntingtin in an inducible PC12 cell model of Huntington's disease." In: *Cell Cycle* 6.23 (Dec. 2007), pp. 2970–81. ISSN: 1551-4005. DOI: 10.4161/cc.6.23.4992.

[222] D. S. Hwangbo et al. "Drosophila dFOXO controls lifespan and regulates insulin signalling in brain and fat body." In: *Nature* 429.6991 (June 2004), pp. 562–6. ISSN: 1476-4687. DOI: 10.1038/nature02549.

[223] L. Poirier et al. "Characterization of the Drosophila gene-switch system in aging studies: a cautionary tale." In: *Aging Cell* 7.5 (Oct. 2008), pp. 758–70. ISSN: 1474-9726. DOI: 10.1111/j.1474-9726.2008.00421.x.

[224] D. Ford et al. “Alteration of Drosophila life span using conditional, tissue-specific expression of transgenes triggered by doxycyline or RU486/Mifepristone.” In: *Exp Gerontol* 42.6 (June 2007), pp. 483–97. ISSN: 0531-5565. DOI: 10.1016/j.exger.2007.01.004.

[225] R. Wong et al. “Quantification of food intake in Drosophila.” In: *PLoS One* 4.6 (2009), e6063. ISSN: 1932-6203. DOI: 10.1371/journal.pone.0006063.

[226] M. E. Giannakou et al. “Dynamics of the action of dFOXO on adult mortality in Drosophila.” In: *Aging Cell* 6.4 (Aug. 2007), pp. 429–38. ISSN: 1474-9718. DOI: 10.1111/j.1474-9726.2007.00290.x.

[227] X.-H. H. Lu and X. W. Yang. “"Huntingtin holiday": progress toward an antisense therapy for Huntington’s disease.” In: *Neuron* 74.6 (June 2012), pp. 964–6. ISSN: 1097-4199. DOI: 10.1016/j.neuron.2012.06.001.

[228] N. H. Skotte et al. “Allele-specific suppression of mutant huntingtin using antisense oligonucleotides: providing a therapeutic option for all Huntington disease patients.” In: *PLoS One* 9.9 (2014), e107434. ISSN: 1932-6203. DOI: 10.1371/journal.pone.0107434.

[229] A. Yamamoto, J. J. Lucas, and R. Hen. “Reversal of neuropathology and motor dysfunction in a conditional model of Huntington’s disease”. In: *Cell* 101.1 (2000), pp. 57–66. ISSN: 1097-4172.

[230] A. E. Molero et al. “Selective expression of mutant huntingtin during development recapitulates characteristic features of Huntington’s disease.” In: *Proc Natl Acad Sci U S A* 113.20 (May 2016), pp. 5736–41. ISSN: 1091-6490. DOI: 10.1073/pnas.1603871113.

[231] A. Weiss et al. “Sensitive biochemical aggregate detection reveals aggregation onset before symptom development in cellular and murine models of Huntington’s disease.” In: *J Neurochem* 104.3 (Feb. 2008), pp. 846–58. ISSN: 1471-4159. DOI: 10.1111/j.1471-4159.2007.05032.x.

[232] R. J. Carter et al. “Characterization of progressive motor deficits in mice transgenic for the human Huntington’s disease mutation.” In: *J Neurosci* 19.8 (Apr. 1999), pp. 3248–57. ISSN: 0270-6474.

[233] L. A. Lione et al. “Selective discrimination learning impairments in mice expressing the human Huntington’s disease mutation.” In: *J Neurosci* 19.23 (Dec. 1999), pp. 10428–37. ISSN: 0270-6474.

[234] B. Ravikumar, R. Duden, and D. C. Rubinsztein. “Aggregate-prone proteins with polyglutamine and polyalanine expansions are degraded by autophagy.” In: *Hum Mol Genet* 11.9 (May 2002), pp. 1107–17. ISSN: 0964-6906. DOI: 11978769.

[235] S. Finkbeiner. "Huntington's Disease." In: *Cold Spring Harb Perspect Biol* 3.6 (June 2011). ISSN: 1943-0264. DOI: 10.1101/cshperspect.a007476.

[236] S. Li and X.-J. J. Li. "Multiple pathways contribute to the pathogenesis of Huntington disease." In: *Mol Neurodegener* 1 (2006), p. 19. ISSN: 1750-1326. DOI: 10.1186/1750-1326-1-19.

[237] E. Diguet et al. "Normal aging modulates the neurotoxicity of mutant huntingtin." In: *PLoS One* 4.2 (2009), e4637. ISSN: 1932-6203. DOI: 10.1371/journal.pone.0004637.

[238] G. Carrard et al. "Impairment of proteasome structure and function in aging." In: *Int J Biochem Cell Biol* 34.11 (Nov. 2002), pp. 1461–74. ISSN: 1357-2725. DOI: 12200039.

[239] D. A. Ferrington, A. D. Husom, and L. V. Thompson. "Altered proteasome structure, function, and oxidation in aged muscle." In: *FASEB J* 19.6 (Apr. 2005), pp. 644–6. ISSN: 1530-6860. DOI: 10.1096/fj.04-2578fje.

[240] J. N. Keller et al. "Autophagy, proteasomes, lipofuscin, and oxidative stress in the aging brain." In: *Int J Biochem Cell Biol* 36.12 (Dec. 2004), pp. 2376–91. ISSN: 1357-2725. DOI: 10.1016/j.biocel.2004.05.003.

[241] W. F. Ward. "Protein degradation in the aging organism." In: *Prog Mol Subcell Biol* 29 (2002), pp. 35–42. ISSN: 0079-6484. DOI: 11908071.

[242] I. Rogers et al. "Ageing increases vulnerability to aβ42 toxicity in Drosophila." In: *PLoS One* 7.7 (2012), e40569. ISSN: 1932-6203. DOI: 10.1371/journal.pone.0040569.

[243] L. Pieri et al. "Fibrillar α-synuclein and huntingtin exon 1 assemblies are toxic to the cells." In: *Biophys J* 102.12 (June 2012), pp. 2894–905. ISSN: 1542-0086. DOI: 10.1016/j.bpj.2012.04.050.

[244] D. J. Selkoe and J. Hardy. "The amyloid hypothesis of Alzheimer's disease at 25 years." In: *EMBO Mol Med* 8.6 (June 2016), pp. 595–608. ISSN: 1757-4684. DOI: 10.15252/emmm.201606210.

[245] B. R. Bettencourt, C. C. Hogan, and M. Nimali. "Polyglutamine expansion in Drosophila: thermal stress and Hsp70 as selective agents." In: *J Biosci* 32.3 (Apr. 2007), pp. 537–47. ISSN: 0250-5991.

[246] P. Brundin, R. Melki, and R. Kopito. "Prion-like transmission of protein aggregates in neurodegenerative diseases." In: *Nat Rev Mol Cell Biol* 11.4 (Apr. 2010), pp. 301–7. ISSN: 1471-0080. DOI: 10.1038/nrm2873.

[247] C. J. Cummings et al. "Over-expression of inducible HSP70 chaperone suppresses neuropathology and improves motor function in SCA1 mice." In: *Hum Mol Genet* 10.14 (July 2001), pp. 1511–8. ISSN: 0964-6906.

[248] M. U. Sajjad et al. "DJ-1 modulates aggregation and pathogenesis in models of Huntington's disease." In: *Hum Mol Genet* 23.3 (Feb. 2014), pp. 755–66. ISSN: 1460-2083. DOI: 10.1093/hmg/ddt466.

[249] Y. Kuo et al. "Suppression of polyglutamine protein toxicity by co-expression of a heat-shock protein 40 and a heat-shock protein 110." In: *Cell Death Dis* 4 (Oct. 2013), e833. ISSN: 2041-4889. DOI: 10.1038/cddis.2013.351.

[250] X.-C. C. Zeng et al. "Hsp70 dynamics in vivo: effect of heat shock and protein aggregation." In: *J Cell Sci* 117.Pt 21 (Oct. 2004), pp. 4991–5000. ISSN: 0021-9533. DOI: 10.1242/jcs.01373.

[251] E. J. Wild and S. J. Tabrizi. "Targets for future clinical trials in Huntington's disease: what's in the pipeline?" In: *Mov Disord* 29.11 (Sept. 2014), pp. 1434–45. ISSN: 1531-8257. DOI: 10.1002/mds.26007.

[252] J. L. Cummings et al. "Effect of Dextromethorphan-Quinidine on Agitation in Patients With Alzheimer Disease Dementia: A Randomized Clinical Trial." In: *JAMA* 314.12 (2015), pp. 1242–54. ISSN: 1538-3598. DOI: 10.1001/jama.2015.10214.

[253] D. M. Lin and C. S. Goodman. "Ectopic and increased expression of Fasciclin II alters motoneuron growth cone guidance." In: *Neuron* 13.3 (Sept. 1994), pp. 507–23. ISSN: 0896-6273. DOI: 7917288.

[254] G. Xiao et al. "Huntington disease arises from a combinatory toxicity of polyglutamine and copper binding." In: *Proc Natl Acad Sci U S A* 110.37 (Sept. 2013), pp. 14995–5000. ISSN: 1091-6490. DOI: 10.1073/pnas.1308535110.

[255] B. Fuss and M. Hoch. "Drosophila endoderm development requires a novel homeobox gene which is a target of Wingless and Dpp signalling." In: *Mech Dev* 79.1-2 (Dec. 1998), pp. 83–97. ISSN: 0925-4773. DOI: 10349623.

[256] J. B. Connolly et al. "Associative learning disrupted by impaired Gs signaling in Drosophila mushroom bodies." In: *Science* 274.5295 (Dec. 1996), pp. 2104–7. ISSN: 0036-8075. DOI: 8953046.

[257] S. Benzer. "BEHAVIORAL MUTANTS OF Drosophila ISOLATED BY COUNTERCURRENT DISTRIBUTION." In: *Proc Natl Acad Sci U S A* 58.3 (Sept. 1967), pp. 1112–9. ISSN: 0027-8424. DOI: PMC335755.

[258] T. Hazelrigg, R. Levis, and G. M. Rubin. "Transformation of white locus DNA in drosophila: dosage compensation, zeste interaction, and position effects." In: *Cell* 36.2 (Feb. 1984), pp. 469–81. ISSN: 0092-8674.

[259] X. Jiang and A. Sorkin. “Coordinated traffic of Grb2 and Ras during epidermal growth factor receptor endocytosis visualized in living cells.” In: *Mol Biol Cell* 13.5 (May 2002), pp. 1522–35. ISSN: 1059-1524. DOI: 10.1091/mbc.01-11-0552.

[260] S. J. Sigrist et al. “Experience-dependent strengthening of Drosophila neuromuscular junctions.” In: *J Neurosci* 23.16 (July 2003), pp. 6546–56. ISSN: 1529-2401. DOI: 12878696.

[261] B. A. Stewart et al. “Improved stability of Drosophila larval neuromuscular preparations in haemolymph-like physiological solutions.” In: *J Comp Physiol A* 175.2 (Aug. 1994), pp. 179–91.